
Development and Synthesis of New Potential ATP-Competitive Myt1 Kinase Inhibitors

Dissertation

zur Erlangung des akademischen Grades

Doctor rerum naturalium

(Dr. rer. nat.)

vorgelegt der

Naturwissenschaftliche Fakultät I

(Biowissenschaften)

der Martin-Luther-Universität Halle-Wittenberg

von

Ghassab M. A. Al-Mazaideh

geb. am 25.08.1979 in Al Tafila, Jordanien

Gutachter/in:

1. Prof. Dr. Wolfgang Sippl, Halle (Saale)

2. Prof. Dr. Peter Imming, Halle (Saale)

3. Prof. Dr. Manfred Jung, Freiburg

Halle (Saale), den 24. May 2012 (Tag der Verteidigung)

To my lovely family

My wife Haya

My daughter Rafef

The two candles that always

enlighten my life

To the spirit of my dear father

Ghassab M. Al-Mazaideh

Table of Contents

Table of Contents	I
List of Abbreviations.....	IV
List of Tables	VI
List of Figures.....	VII
List of Schemes	VIII
1 Introduction	1
1.1 Objectives.....	3
2 Biochemical Background	4
2.1 Protein Kinases.....	4
2.2 Cell Cycle.....	4
2.3 Cyclin-Dependent Kinases	5
2.4 Wee Kinases Family.....	6
2.4.1 Wee1 Kinases	7
2.4.2 Myt1 Kinase	8
3 Protein Kinase Inhibitors	11
3.1 Kinase Inhibition	11
3.1.1 Wee1 Kinase Inhibitors	13
3.1.2 Myt1 Kinase Inhibitors.....	13
3.2 Design of Novel Potentially ATP-Competitive Inhibitors	14
3.2.1 Carbohydrate Domain	15
3.2.2 Spacer Groups	17
3.2.3 Basic Moiety	17
3.2.4 Triazole-Alkyne Moieties.....	17
3.3 Molecular Docking.....	18
3.3.1 Docking Studies on Human Myt1 Kinase	19
3.3.2 Docking Results	20
4 Results and Discussion	26
4.1 Method A: Reaction of <i>N</i> -Containing Compounds with Glycosyl Intermediates.....	27
4.2 Glycosylation Methods	27

4.2.1	GBF via Trichloroacetimidate Method	29
4.2.2	GBF via using Borontrifluoride Etherate	30
4.2.3	GBF using Phase Transfer Catalysts	32
4.3	Reaction of Carbohydrate Intermediates with Basic Moieties	33
4.4	Method B: Reaction of Glycosyl Donors with Acceptor Intermediates.....	35
4.4.1	Basic Moiety and Spacer Groups	35
4.4.2	Reaction of Basic Moiety Intermediates with Carbohydrate Donors.....	37
4.5	Removal of Protecting Groups.....	38
4.6	Acetyl Protecting Group.....	39
4.6.1	Synthesis of Glycosyl Acetates	39
4.6.2	Synthesis of Acetylated Glycoside Intermediates	39
4.6.3	Reaction of Glycosyl Acceptors with Donor.....	40
4.6.4	Synthesis of Perhydroxylated Compounds.....	40
4.7	Click Chemistry Background and Synthesis	42
4.7.1	Synthesis of the Azide Moieties	44
4.7.2	Synthesis of the Acetylene Derivatives	44
4.7.3	Click Reaction	45
5	Discussion and Summary.....	47
6	Experimental Section	50
6.1	Materials and Methods	50
6.1.1	Chemicals and Solvents	50
6.1.2	NMR-Spectroscopy	51
6.1.3	Mass Spectroscopy	51
6.1.4	Melting points	51
6.1.5	Chromatography	52
6.2	Synthetic Procedures	52
6.2.1	Synthesis of Benzylated Glycoside Intermediates	52
6.2.2	Synthesis of Benzylated Glycopyranosidyl Alkyl Acceptors	57
6.2.3	Synthesis of Acceptor Intermediates	60

6.2.4	Synthesis of Glycosyl Acetates	63
6.2.5	Synthesis of Acetylated Glycoside Intermediates	64
6.2.6	Synthesis of Acetylated Glycopyranosidyl Alkyl Acceptors	65
6.2.7	Synthesis of Perhydroxylated Compounds.....	69
6.2.8	Synthesis of Azidoglucosides and Azidogalactosides.....	72
6.2.9	Synthesis of Terminal Acetylenes.....	73
6.2.10	Synthesis of Acetylated Gluco-and Galactotriazole Derivatives	75
6.2.11	Synthesis of Gluco-and Galactotriazole Derivatives.....	82
7	Bibliography.....	87
8	Appendix.....	95
9	Acknowledgments.....	112
10	Curriculum Vitae	113
11	Declaration of Independence.....	115

List of Abbreviations

δ	Chemical shift
Å	Angstrom
Ac	Acetyl
ATP	Adenosine triphosphate
BnCl	Benzyl chloride
BF ₃ ·Et ₂ O	Borontrifluoride etherate
Cdc2	Cell division control protein 2
Cdc25	Cell division control protein 25
Cdk	Cyclin-dependent kinase
c-KIT	Tyrosine-protein kinase kit
CML	Chronic myeloid leukemia
CuAAC	Cu(I)-catalyzed azide–alkyne cycloaddition
DCM	Dichloromethane
DMAP	4-Dimethylaminopyridine
DMF	Dimethyl formamid
d	Doublet
dd	Doublet of doublet
GAs	Genetic algorithms
GBF	Glycosidic bond formation
GOLD	Genetic optimization for ligand docking
HeLa Cell	Human endothelial cells of cervical cancer of henrietta lacks
¹ H-NMR	¹ H-nuclear magnetic resonance
Hz	Hertz
J	Coupling constant
KIs	Kinase inhibitors

List of Abbreviations

KOH	Potassium hydroxide
m	Multiplet
MeOH	Methanol
mmol	Millimol
M.p.	Melting point
MPF	Maturation-promoting factor
NaH	Sodium hydride
NaN ₃	Sodium azide
NaOMe	Sodium methanolate
PDB	Protein data bank
PDGF	Platelet-derived growth factor
Ph	Phenyl-C ₆ H ₅
PKMYT1	Protein kinase Myt1
PKs	Protein kinases
Plk1	Polo-like kinase1
ppm	Parts per million
PTC	Phase transfer catalyst
RMSD	Root mean square deviation
RT	Room temperature
s	Singlet
t	Triplet
TEA	Triethylamine
THF	Tetrahydrofuran
TLC	Thin layer chromatography
TrCl	Triphenylmethyl chloride
Trp	Tryptophan

List of Tables

Table 1: Gold score (G) and corr.Gold score (corr.G) values	21
Table 2: Results of GBF of glycopyranoside derivatives.....	31
Table 3: Yields and conditions of glycopyranoside derivatives by PTC	33
Table 4: Yields of glycosidic intermediates coupled with BHP derivative.....	34
Table 5: Reaction conditions used for alkylation of BHP with several spacer groups	35
Table 6: Reaction conditions used for alkylation of DPH with several spacer groups	36
Table 7: Results of different acceptors with sugar donor.....	37
Table 8: Results of coupling acetylated glycoside intermediates with different acceptors.....	40
Table 9: Results of deacetylated reaction with different glycoside intermediates	41

List of Figures

Figure 1: A functional cell cycle	5
Figure 2: Control of Cdc2 (Cdk1) activity by inhibitory phosphorylation.....	6
Figure 3: Wee kinases family	7
Figure 4: Influence on the G2-M transition by Plk1	7
Figure 5: Kinase domains of Myt1 and Wee1	9
Figure 6: Crystal structure of the catalytic domain of Myt1	9
Figure 7: Chemical structure of Imatinib	12
Figure 8: Structure of Dasatinib	13
Figure 9: The general structure of novel compounds.....	15
Figure 10: The chemical structure of heterocyclic-bond acceptor systems.....	17
Figure 11: Set of terminal acetylenes	18
Figure 12: Comparison between homology model and crystal structure of Myt1 kinase	20
Figure 13: Simulation of the binding of ligands in the binding pocket of the Myt1	24
Figure 14: General structure of final compounds.....	26
Figure 15: Benzylated glycopyranosidyl alkyl acceptors.....	34
Figure 16: General structure of click compounds	42
Figure 17: General structure of the final compounds.....	47

List of Schemes

Scheme 1:	Synthesis of compound 3.....	16
Scheme 2:	Illustration of synthesis methods of compound 6.....	27
Scheme 3:	Glycosylation reaction.....	28
Scheme 4:	The trichloroacetimidate glycosylation method	29
Scheme 5:	Synthesis of glycopyranoside derivatives by GBF-trichloroacetimidate method.....	30
Scheme 6:	Comparison between several methods to prepare 8b,c.....	32
Scheme 7:	General reaction of <i>O</i> -alkylation of glycosyl donors by PTC	33
Scheme 8:	Reaction of <i>N</i> -alkylated BHP and DPH with sugar.....	37
Scheme 9:	Removal of benzyl ether protecting groups.....	38
Scheme 10:	Synthesis of acetylated glucopyranose	39
Scheme 11:	Synthesis of acetylated glycoside intermediates.....	39
Scheme 12:	Synthesis of acetylated glycopyranosidyl alkyl acceptors.....	40
Scheme 13:	Synthesis of perhydroxylated final compounds GS (29-34).....	41
Scheme 14:	CuAAC at elevated temperature or the addition of Cu(I) ions	43
Scheme 15:	Proposed catalytic cycle for azide-alkyne coupling	43
Scheme 16:	Synthesis of β -azidoglycoside at the position C-1.....	44
Scheme 17:	Synthesis of perhydroxylated glyco-triazole compounds.....	45

1 Introduction

Cancer is the unregulated growth of abnormal cells in the body. Cases of cancer are more common with increasing age and are a great threat to human life [1]. Cancer can develop in almost any organ or tissue, such as the lungs, stomach and blood or nerve tissues. Consequently, the development of new drugs plays a central role. Conventional therapy acts nonspecifically and damages healthy cells as well as cancer cells by means of cancer treatment drugs which include platinum compounds, alkylating agents and DNA topoisomerase inhibitors. Even if the activity against tumor cells is very high, these drugs have inconvenient negative side effects, which result in the discontinuation of the therapy and physical effects such as hair loss, nausea, vomiting, heart muscle damage, myelosuppression and the emergence of drug resistance during cancer therapy [2].

A number of new treatment approaches have been developed in the last few years to avoid these disadvantages according to the understanding of the processes at the molecular level. A good example of the success of such molecular treatment strategy is the tyrosine kinase inhibitor Imatinib (Gleevec), which was introduced in 2001 as an important therapeutic agent in modern cancer therapy for treatment of chronic myeloid leukemia (CML) [3]. The mechanism is based on the disruption of signaling cascades, such that signals for cell proliferation and cell growth are no longer forwarded or only so in an altered form.

Another promising approach is the manipulation of kinases that are involved in regulating the cell cycle. The cell cycle is the series and ordered set of events that takes place in a cell, leading to its replication and division. These actions are controlled by well balanced mechanisms including two main instances: the G1 at the inter-phase of G1 and S phase, and the G2 checkpoint which controls the entry into mitosis.

The kinases, Myt1, Wee1 and Chk1 are key regulators of this G2 checkpoint, which act directly or indirectly to inhibit Cdc2 (Cell division control protein 2, synonymous to human Cdk1) activity. The human membrane-associated tyrosine and threonine Myt1, is an important dual-specific kinase. This protein kinase is of major importance in cell cycle regulation, particularly at the G2-M transition. Myt1 inactivates Cdc2-Cyclin B complexes by phosphorylating Cdc2 on Thr14 and Tyr15 [4]. In contrast, Wee1 kinase selectively phosphorylates the Tyr15 residue only. Additionally, the entire mitosis, Myt1 plays an important role in intra-cellular membrane dynamics, such as the formation of the Golgi complex [5, 6].

Thus the arrested cell is able to correct damaged DNA. Due to mutations of the p53 tumor suppressor gene, many cancer cells lose the important checkpoint at the G1/S transition and rely, therefore, totally on the second checkpoint after G2 phase in order to repair DNA damage. For this reason, the Wee kinases are interesting targets for drug development. If the inhibitory properties of the Wee kinases are stopped, premature activation of the Cdc2-Cyclin B complexes can be introduced, leading to premature mitosis and apoptosis [7].

Furthermore, Myt1 could be brought into context with many other physiological processes such as participation in the development of eyes in *Drosophila melanogaster*, as well as with pathological changes including carcinogenesis of UVA-induced skin cancer [8] and at gene (PKMYT1) level, as a potential biomarker of clear cell renal cell carcinoma [9]. Induced activation leads to a prolongation of S-and G2-phase of the cell cycle, allowing to gain additional time to later induce the replication of the virus [10]. In addition, this gene is differentially expressed in fetal compared to the adult brain of Klinefelter syndrome, correlated with verbal cognitive dysfunction. However, the significance of the latter finding still needs to be demonstrated [11].

In 2001, PD-166285 was described as a Wee1 kinase inhibitor, but is also considered as a broadly active tyrosine kinase inhibitor, it led to an abrogation of the G2 checkpoint in irradiated cancer cells [12]. Recently, studies identified a compound named MK-1775 to be a potent inhibitor of Wee1 kinase. In combination with conventional cytotoxic drugs, this treatment strategy leads to apoptosis of the cell [13]. Meanwhile, this compound passed phase I clinical trials and is currently undergoing phase II clinical evaluation against a variety of tumors [14]. Consequently, selective Myt1 inhibitors would be very interesting as well.

1.1 Objectives

There are no potent and selective inhibitors for Myt1 kinase available until now. The mechanism of the real ability of Myt1 as a target for cancer therapy is not yet foreseeable [15]. Selective inhibitors might help to better understand the biological role of this enzyme and, on this foundation, allows for intervention in pathological changes. For this purpose, it is necessary to do basic research.

As a base, in the search for new lead structures that interfere selectively in cellular regulatory processes, Dr. M. Schmidt and his research group neosynthesized bioactive glyco-glycerolipids, originally derived from marine algae extracts, according to the report of ZHOU et al. [16] and some intermediates of this synthesis route were also used in this work.

The aim of this work is to synthesize new potential lead structures of ATP-competitive compounds and to contribute to the development of both potent and selective Myt1 kinase inhibitors. Moreover, 1,3-dipolar cycloaddition reaction between azides and alkynes should be realized to afford glyco-triazoles as another class of potential inhibitors. The synthesis approach is also intended to provide a basis for structural modifications. It should allow changing the substitution of the carbohydrate building block, alkyl chain length, basic moiety and the triazole alkyne moiety.

Based on the results of KRISTIJANSDOTTIR and RUDOLPH [17] that Staurosporine inhibits Myt1 kinase, this compound will be used as a positive control in docking and modeling studies applied on a Myt1 kinase homology model and on the crystal structure of the kinase domain, available since September 2010.

These compounds could then be tested by biochemical assays and would thus allow the derivation of structure-activity relationships and conclusions about the type of inhibition.

2 Biochemical Background

2.1 Protein Kinases

Protein kinases (PKs) have profound effects on any cell; as they are regulators of many cell functions. PKs are the largest protein family and most influential within the human genome [18]. The human genome contains 518 protein kinase genes; they constitute about 2 % of all human genes. PKs mediate a chemical reaction that the γ -phosphate group of adenosine triphosphate (ATP) is transferred to the hydroxyl group of serine, threonine or tyrosine residues in the substrate protein. This phosphorylation positively or negatively affects activity, localization and overall function of many other proteins. The protein phosphorylation is reversible by the action of protein phosphatases. 30 % of all proteins may be modified by kinases. So, kinases are known to regulate the majority of cellular pathways, especially those involved in signal transduction and the transmission of signals within the cell. Dysregulation of kinase activity is a frequent cause of disease, especially cancer [19].

2.2 Cell cycle

The replication cycle of a eukaryotic somatic cell consists of four main phases: The G1-phase is characterized by cell growth and preparation for replication. DNA replication occurs during S-phase (Fig.1). The subsequent G2-phase is a further phase of growth. The cell growth stops at the transition to the mitosis (M-phase) and the cellular energy is focused on the orderly division into two daughter cells [20]. Optionally, in the G0-phase the cell may leave the cycle and temporarily stop dividing (state of resting). At any time, e.g. induced by mediators such as cytokines, the cell can reenter and precede the cell cycle. These repetitive control mechanisms that ensure the fidelity of cell division are called cell cycle checkpoints, except the G0-phase which does not always occur. A prominent role in the checkpoint control play the cyclin-dependent kinases [21].

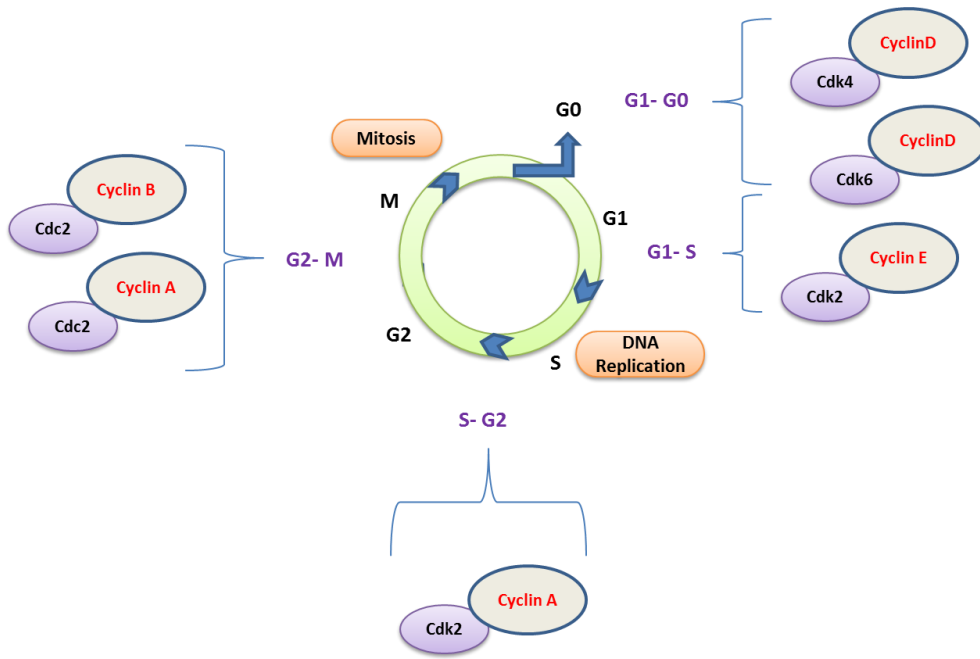


Figure 1: A functional cell cycle [22]

2.3 Cyclin-Dependent Kinases

The cyclin-dependent kinases (Cdks) are a family of PKs that play key roles in cell division. The phosphorylation and inactivation of the retinoblastoma (Rb) tumor suppressing proteins are produced throughout late G1, S and G2-M phases [23].

The human Cdk1, also referred to as Cdc2, is required for the onset of mitosis. Cdc2 controls entry of cells into mitosis by inhibitory phosphorylation on Thr14 and Tyr15, which inhibits the activity of enzyme and prevents premature initiation of mitosis. Cdc2 as a monomer is catalytically inactive and is rendered active by association with activators, e.g. Cyclin B [24]. The complex of mitotic B cyclins with M-phase Cdc2 is also termed Maturation-Promoting Factor (MPF) [4]. This complex in the G2-M phase is shown in Figure 2.

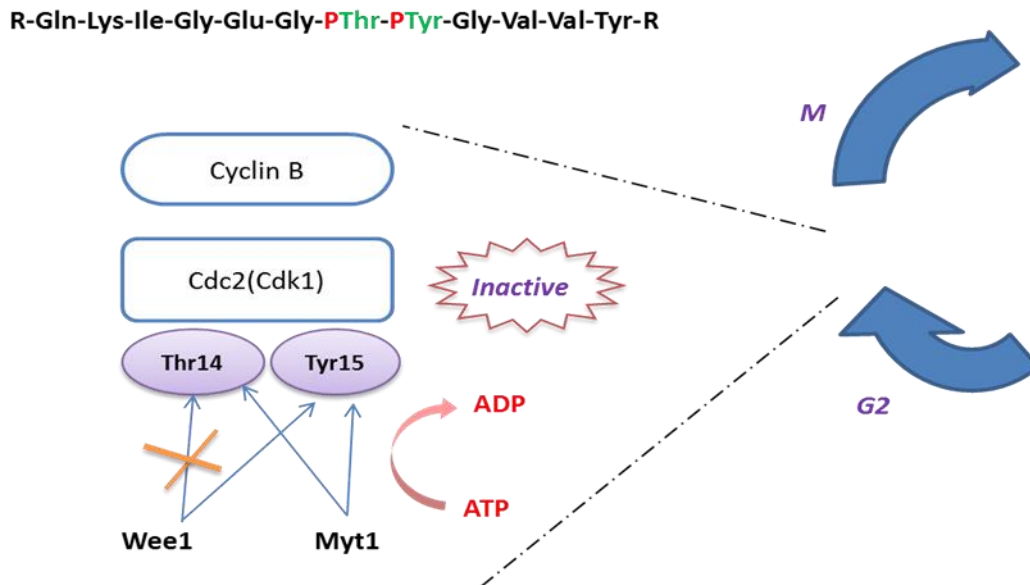


Figure 2: Control of Cdc2 (Cdk1) activity by inhibitory phosphorylation

The activity of Cdc2 is regulated by inhibitory phosphorylations: during the interphase, Cdc2 associates with Cyclin B to form a catalytically active complex. Phosphorylation of Cdc2-cyclin B complex at the activation loop of Cdc2 at Thr14 and Tyr15 residues by Myt1 and at Tyr15 by Wee1 leads to a blockade of the activity of the complex. The G2-M transition, the dual-specific Cdc25 phosphatases remove the inhibitory phosphate groups on both Thr14 and Tyr15 and are therefore important determinants of cyclin-Cdk activity [20].

In mammalian cells, there are three Cdc25 isoforms: Cdc25A, Cdc25B, and Cdc25C, all of these isoforms except Cdc25C are over expressed in several human cancers [25]. The discovery of mitosis-controlling aspects showed that both the Cdc2-cyclin complexes and its regulatory enzymes were mainly located in specific cellular compartments. In HeLa cells, it could be shown that Cdc2-cyclin B complexes shuttle between the cytosol and the nucleus during interphase [26].

2.4 Wee Kinases Family

The Wee kinases (Wee1, Wee1B and Myt1) are key regulators of mitotic entry throughout the G2-M transition of the cell cycle. The function of these kinases leads to phosphorylation of tyrosine and threonine residues of Cdc2 (Fig.3). At the amino acid sequence, Wee kinases share the greatest level of similarity in their kinase domain [27]. However, the percentage sequence identity between Myt1 and Wee 1 kinases are lower than 35 % [28].

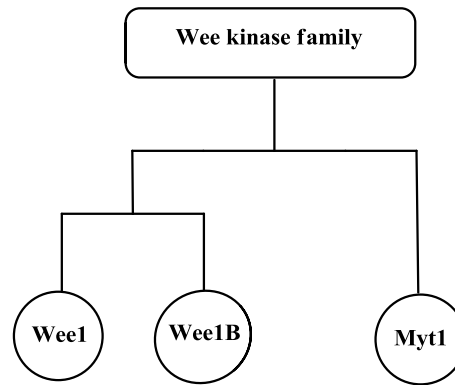


Figure 3: Wee kinases family

Essentially, there are five conserved residues found in the kinase domain. These are a Trp in the subdomain IV, Glu and Asp in subdomain VIII and a Trp and Arg in subdomain X. These conserved residues define Wee kinase family identity, because they are not commonly found in other non-Wee kinases at this position. The activity of the Wee kinases is furthermore hierarchically controlled by Polo-like kinase 1 (Plk1) and the activity of Cdc25 phosphatases (Fig.4), which act as activators of MPF. Plk1 phosphorylates and activates Cdc25 leading to further amplification of Cdk1-cyclin B activity in mitosis [29].

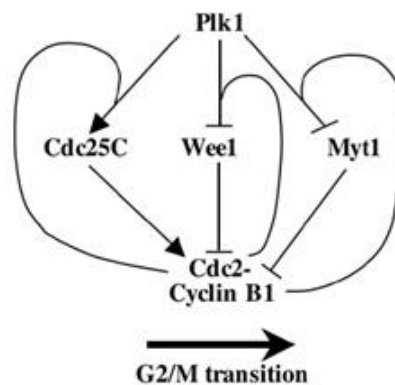


Figure 4: Influence on the G2-M transition by Plk1[30]

2.4.1 Wee1 Kinases

Wee1 and Wee1B are soluble and located to the nucleus. The WEE1 gene was first identified by a NURSE in 1975 [31]. The somatic Wee1 kinase (Wee1A) is a 72 kDa protein containing 646 amino acids and consisting of three-domains: an *N*-terminal regulatory domain, a central kinase domain, and a short *C*-terminal regulatory domain (serine/threonine kinases) [32]. The catalytic kinase domain comprises 271 amino acids from Phe299 to Leu569. It leads to phosphorylation of the Cdc2-cyclin B complex on the glycine rich loop on Tyr15 in the active site of Cdc2-cylin B. The activity of Wee1 is blocked in the

M-phase of the cell cycle by Plk1 mediated phosphorylation, while the activity will be the maximum during S and G2-phase [4, 33-35].

2.4.2 Myt1 Kinase

Myt1 also belongs to the family of Wee kinases. It is a membrane associated kinase and localizes to the endoplasmic reticulum and Golgi complex. It consists of 499 amino acids and the kinase domain consists of 250 amino acids with a molecular weight of about 55 kDa. Myt1 is a dual-specific kinase and has the capacity to phosphorylate both Thr14 and Tyr15 residues of Cdc2. Inhibition of Myt1 kinase is predicted to cause premature activation of Cdc2 [27]. Therefore, inhibitors of Myt1 kinase are supposed to rapidly kill proliferating cells and interfere with G2 checkpoint control. Such inhibitors could play key role as targets for development of new drugs and could help overcoming resistance.

At the end of G2-phase, Cdc25 phosphatases dephosphorylate Thr14 and Tyr15 leading to activation of Cdc2-cyclin B and thus promoting mitosis. In addition, the human protein kinase Myt1 is hyperphosphorylated by Plk1 during M-phase [36-41], interestingly, without affecting the Myt1 kinase activity in a direct manner.

Myt1 Homology model

In the beginning of this work, no crystal structure of the full length Myt1 kinase was available and only the amino acid sequence was known (PKMyt1_human: Q99640). A homology model of Myt1 kinase was developed in the group of Prof. Sippl in the Institute of Pharmacy based on homology to the crystallized Wee1. The human Wee1 kinase shows a sequence identity of 32 % and sequence homology of 46 % [28]. According to the model, the crystal structure of human Wee1 kinase (pdb code: 1X8B) kinase domain is complexed with inhibitor PD0407824 (Fig.5-B), four other related kinases as template (pdb code: 1O1U for (CDK2), 1ZYC for (GCN2), 2IW8 and 2G9X for (CDK2).

The catalytic domain of kinases consists mainly of two lobes (or subdomains): *N*-terminal lobe and *C*-terminal lobe and they are connected via a short polypeptide chain, which is known as the hinge region. The active centre, *N*-terminal lobe (top) through the five twisted β -sheets and the glycine rich loop limit the hinge region marking the end of the pocket. The *C*-subdomain differs from the *N*-terminal domain in size, sequence and helicity.

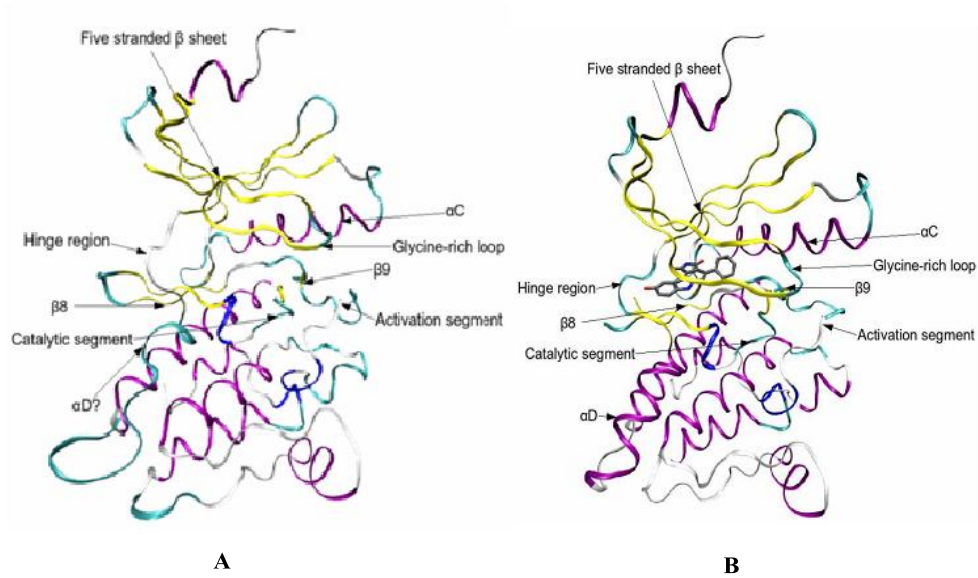


Figure 5: Kinase domains of Myt1 (homology model, A) and Wee1 (B) [27]

Myt1 is striking about the absence of the helix of discharge. However, it has the typical DFG motif (D251, F252, and G253). In contrast, the Wee1 kinase has a DLG motif instead of DFG [27].

Myt1 crystal structure

There is a crystal structure for PKMYT1 available since September 2010. This crystal structure consists only of the catalytic domain of Myt1, ranging from 75-362 amino acids as shown in Figure 6 where β -sheets are shown in green and α -helices in red at a resolution of 1.9 Å.



Figure 6: Crystal structure of the catalytic domain of Myt1 (PDB: 3P1A) [42].

The peptide backbone in the hinge region plays a key role in the binding of the co-substrate ATP, by being responsible for the formation of the crucial hydrogen bonds. α - and β -phosphate groups of ATP could be fixed for the catalytic reaction through interaction with a divalent magnesium ion and a conserved lysine residue [43, 44].

3 Protein Kinase Inhibitors

3.1 Kinase Inhibition

Protein kinase inhibitors (PKIs) work as therapeutic agents for a variety of human diseases by blocking the activity of kinases involved in the signaling pathways of growth [44]. PKs are divided into three general classes, characterized with regard to their substrate specificity [45]:

- Serine/threonine-protein kinases.
- Tyrosine-protein kinases.
- Dual specific protein kinases (phosphorylate both threonine and tyrosine on target proteins).

In addition, these inhibitors are indispensable to fully understanding the actual role a kinase plays in the cellular environment. There are three mechanisms of inhibitors of serine/threonine and tyrosine protein kinases [46]:

- Catalytic site inhibitors, competing with ATP at the active site.
- Regulatory site inhibitors, that bind at a regulatory site and compete with endogenous regulators of the kinase.
- Substrate inhibitors, which compete with the protein substrate, thus preventing its engagement with the kinase; this group contains large peptides or peptidomimetics.

Most recent studies are seeking inhibition of the enzyme activity in a competitive manner. Generally, there are different types of inhibitors [47, 48]:

Type I: Inhibitors bind exclusively to the ATP binding site, are the most common and known as ATP-competitive (e.g. Sunitinib).

Type II: Inhibitors bind to an extended ATP binding site, which assumes the DFG-out conformation (inactivated conformations) of the kinase (e.g. BIRB796, a highly selective p38 kinase inhibitor).

Type III: Inhibitors bind exclusively outside of the ATP binding site, are known as ATP-noncompetitive (e.g. MEK inhibitors such as PD184352).

Type IV: Covalent irreversible inhibitors. There is no agreement in the literature in concerning the use of these types, inhibition occurred when the compounds combined

covalently with enzymes so as to inactivate them irreversibly (e.g. Canertinib, also known as CI-1033). All of these kinase inhibitors are fully reversible inhibitors except type IV.

Imatinib

In recent years, major trends of research have leaned towards even more selective and potent inhibitors in an attempt to reduce the risk of side effects. The first example as an approved and marketed drug was Imatinib (Gleevec, also known as STI-571) (Fig.7). Its main target is the ABL tyrosine kinase, which plays a role in regulation of cytoskeletal function and dynamic progression through the cell cycle and cell death [47].

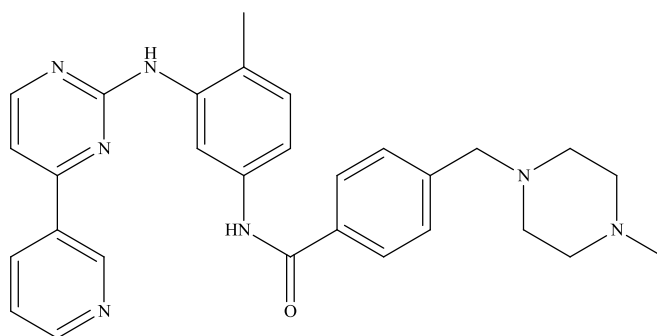


Figure 7: Chemical structure of Imatinib (STI 571, Gleevec)

Currently, Imatinib is used for treatment of CML caused by an abnormal chromosome called the Philadelphia chromosome. The outcomes of the exchanged genetic information are two genes, BCR (breakpoint cluster region) and ABL, to producing the fused protein with constitutive kinase activity (BCR-ABL). These processes cause abnormal production of CML cells in the blood. Additionally, Imatinib shows a multikinase activity which has led to its exploitation in different cancer types and inhibits several structurally related tyrosine kinases like c-KIT (tyrosine-protein kinase Kit), and the receptor tyrosine kinases for platelet-derived growth factor (PDGFR) [49]. Despite the unintended Imatinib targets, the clinical evaluation showed that Imatinib had a relatively low toxicity level coupled with a high efficiency rate.

Dasatinib

Dasatinib, previously known as BMS-354825, and approved since 2006, is an anti-cancer drug [50] (treatment of newly diagnosed CML, together with a resistance against Imatinib and Nilotinib) and was introduced 5 years after Imatinib as a potent tyrosine kinase inhibitor. The structure of Dasatinib (Fig.8) differs from Imatinib and it acts not only by

inhibition of the BCR-ABL protein kinase, but also by inhibition of other kinases [51]. Dasatinib is more promiscuous and inhibits c-Src kinase as another primary target, in contrast to Nilotinib and Imatinib, which do not address this kinase [52-54].

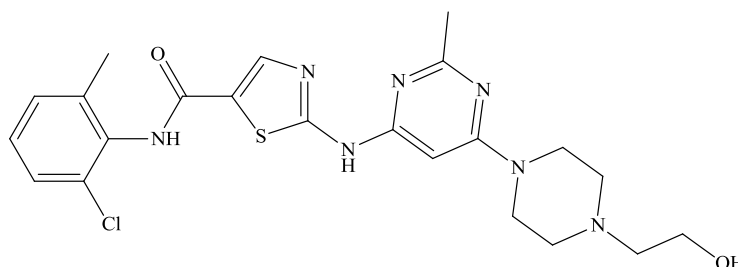


Figure 8: Structure of Dasatinib

3.1.1 Wee1 Kinase Inhibitors

MK-1775 was described in 2009 by HIRAI et al. [13] as a potent and selective small molecule inhibitor for Wee1. The results showed that this drug abrogates the G2 checkpoint and stimulates the cytotoxicity of the DNA-damaging agents Gemcitabine, and Cisplatin selectively in p53-deficient cells (which rely on the G2-checkpoint much more than normal cells). For that, such tumors are selectively sensitized to DNA-damaging agents by Wee1 inhibition. MK-1775 has been introduced as a chemosensitizer and is currently being evaluated in phase II clinical trials in patients with advanced solid tumors, integrated with Gemcitabine or Cisplatin and Carboplatin. A previous report showed that MK-1775 is well tolerated and might also show single agent anti-tumor activity in combination with chemotherapy alike [55].

PD-166285 is described as G2 checkpoints abrogator and potent ATP-competitive inhibitor. This compound is a broadly active tyrosine kinase inhibitor and has many other cellular targets besides Wee1 including c-Src, epidermal growth factor receptor and platelet-derived growth factor receptor [56].

3.1.2 Myt1 Kinase Inhibitors

To date, there are no studies dealing with potential anti-cancer human Myt1 kinase inhibitors. Because this type of kinases is hard to obtain, and assay, there are few data available so far. One report deals with the interaction of glycolipids and Myt1 [16]. Few patents [57-59] were found preparing some compounds to inhibit the Myt1 kinase, but no inhibition data for the patented structure are accessible. These patents claimed to have invented compounds for potent Myt1 kinase inhibition to treat various indications,

including cancer, but testing and determining the potency and effectiveness of these compounds with full-length Myt1 were not described. Even if these compounds will bind to the ATP binding site. Until now there is no potent and selective Myt1 kinase inhibitor available.

3.2 Design of Novel Potentially ATP-Competitive Inhibitors

Most of kinase inhibitors are ATP competitive. These inhibitors act by binding the ATP binding site of the kinase like selective kinase inhibitors and multi kinase inhibitors (staurosporine). It is difficult to design ATP competitive inhibitors, because the structure of ATP binding sites which bind with PKs are structurally highly related even in divergent kinase domains. Additionally, other inhibitors work by binding to the lipid binding site like glycolipids, MEK inhibitors such as CI-1040 (PD184352) and AKT1, AKT2 inhibitors (allosteric inhibitors) [16, 47].

The starting point of our investigations focused on was the work of GÖLLNER et al. [60] (the research group of Dr. M. Schmidt) with neosynthesis of reported glyco-glycerolipids and the new derivatization of molecule domains. Based on their structure, we suppose that these compounds are type III inhibitors (allosteric inhibition). The compounds described herein are designed to be type I or type II inhibitors, because they should bind ATP-competitively.

By taking this synthesis strategy we looked for new compounds with a carbohydrate core structure connected via different spacer groups to a heterocyclic *H*-bond acceptor system. The structure of these new inhibitors was determined and modified based on the results of the docking and modeling studies. The synthesized compounds might create a new class of potential ATP-competitive inhibitors of Myt1. Depending on the first results obtained from a binding assay for glyco-triazole compounds prepared in our group [61], we found that two glyco-triazole compounds have positive results. For these results, the further development of this structure will be very interesting. The 1,3-dipolar cycloaddition (Fig.9) between azidoglucoside or azidogalactoside connected with alkynes, gives several class of agents.

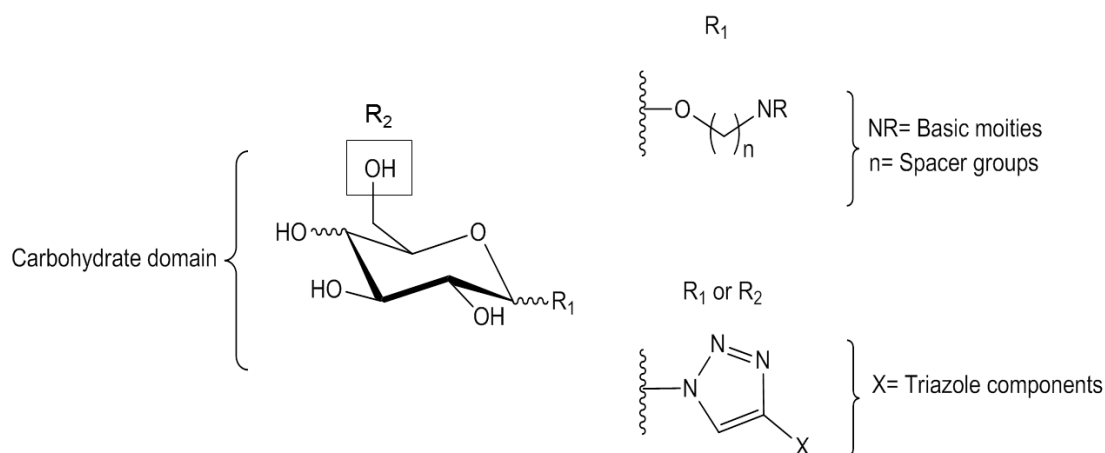


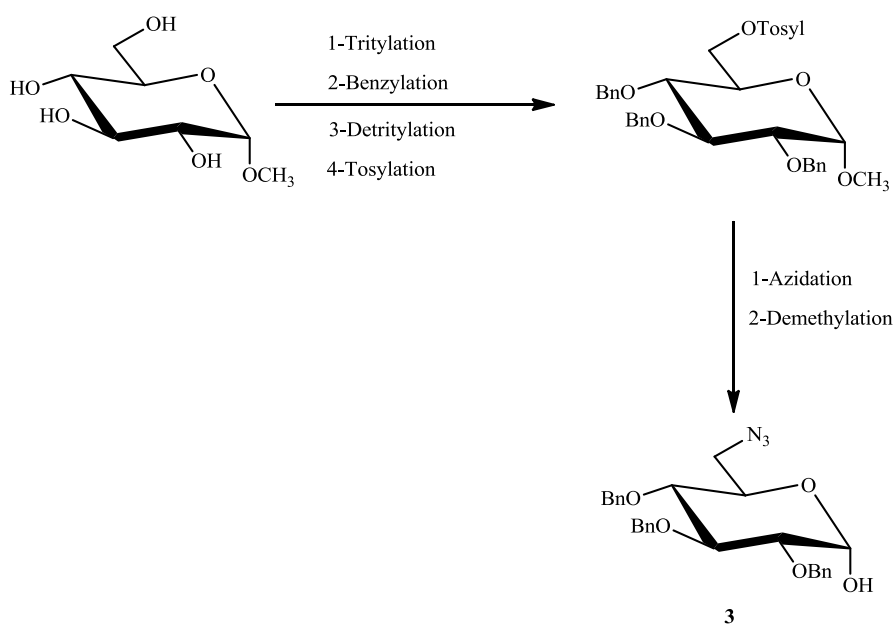
Figure 9: The general structure of novel compounds

The binding modes of the synthesized final compounds can be predicted using methods of computer-based drug design.

3.2.1 Carbohydrate Domain

Carbohydrates are an important class derived from natural products, the continued interest is due to the chemical and the biological importance of these molecules. Such scaffolds are used to mimic bioactive molecules. They provide a good platform to display chemical functionalities that have the potential to interact with kinases. They are chemically stable moieties (rigid core) with a number of reactive orthogonal functional groups (mostly hydroxyl functions) and also have a low molecular weight. Therefore, carbohydrate sugars are also important from a pharmaceutical point of view due to their involvement in cell recognition processes and signal transduction. They provide a series of scaffolds as chiral-pool material, are available by the inversion of individual positions and as building blocks for the synthesis of natural products and drugs [62].

In this study, two benzylated glucopyranoside derivatives were used: the commercially available 2,3,4,6-tetra-*O*-benzyl-*D*-glucopyranose and the synthetic 6-azido-2,3,4-tri-*O*-benzyl-6-deoxy- α -*D*-glucopyranose **3** (Scheme 1) which was described by GÖLLNER et al. [60].



Scheme 1: Synthesis of compound 3

The described procedure involves synthesis of compound **3** from α -methyl-D-glucopyranoside via the following steps:

1. Selective protection of the primary hydroxyl group at position C-6 by using Triphenylmethyl chloride (TrCl) in dry pyridine in the presence of 4-dimethylaminopyridine (DMAP) with heating (Tritylation).
2. Benzylation of other secondary hydroxyl groups in presence of excess benzyl chloride (BnCl) and strong base NaH with heating (Benzylation).
3. Removing of the trityl group with trifluoroborane etherate ($BF_3 \cdot Et_2O$) complex at RT (Detritylation).
4. Using 4-toluenesulfonyl chloride and triethylamine (TEA) as a base in cooling conditions to protect position C-6 as toluenesulfonate ester as a good leaving group (Tosylation).
5. Nucleophilic substitution reaction applied by using sodium azide (NaN_3) in solvent with heating (Azidation).
6. Acid hydrolysis of the methoxy group by a mixture of sulphuric acid and acetic acid to form compound **3** ready for glycosylation (Demethylation).

Debenzylation (hydrogenation) was applied in the final step of the synthesis. In addition, acetyl groups were used instead of benzyl group to prepare final compounds; a deacetylation procedure was applied in order to obtain perhydroxylated compounds.

3.2.2 Spacer Groups

Acyclic aliphatic saturated hydrocarbons were used as a linker between glucosyl donors and heterocyclic *H*-bond acceptor systems. Primary alkyl halides or haloalkanes and halo alcohols were used as a source of widely used connectors. Haloalkanes contain a sp^3 hybridized carbon atom bound to fluorine, chlorine, bromine, and iodine. The polarity makes the carbon atom electrophilic and the halogen is nucleophilic. Halogenids (Cl^- , Br^- and I^-) are good leaving groups and haloalkanes are more reactive than the parent alkane chains. Consequently, the carbon atom can be easily attacked by nucleophiles via nucleophilic substitution reactions S_N1 or S_N2 [63].

3.2.3 Basic Moiety

Different heterocyclic *H*-bond acceptor systems were connected to glycoside donors intermediates. Figure 10 shows the structure of basic moieties used as acceptors for coupling with (haloalkyl) glycosides.

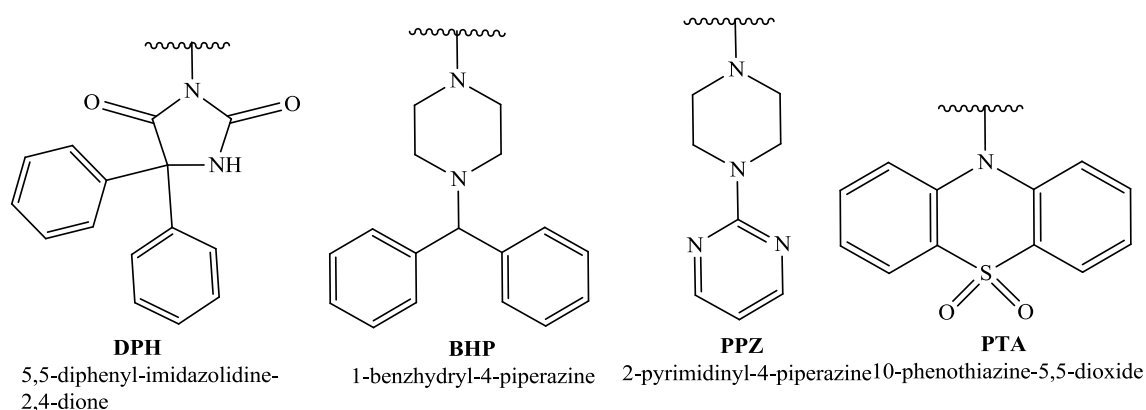


Figure 10: The chemical structure of heterocyclic-bond acceptor systems

3.2.4 Triazole-Alkyne Moieties

Several alkynes (Fig.11) were connected with azido glycosugars such as **DIH**, **BIP**, and **PPI** to establish a glyco-triazol sugars library. Two *C*-alkylated aromatic ketones **BIF**, **DIB** were used also to generate different classes of glyco-triazole compounds at position C-1 and at position C-6. **BIF** and **DIB** were connected to 6-azido glucopyranosides by B.SAUER [61] and showed an effect in a binding assay.

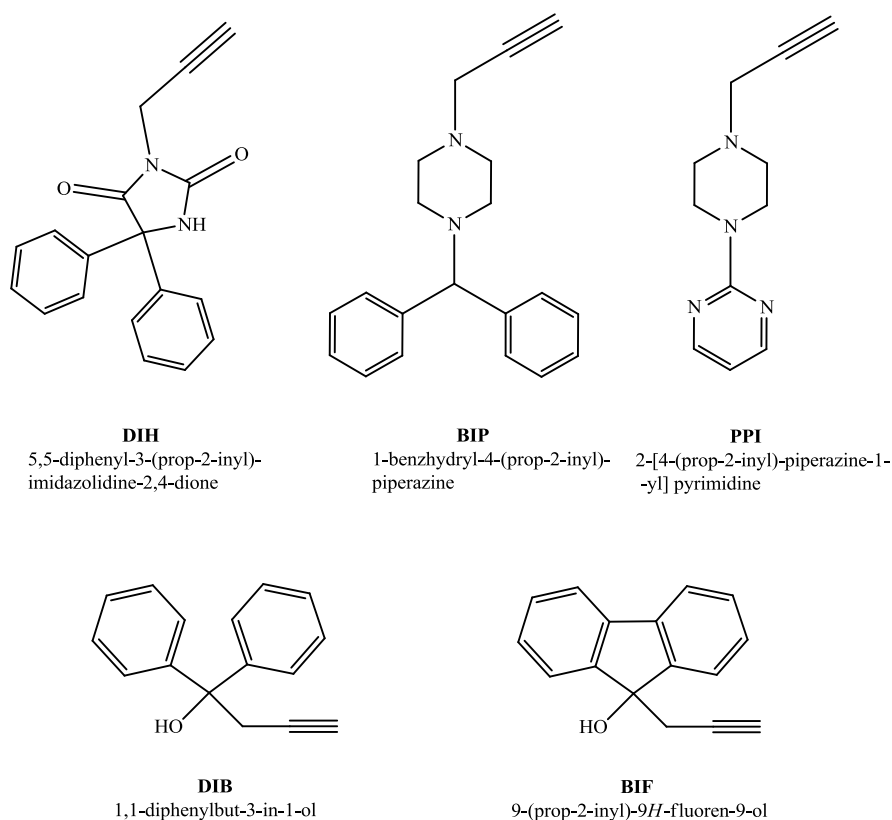


Figure 11: Set of terminal acetylenes

3.3 Molecular Docking

Molecular docking is an important tool in computer assisted molecular design, rational design of drugs and structural biology. Docking is defined as the fitting of ligands into the binding pocket of a protein. The main goal of this method is to predict the binding mode of a ligand together with a protein with a known 3D-structure. The target prediction and assessment of the ligand in the binding pocket of the protein-ligand complex may help to find new leads.

A docking program consists of two main parts. The first part generates new conformations of the docked ligand inside the defined binding pocket of the protein, and the second part is the scoring function, evaluating the interaction. In this part all conformations are scored according to their position inside the pocket. The score is later used to rank the conformations [64, 65]. One of the best known and most extensively tested programs for docking in the field of pharmaceutical research and biotechnology is GOLD (Genetic Optimization for Ligand Docking). It is a reliable docking program developed by JONES et al. in 1995 [66]. GOLD was one of the first docking programs and is based on a genetic algorithm (GA) for flexible docking. The role of all the algorithms which are used in

docking is the reproduction of the lowest energy conformation of the ligand in the binding pocket through imitation of natural evolutionary processes.

GAs mimic the process of natural evolution by manipulating a collection of data structures so-called chromosomes [67]. The first step of a GA for docking is the randomized creation of a large population of different ligand conformations. After the creation, each member of the population is scored by the scoring function. The scoring function implements terms for protein-ligand hydrogen bonding, van der Waals energy, ligand torsional energy and internal van der Waals energy. In the second step of a GA all individuals having a lower score than a specific cut-off value are rejected. In a third step the remaining individuals undergo some genetic operations like cross-over, single-point-mutation and so on. The last step is used to create as many new individuals from the remaining ones, that are needed to come back to the starting population [68].

Gold score was selected as the scoring function for the approach chosen in this work. To eliminate the influence of the molecular weight, the gold score can be corrected by dividing the original score over the square root of the number of non-hydrogen atoms (heavy atoms) [65].

3.3.1 Docking Studies on Human Myt1 Kinase

The homology model of human Myt1 kinase was developed in a theoretical approach in the group of Prof. Sippl based on known crystal structures of Wee1. The docking study was applied on this homology model and in comparison with the crystal structure for the kinase domain of Myt1 available since September 2010. In a docking study we followed the structure of the native substrate ATP and investigated a range of potential ATP-competitive compounds in comparison with the known unspecific kinase inhibitors such as staurosporine and K 252c. Docking and modeling studies on a Myt1 homology model and new crystal structure led to modified inhibitor structures. All of the dock works and simulations were done by German Erlenkamp (AG Medicinal Chemistry, Prof. Dr. W. Sippl). For docking works the program GOLD version 5 [69] and a fragment of the Myt1 kinase listed in the RCSB Protein Data Bank (PDB code 3P1A, X-ray structure of Myt1) were used.

3.3.2 Docking Results

All the simulated compounds have acceptable gold score values. Due to this GOLD is able to correctly predict the binding mode of Wee1 kinase inhibitors [70, 71]. The examination of the scoring values is necessary for plausibility.

RMSD (root-mean-square deviation) value between these two kinase domains is approximately 2 Å. This value is the measure of the average distance between the atoms (usually the backbone atoms- the $C\alpha$ atomic coordinates). Therefore, they are quite similar and the same protocol was used for Myt1 docking as for Wee1 docking [28].

Herein (Fig.12) the docking study was applied on the hinge region of the Wee1 homology model (blue) and crystal structure of the catalytic domain of Myt1 (green) at 1,9 Å resolution.

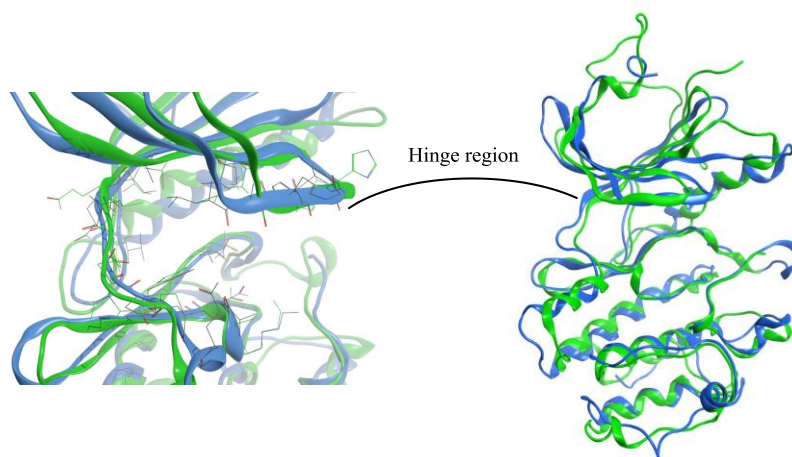
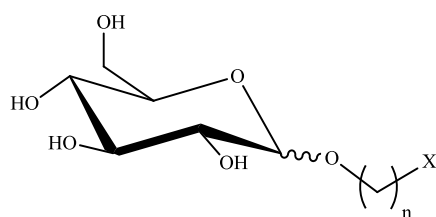
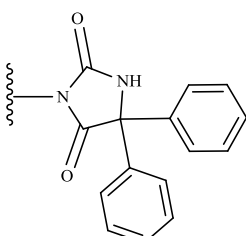
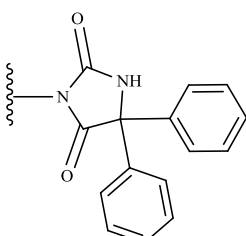
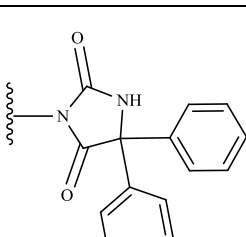
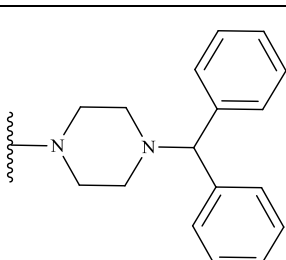


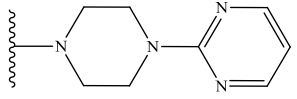
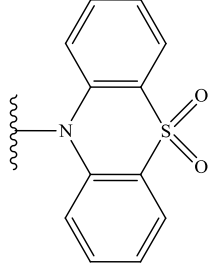
Figure 12: Comparison between homology model and crystal structure of Myt1 kinase

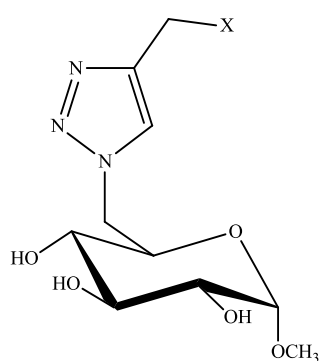
Gold scores showed acceptable values for these compounds compared to staurosporine. Very probable orientations within the binding pocket are combined, so that a real interaction is possible in a biological assay. Table 1 summarizes the docking results for the final compounds.

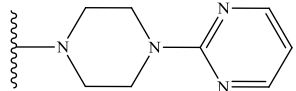
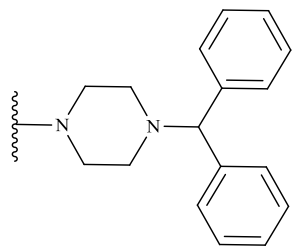
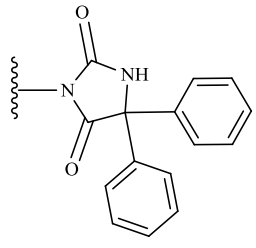
Table 1: Gold score (G) and corr.Gold score (corr.G) values

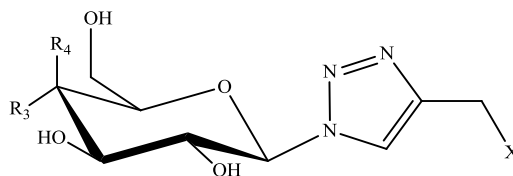


Cpds	n	X	Homology model		Crystal structure	
			G	corr.G	G	corr.G
Staurosporine	-	-	55.35	9.35	59.50	10.19
GS29	2		47.88	8.33	59.25	10.15
GS30	3		55.92	9.59	46.11	7.90
GS31	4		54.20	9.16	63.18	10.67
GS32	3		19.54	3.35	29.27	5.01

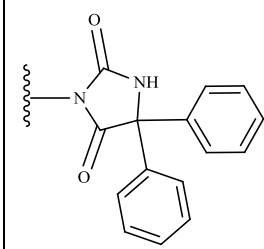
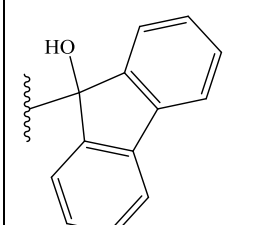
GS33	3		44.25	8.36	45.85	8.66
GS34	3		26.53	4.76	26.58	4.77



Cpds	X	Homology model		Crystal structure	
		G	corr.G	G	corr.G
GS35		54.93	10.20	52.15	9.68
GS36		37.54	6.25	41.59	6.93
GS37		57.53	9.58	70.90	11.81



Cpds	R3	R4	X	Homology model		Crystal structure	
				G	corr.G	corr.G	G
GS38	OH	H		51.32	9.52	56.09	10.41
GS39	OH	H		19.40	3.23	40.19	6.69
GS40	OH	H		58.37	10.48	60.35	10.83
GS41	OH	H		43.34	7.78	59.84	10.74
GS42	H	OH		40.40	7.50	54.61	10.14
GS43	H	OH		48.39	8.06	51.66	8.61

GS44	H	OH		56.43	9.40	64.56	10.76
GS45	H	OH		55.98	10.05	59.99	10.77

In the evaluation, the table shows the simulation results of various ligands within homology model and crystal structure of Myt1 kinase. The location of the ligand is considered within the binding pocket. The highest gold score **70.90** and corr.gold scores **11.81** was obtained with compound **GS37**, which is one of the most interesting compounds. Furthermore, the compounds **GS31**, **GS40**, **GS44** and **GS45** have good scores compared to staurosporine, especially values obtained from the crystal structure. These ligands have a very probable orientation (Fig. 13) combined with the binding pocket (likely binding mode). In this case, a hydrogen bond set between the ligand and the hinge region (Cys190) of Myt1 was set as a constraint, because it is considered necessary for an interaction.

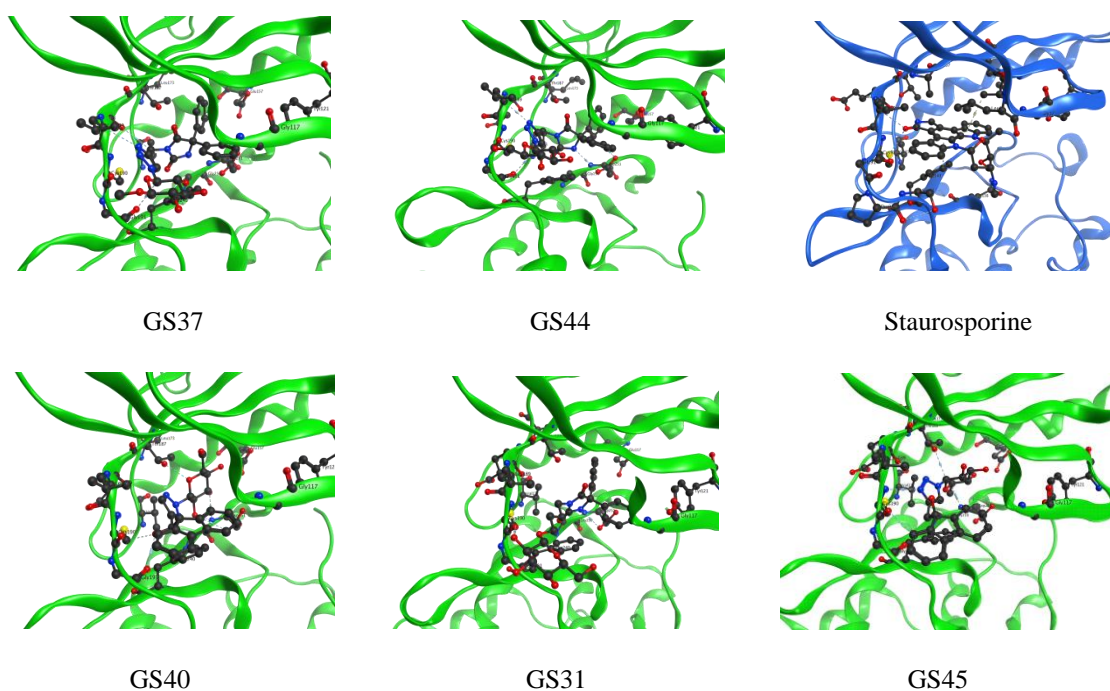


Figure 13: Simulation of the binding of ligands in the binding pocket of the Myt1 crystal structure (green), model (blue)

Most of the ligands showed good scores with both crystal structure and homology model, and the real interactions with Myt1 were likely except with **GS29**, **GS32**. However, these two compounds were likely binding with the model. **GS30**, **GS32**, **GS33**, **GS38** were showed an unlikely binding mode with the model and probable with crystal structure. We found that the better simulations were obtained with crystal structure according to good scores and corrected binding mode with most of the ligands.

Based on the results of the docking studies, the synthesis of these compounds was carried out to afford new promising potential ATP-competitive Myt1 kinase inhibitors and it will be tested in bioassays.

4 Results and Discussion

The present work provides synthesis of glucopyranosidyl alkyl acceptors with structure showed in fig.14.

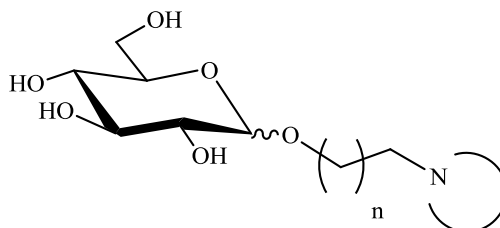


Figure 14: General structure of final compounds

Wherein:

n: is chosen from 1-3 (alkyl linker)

N: basic moiety

According to scheme below (Scheme 2), this represents general steps of the synthesis methods of the unprotected sugar **6**. This scheme involves two methods to prepare the protected sugar **5**:

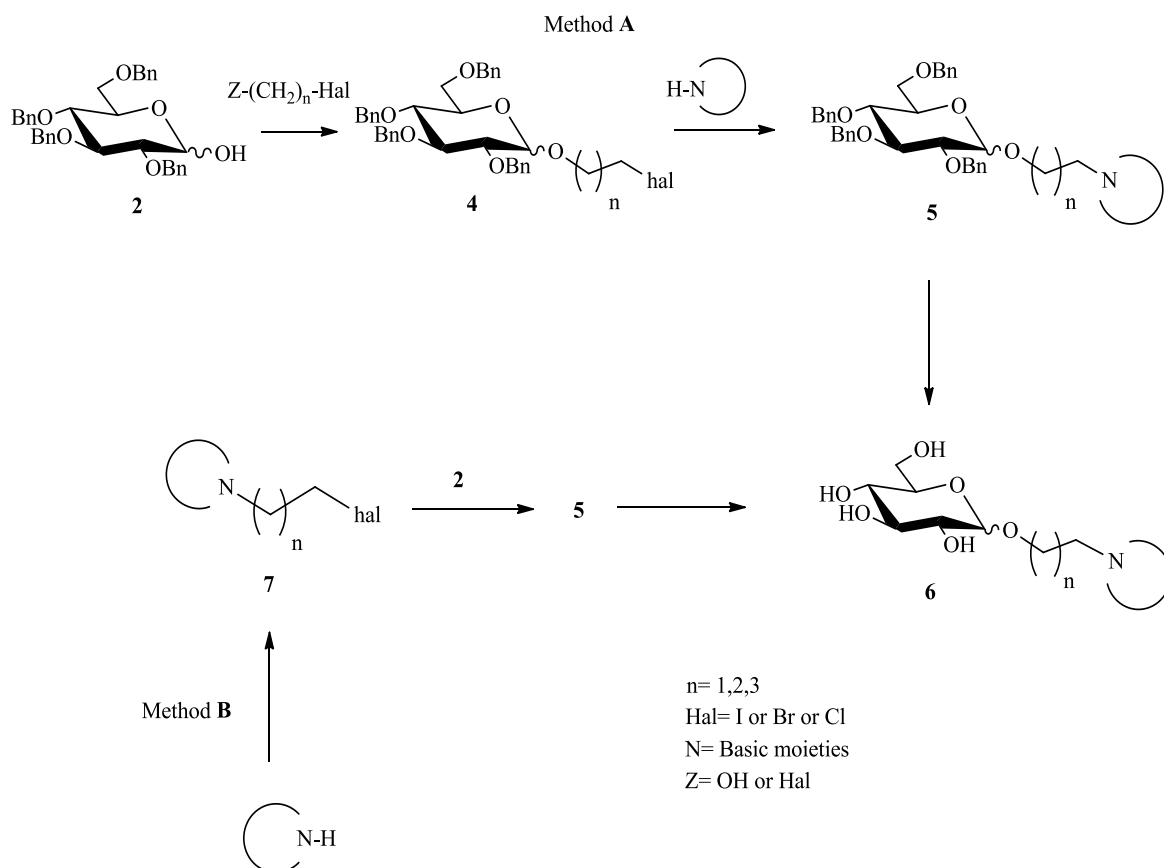
- Method A: Reaction of *N*-containing compounds with glucosyl intermediate

This method represents a reaction of glucopyranoside derivatives with different alkyl halides or halo alcohols to form protected glucopyranoside intermediates (compound **4**). After that several aromatic heterocyclic compounds were reacted with these intermediates.

- Method B: Reaction of glucosyl donors with acceptors intermediate

In this method, different acceptors (aromatic heterocyclic compounds) were used to react with alkyl halide or halo alcohol to form compound **7** as acceptors intermediate. Then these intermediates were reacted with glucopyranoside derivatives. Therefore, these two methods were studied to identify the best way to prepare **5**.

Finally, the catalytic transfer hydrogenation reaction was applied to convert **5** to the target final target **6**.



Scheme 2: Illustration of synthesis methods of compound 6

4.1 Method A: Reaction of *N*-Containing Compounds with Glycosyl Intermediates

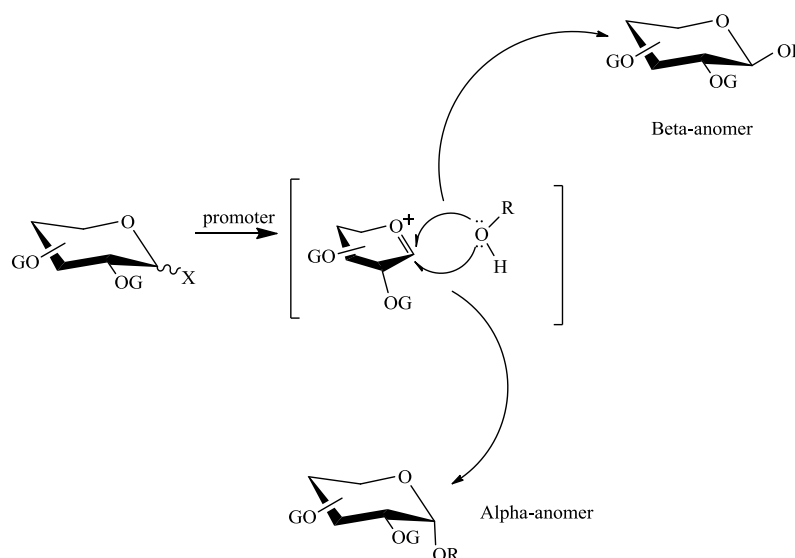
A series of glycosylation reactions between the benzylated sugar donors and different spacer groups, particularly 1-*O*-alkylation, were carried out to obtain compound **4** with good yield. After that, *O*-glycosyl intermediates were reacted with several heterocyclic acceptors to form compound **5** and deprotection was applied to obtain structure **6** as novel compounds.

4.2 Glycosylation Methods

Glycoside reaction is a very common reaction in nature providing a wide variety of glycoconjugates and oligosaccharides as glycolipids, glycopeptides and glycoproteins. Basically, the compound that gives the glycosyl moiety is called the glycosyl donor, and the alcohol that receives it, is referred to as glycosyl acceptor. Glycosylations are based on the activation of the anomeric carbon of the protected sugar residue, to be coupled served as the electrophile (the glycosyl donor) and the alcohol (the glycosyl acceptor) as the nucleophile. As a result, glycosidic bond is formed by nucleophilic substitution at the anomeric carbon of the glycosyl donor. In addition, the reaction is performed in the presence of an activator

called promoter, generally Lewis acids such as $\text{BF}_3 \cdot \text{Et}_2\text{O}$ or TMSOTf are used in catalytic amounts. Additionally, other mild activating species, such as, AgOTf [72] have also been used. Consequently, anomeric product was obtained. Also the reaction solvent plays an important role in terms of influencing of the stereoselectivity at the anomeric center. Basically, solvents of low polarity, like DCM, ether, toluene and 1,2-dichloroethane are commonly used. These solvents enhance the formation of α -glycosides. On the other hand, polar solvents, such as acetonitrile or nitromethane at low temperature, shift stereoselectivity towards the formation of β -glycoside. This is due to exocyclic complex formation with the solvents that hinder the β and α faces, respectively [73, 74].

Generally, distinct experimental conditions are needed to perform the reaction, such as: inert atmosphere, the use of dry solvents and molecular sieves (acids activator). In some cases the order of adding the reagents is important. In the most common approach a glycosyl donor is activated at the anomeric center with a promoter to give a glycosyl cation (oxocarbenium ion) susceptible to nucleophilic attack by glycosyl acceptor. Scheme 3 shows the general mechanistic pathways for glycosidic bond formation (GBF).



Scheme 3: Glycosylation reaction [74]
R: alkyl, G = Non-participating group (benzyl, azido, etc.)

The general strategy for GBF synthesis is based on two steps: activation step and glycosylation step. In the first step the anomeric center should be activated under formation of a stable glycosyl donor and best by a catalyzed attachment of a leaving group to the anomeric hydroxyl group.

Activation of the sugar residue can be achieved in three main ways [75]:

- KOENIGS–KNORR: method where the general principle of this method depends basically on exchange of the anomeric hydroxyl group with halide leaving group to give glycosyl halide, which is then activated by heavy metal salts.
- FISCHER-HELPERICH: method where the anomeric hydroxyl group is activated by a proton catalyst.
- In the trichloroacetimidate method and other types of anomeric oxygen activation, a simple base-catalyzed addition of the anomeric hydroxyl group to trichloroacetonitrile yielding *O*-glycosyl trichloroacetimidate, which generate highly reactive glycosyl donors under very mild acid-catalysis (Lewis acid).

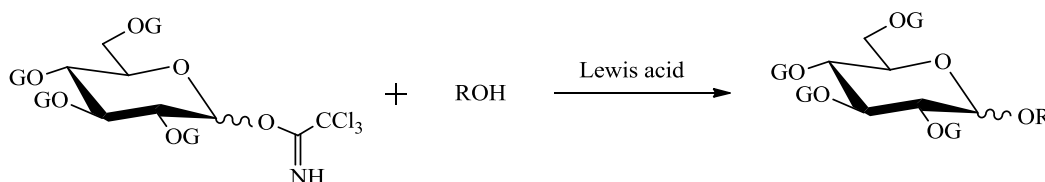
The second step depends on uniform high-yielding glycosyl transfer to the glycosyl acceptor based on glycosyl donor activation with catalytic amounts of promoter.

In this study, three methods were applied:

- GBF via trichloroacetimidate method
- GBF via using borontrifluoride etherate
- GBF using phase transfer catalysis

4.2.1 GBF via Trichloroacetimidate Method

Glycosylation reactions using trichloroacetimidate were first introduced and explored by MICHEL and SCHMIDT in 1980 [76] and since then have become a universal method which avoids the use of heavy metal salts as activators. This developed method is first base catalysis, and then deprotonation of the anomeric position of the otherwise protected sugar. Furthermore, the activation for the glycosylation reactions involve with catalytic amounts of Lewis acids (Scheme 4).

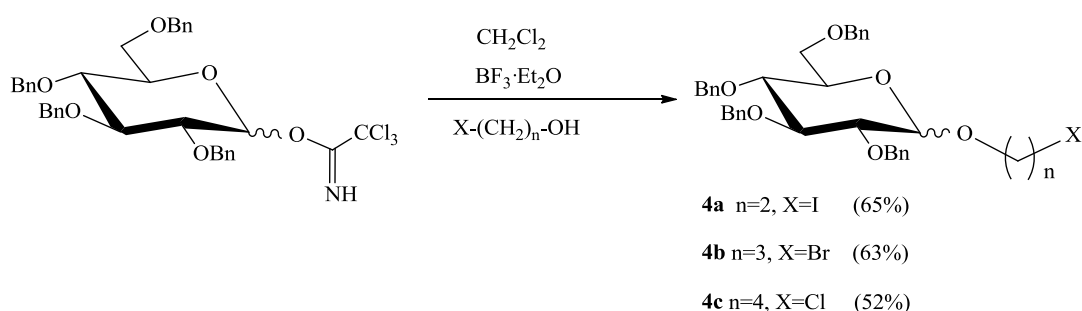


Scheme 4: The trichloroacetimidate glycosylation method

The resulting 1-*O*-alkoxide is trapped by the electrophilic nitrile group of trichloroacetonitrile depending on the reaction conditions for the stable α - or β -trichloroacetimidate. The thermodynamic control, using NaH or KOH [77] as base with phase transfer catalyst promotes the formation of the stabilized intermediate by the anomeric effect of α -form. On

the other hand the kinetically controlled reaction using K_2CO_3 as base leads due to the higher nucleophilicity of the equatorial preference to the formation of alkoxide β -anomer. Here, the choice of solvent, temperature and acid are crucial for the stereoselectivity of the glycosylation. The advantages of this imidate synthesis are certainly to be found in the stability and the good yields and the imidates in stereoselectivity. However, using trichloroacetonitrile method provides a disadvantage in the problematic separation of the methyl group at the anomeric position, which at relatively simply structured carbohydrates nor compensated, but for more complicated molecules can be fatal [78].

In this work, in situ reaction was applied according to SCHMIDT et al. [79] preparing *O*-glucosyl trichloroacetimidates which are suitable intermediates, since they can be obtained by glycosylating the anomeric hydroxyl group via dissolving protected glucopyranoside derivatives in dry DCM as solvent under inert atmosphere (Argon) in the presence of sodium hydride as base at RT. After addition of *O*-nucleophile (alcohol components) to the reaction, $BF_3 \cdot Et_2O$ was added as acid catalysis. The mixture was cooled to $-20\text{ }^\circ\text{C}$ to start the glycosylation of acceptors. After completion of the reaction, water is added and organic layer was separated by extraction, dried over sodium sulfate, removal the solvent under vacuum produced yellow oil substance, which was purified by column chromatography. Scheme 5 represents GBF by using trichloroacetimidate method and the percentage yield obtained by this method for glucosyl donors **4a-c**.



Scheme 5: Synthesis of glycopyranoside derivatives by GBF-trichloroacetimidate method
X= halide (Cl, Br, I)

4.2.2 GBF via using Borontrifluoride Etherate

Glycosides involve a fully protected saccharide with a leaving group at the anomeric position, and a haloalkanol (aglycone) with only one hydroxyl group. Oxocarbenium formed by using activators which will then be attacked by the aglycone.

The reactivity of glycosyl donors depend on the employed protecting groups and the intrinsic structure-associated reactivity, so that several methods designed for activating glycosyl donors like "BF₃-Mediated Glycosylation" [80, 81]. Formation of haloalkyl glycosides was accomplished through a glycosidation using glycosyl donor derivatives and aglycone primary halide, in which the hard Lewis acid BF₃·Et₂O activate the presence of free hydroxyl groups at RT in the presence of DCM as solvent and without using sonication. Glycosyl cation was obtained and liable in situ to nucleophilic attack by acceptors. The results of these glycosylation reactions are shown in table 2. This reaction is not complicated and the desired α/β -mixture of haloalkyl glycosides **4a-c** is generally obtained in good yields.

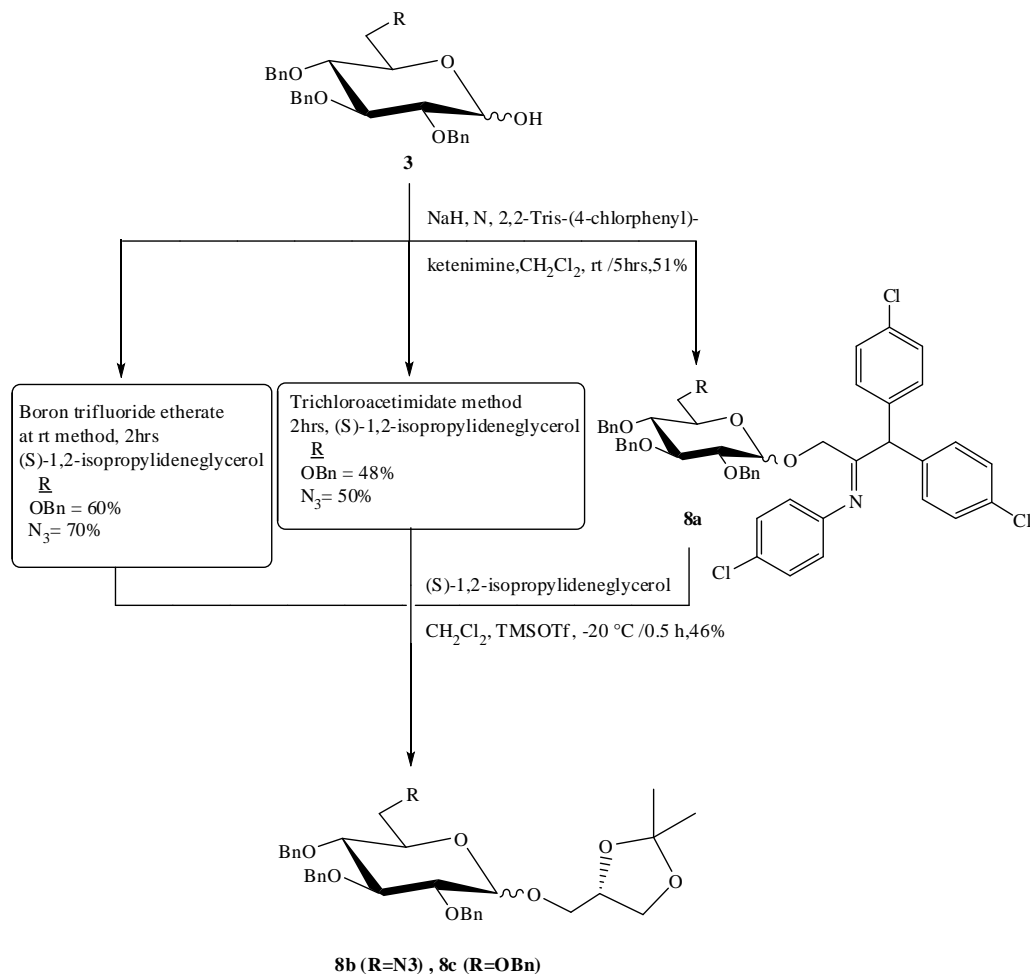
Table 2: Results of GBF of glycopyranoside derivatives

	X	n	Time (hours)	Yield %
4a	I	2	0.5	84
4b	Br	3	1	80
4c	Cl	4	4.5	60

Herein, the boron trifluoride etherate catalyzed coupling of alcohol components with *O*-protected sugars. The product was obtained with different percentage yield with respect to the time; the best conversion appeared with **4a** at 0.5 h. This method gave good yields comparing to other glycosylation ways depending on the yields, reaction condition and simplicity in the purification.

This reaction was applied also to prepare 3-*O*-(6-azido-2,3,4-tri-*O*-benzyl-6-deoxy-D-glucosyl)-1,2-isopropylidene-*sn*-glycerol **8b** by one step with good yield 70 % as a mixture of α/β -anomers and 50 % with using trichloroacetimidate method (Scheme 6). Actually, this method is more interesting than others, the compounds were prepared by two steps.

Firstly the reaction of compound **3** (Scheme 1) with *N*-2,2-tris-(4-chlorophenyl) ketenimine to get **8a** with 51 % yield as β -anomer. Secondly, this intermediate **8a** was reacted with (*S*)-1,2-isopropylidene-glycerol to get **8b** with 46 % yield as α -anomer.

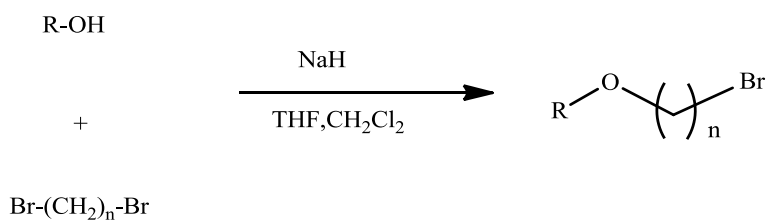
Scheme 6: Comparison between several methods to prepare **8b**, **8c**

Also the same procedure was applied to get 3-*O*-(2,3,4,6-tetra-*O*-benzyl-6-deoxy-D-glucosyl)-1,2-isopropylidene-*sn*-glycerol **8c** with yield 60 % compared to trichloroacetimidate method (48 %). The resulting yields showed that using BF₃·Et₂O method at RT is the best way.

4.2.3 GBF using Phase Transfer Catalysts

Phase transfer catalysis (PTC) in the glycosylation reactions with primary alkyl halide and sugar donors proceeds well. Standard preparative procedures for this glycosidation step require strong base such as sodium hydride. In this method, direct 1-*O*-alkylation of protected sugars was achieved in the presence of a strong base and dibromoalkane inside two solvents. This liquid-liquid phase system consists of two polar aprotic solvents. PTC [82] was carried out by using different acceptors and adding aprotic solvent to the reaction mixture after certain time, where a solution of the sugar, base and glycosyl acceptor dissolved in dry dichloromethane, stirred under inert condition and at ambient temperature.

After that an equal volume of dry THF was added as a second solvent to the mixture to start the alkylation and produced bromoalkyl glycosides (Scheme 7). The reaction might be monitored by TLC, then the compounds isolated **4b** or **4d** and purified via column chromatography.



Scheme 7: General reaction of *O*-alkylation of glycosyl donors by PTC

THF was added to the mixture getting more activation and good yield by using benzyl sugars moieties. The reaction principle has already been successfully applied to a variety of combinations between glycosyl donor bodies (table 3) and haloalkane obtained a mixture of α/β products.

Table 3: Yields and conditions of glycopyranosed derivatives by PTC

	n	Time (hours)	Yield %
4b	3	12	75
4d	4	50	65

4.3 Reaction of Carbohydrate Intermediates with Basic Moieties

Herein, glycosyl derivatives react with different basic moieties (Fig.15) with different conditions. Several spacer groups that contain halogens X like iodine, bromine and chlorine were used.

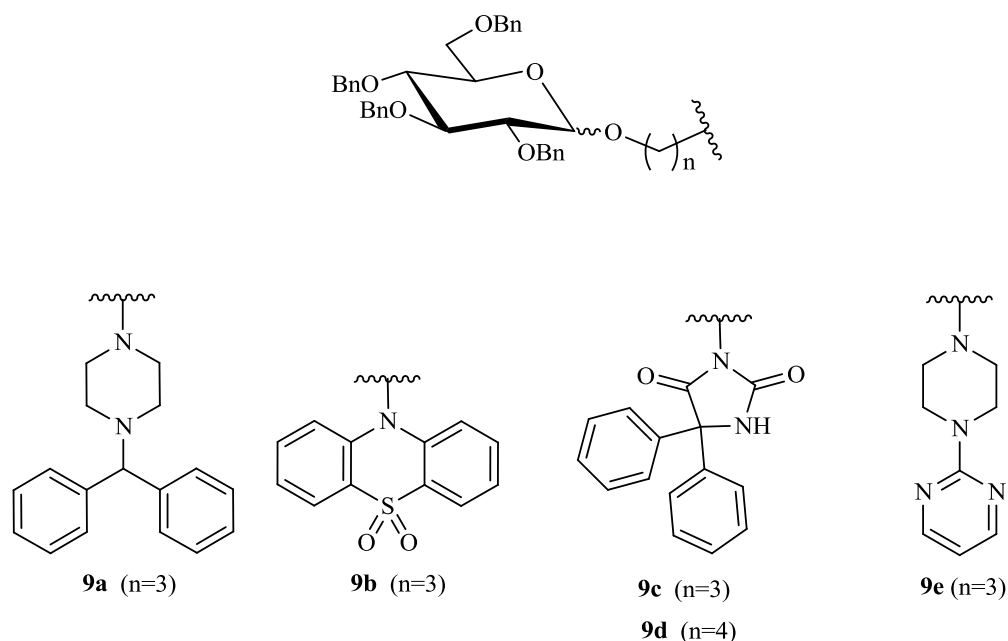


Figure 15: Benzylated glycopyranosidyl alkyl acceptors

These novel benzylated glucopyranosidyl alkyl acceptor derivatives were synthesized depending on the optimization of the method of SADASHIVA et al. [83], the *N*-alkylation reactions were carried out by coupling the protected haloalkyl glucosides with different free secondary amine by using dry potassium carbonate in DMF under Argon. Potassium iodide was added with bromo-, chloroglucosyl intermediates to facilitate the alkylation reaction. *N*-alkylation depends on the reactivity of basic moiety, the leaving groups (table 4) in the glucosides intermediate and temperature. The same procedure was applied to couple other basic moieties with glycopyranosidoyl derivatives like PPZ, DPH and PTO (**9a-e**).

Table 4: Yields of glycosidic intermediates coupled with BHP derivative

R₁	n	X	T (°C)	Time (hours)	Yield %
9a	3	Br	RT	20	65
			80		35
9b	3	Br	RT	24	60
9c	3	Br	RT	20	67
9d	4	Cl	RT	36	55
9e	3	Br	RT	24	55
		Cl	55	20	43

According to these results, we can observe the following:

- If the reaction is carried out at RT, the yields will be increased compared to heating conditions.
- The reaction rate depends strongly on the leaving group in the following order: I > Br > Cl. Also when the length of the alkyl chain increases the yield of coupling reactions decreases according to this arrangement: ethyl > propyl > butyl.

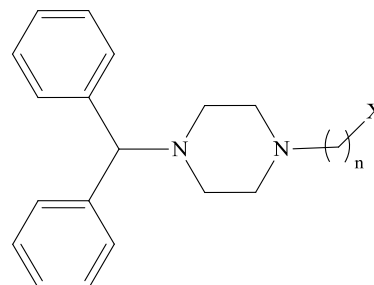
4.4 Method B: Reaction of Glycosyl Donors with Acceptor Intermediates

4.4.1 Basic Moiety and Spacer Groups

N-alkylation [84] occurred between basic moiety compounds and dihaloalkane, haloalkanol to get glycosyl acceptors with general formula like compound **7** (Scheme 2). In this alkylation different halides and alkyl chains were used. In addition different conditions like: temperature, solvents, base and time applied to improve the percentage yield. Piperazine BHP and hydantoin DPH derivatives were synthesized by modifying the method of KOMISSARENKO [85]. Synthesis of substituted BHP with condensing various dihaloalkane, haloalkanol, was succeeded with piperazine derivative. BHP reacted with linkers using acetone, DCM and DMF as solvent with several base to optimize the actual yields of BHP-3-X. Table 5 shows a series of substituted BHP **10a-c** which were synthesized under different conditions to improve the yields of the *N*-alkylation.

Table 5: Reaction conditions used for alkylation of BHP with several spacer groups

	n	X	Conditions	T (°C)	Time (hours)	Yield %
10a	3	Cl	Acetone, 25 % NaOH	rt	22	80
10b	3	Br	Acetone, 25 % NaOH	rt	23	50
			CH ₂ Cl ₂ , NaH	rt	24	20
			CH ₂ Cl ₂ , Et ₃ N	30	1	30
			CH ₂ Cl ₂ , K ₂ CO ₃	rt	24	80
			CH ₂ Cl ₂ , Et ₃ N	rt	24	17
10c	3	OH	CH ₂ Cl ₂ , K ₂ CO ₃	rt	24	60
			DMF, K ₂ CO ₃	60	12	55

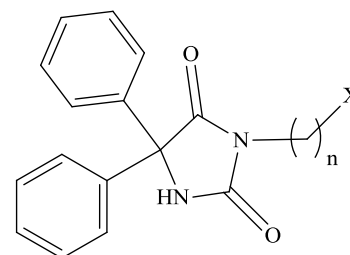


The results showed that the best yields are obtained by using propyl alkane **10a**, **10b** (80 %) with different halide in acetone with sodium hydroxide and K_2CO_3 in DCM respectively, where these conditions are maximized at normal temperature. But poor yields (20 %) were obtained in the case of **10b** with using strong base in DCM as a solvent, due to the equal reactivity of the halide (dibromopropane) and creation of alkylation from both sides. No significant difference was obtained in the case of **10c** using haloalkanol at RT and heating with changing the solvents in the same base K_2CO_3 .

Table 6 shows the effect of other conditions used to prepare DPH derivatives **11a-c**. Hydantoin derivatives were synthesized by modifying the method of KOSASAYAMA [86]. DMF with strong bases and tetra butyl ammonium iodide (TBAI) as a source of iodide were found to perform best with the DPH. In addition, THF and potassium tertiary butoxide ($(CH_3)_3COK$) was used to prepare DPH-3-OH.

Table 6: Reaction conditions used for alkylation of DPH with several spacer groups

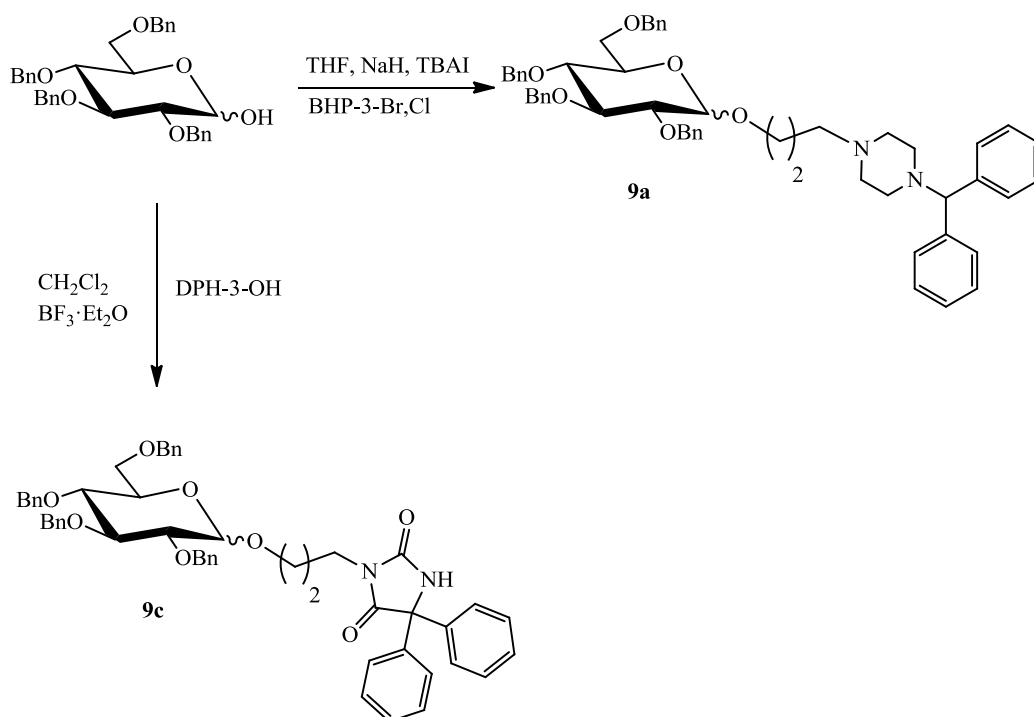
Nr.	n	X	Conditions	T (°C)	Time (hours)	Yield %
11a	3	Br	DMF , NaH , TBAI	rt	0.5	85
				80	0.5	70
11b	3	OH	DMF , NaH , TBAI	rt	1	85
		OH	DMF , NaH , TBAI	100	1	78
		OH	THF , $(CH_3)_3COK$	55	15	80
11c	4	OH	DMF , NaH , TBAI	100	2	50



Based on these results, DPH gave good yields with all types of spacer groups (dihaloalkane and haloalkanol) practically in the case of propyl chain. Additionally using different solvents, temperature and bases had no more effects on the yields. The reactivity of the alkylation of DPH can be arranged according to the yields: propyl > butyl.

4.4.2 Reaction of Basic Moiety Intermediates with Carbohydrate Donors

Glycosidation and substitution reaction were occurred between *N*-alkylated products with fully protected D-glucopyranose (scheme 8). Herein, *N*-halopropyl BHP and DPH have been used as acceptors in this reaction. To find the best method to prepare compound **9a** and **9c**, different conditions were applied according to the types of acceptor. THF, strong base and TBAI were applied in the case of *O*-alkylation of protected sugar and bromo- or chloropropyl BHP to get **9a**.



Scheme 8: Reaction of *N*-alkylated BHP and DPH with sugar

Actually the best yield (table 7) is found with bromo- rather than chloropropyl BHP in RT and 5 hrs (45 % of **9a**). Also a coupling reaction between hydroxypropyl DPH occurred with activating the donor using Lewis acid in DCM to form **9c**, the yield is 53 % at RT.

Table 7: Results of different acceptors with sugar donor

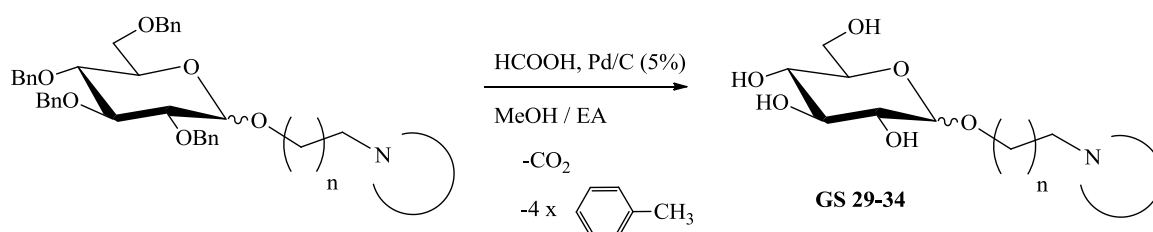
	Glycosyl acceptor	T (°C)	Time (hours)	Yield %
9a	BHP-3-Cl	rt	24	43
	BHP-3-Br	50	12	42
9c	DPH-3-OH	rt	1	45
			2	53

Based on the results mentioned above, BF_3 -Mediated glycosylation is a better method for preparing haloalkyl glycosides, due to give good yields with fully benzylated sugar and it requires a shorter time compared with other methods. In addition the coupling between glycoside intermediate with acceptor is more interesting and gives more yield. For this reasons, method A is more favored to prepare glycopyranosidyl alkyl acceptor than method B.

4.5 Removal of Protecting Groups

Numerous variants methods are described in the literature [87, 88] for removal of benzyl ether protecting groups. A very frequently used method for the removal of benzyl ether protecting groups is palladium-catalyzed hydrogenation under mild conditions, using heterogeneous palladium on carbon (Pd/C) catalyst in the presence of hydrogen gas or hydrogen donors such as formic acid and ammonium formate.

In this experiment, benzylated glucopyranosidyl alkyl acceptors were used with palladium-carbon catalyst or palladium hydroxide 5 and 10 % in different solvents like: dry methanol, isopropanol/methanol and ethanol/ethyl acetate. Using formic acid (Scheme 9), palladium 5 % with 3 bar pressure and dry methanol/ethyl acetate was the succeed conditions. A good conversion could be observed by thin-layer chromatography (TLC). The perhydroxylated compounds were purified by column chromatography with a mixture of chloroform/methanol.



Scheme 9: Removal of benzyl ether protecting groups

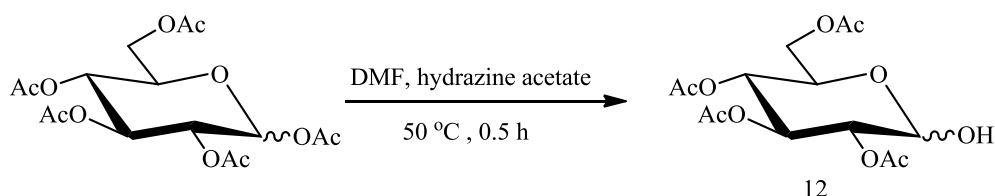
Acetyl protecting group was used in order to improve the yields of perhydroxylated compounds.

4.6 Acetyl Protecting Group

The acetyl protecting groups were used in order to study the reactivity of glycosyl donors as a result of employed protecting groups and comparing with benzylated results.

4.6.1 Synthesis of Glycosyl Acetates

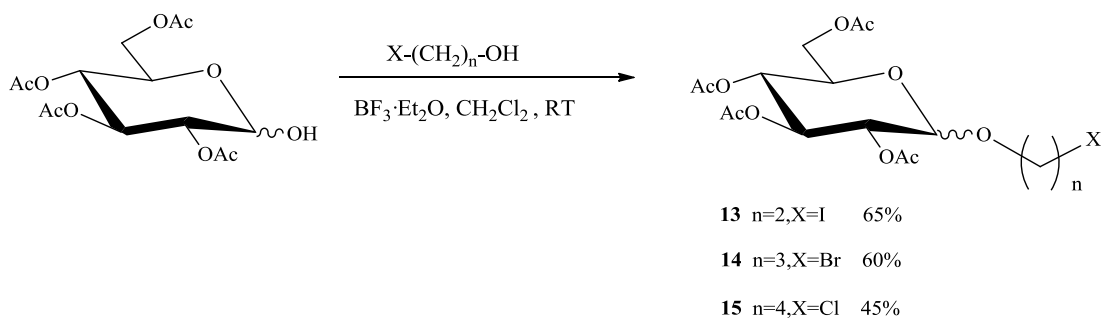
The first step within the synthesis of acetylated glycopyranosidyl alkyl acceptor was the glycosylation of inexpensive fully acetylated glucose with haloalkanol using method A, which was applied with benzylated sugar. Initially the anomeric acetyl group of pentaacetyl glucose was removed chemoselectively with hydrazine acetate in dry DMF by heating at 50 °C (Scheme 10) and stirring under inert atmosphere (Ar) for 3hrs [89, 90]. After extraction and washing the yield was 95 % of 2,3,4,6-tetra-*O*-acetyl-D-glucopyranose **12**, could be obtained as the glycosyl donor.



Scheme 10: synthesis of acetylated glucopyranose

4.6.2 Synthesis of Acetylated Glycoside Intermediates

The hemiacetal reacted with haloalkanol (Scheme 11) in dry DCM under inert conditions and 1 ml of $\text{BF}_3 \cdot \text{Et}_2\text{O}$ was added and the solution stirred for certain time controlled by TLC. Following extraction, washing, drying with Na_2SO_4 anhydrous and the solvent was removed in a vacuum. The crude product was purified by flash chromatography using chloroform/methanol mixture. The yields of glucoside intermediates **13-15** depend on the nature of haloalkanol (X) and the alkyl chain length (n).

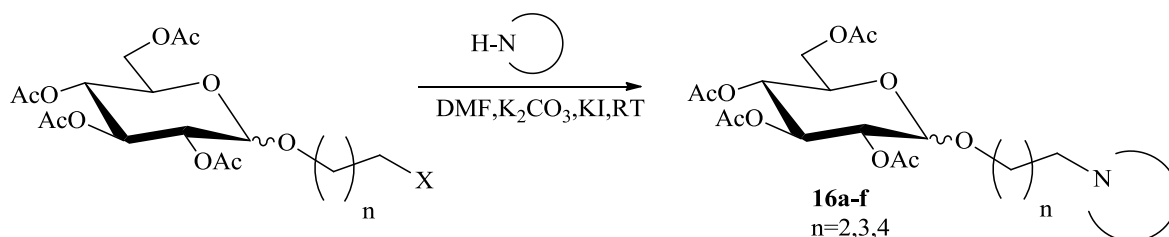


Scheme 11: synthesis of acetylated glycoside intermediates

Additionally, the glycosylation of fully acetylated sugar with 3-chloro-1-propanol was succeed by sonication [81].

4.6.3 Reaction of Glycosyl Acceptors with Donor

The acetylated glucoside intermediates were coupled with different acceptors in DMF by using K_2CO_3 , KI at RT (Scheme 12). The time requires for this step was different according to the length of alkyl chain, type of acceptors and nature of halide used.



Scheme 12: Synthesis of acetylated glycopyranosidyl alkyl acceptors

Glucoside butyl chloride required heating to get more coupling yield (poor leaving group). Extraction using ethyl acetate, washing with water, brine and evaporating the solvent were used to get the products (table 8), purified by column chromatography with chloroform-ethyl acetate mixture.

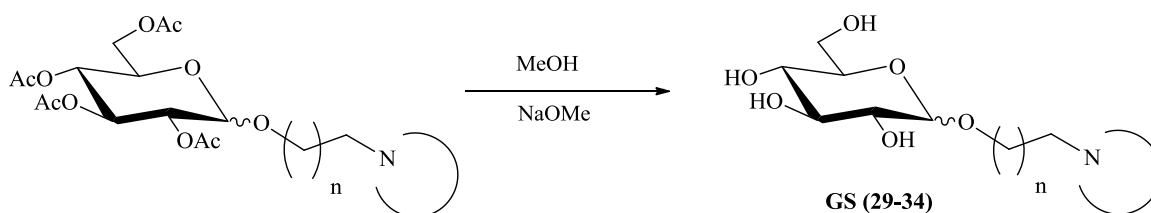
Table 8: Results of coupling acetylated glycoside intermediates with different acceptors

	n	HN-	Yield%
16a	2	DPH	88
16b	3	DPH	75
16c	3	PPS	73
16d	3	BHP	68
16e	3	PTA	65
16f	4	DPH	55

4.6.4 Synthesis of Perhydroxylated Compounds

Finally, the acetyl groups were deprotected under ZEMPLÉN conditions (Scheme 13). Peracetylated compounds were dissolved in dry methanol and the deacetylation was affected by adding in portions a catalytic amount of sodium methoxide. The reaction was monitored by TLC. Stirred under Ar, the solvent removed and

the residue was purified by a silica gel column using chloroform/methanol mixture to get the final compounds **GS (29-34)** as a mixture of α - and β -anomers (table 9).



Scheme 13: Synthesis of perhydroxylated final compounds GS (29-34)

From the result, we found that the final compounds have a mixture of two anomers α/β . The ratio of α increased with increasing the alkyl chain (**GS29-31**) with the same acceptors (DPH). For the same alkyl chain ($n=3$), the α -anomers was the most ratio with PPZ (**GS 33**) and less favored with other acceptors, due to the nature of this receptor which sterically less hindered.

Table 9: Results of deacetylated reaction with different glycoside intermediates

	n	N-	Yield %	$\alpha : \beta$
GS29	2	DPH	86	13:87
GS30	3	DPH	82	25:75
GS31	4	DPH	80	31:69
GS32	3	BHP	84	30:70
GS33	3	PPZ	82	79:21
GS34	3	PTA	79	48:52

The acetyl and benzyl groups were used to prepare the final compounds, the effect of these groups were clear. The acetyl compounds were placate, simply deacetylated and purified with high purity compared with the benzylated compounds.

4.7 Click Chemistry Background and Synthesis

The term click chemistry was introduced by K. BARRY SHARPLESS [91], and is the reaction between azide and alkyne yielding five membered heterocycle. The click reaction refers to reaction which is characterized by including broad applicability, functional group tolerance, stereospecific, high purity, shorter reaction time and high in yield [92]. These advantages should be exploited in this work for derivatization of potential Myt1 kinase inhibitors (Fig.16).

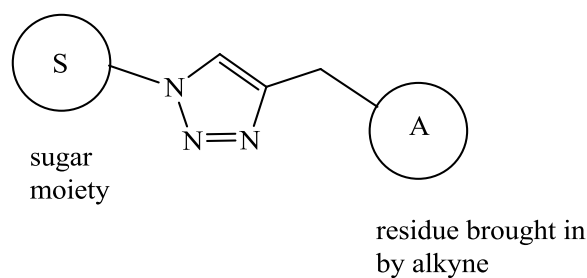
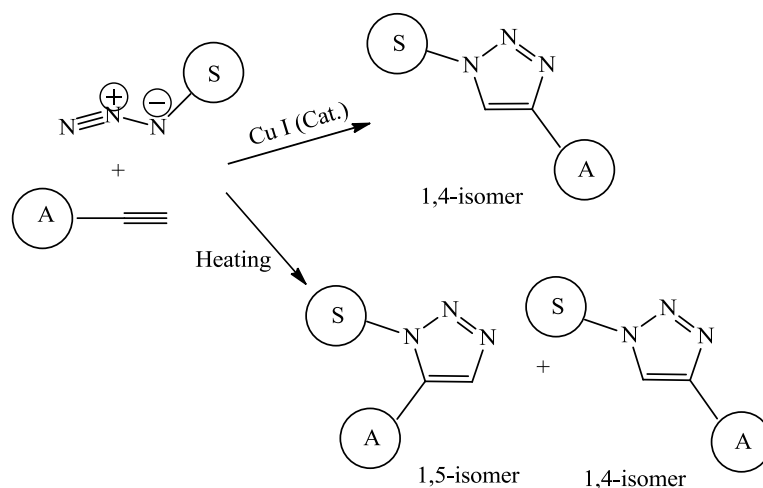


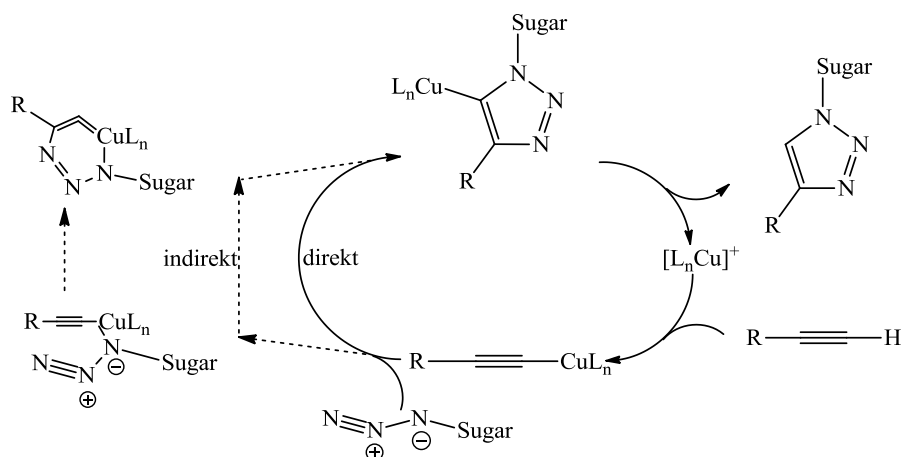
Figure 16: General structure of click compounds

The HUISGEN 1,3-dipolar cycloaddition reaction describes a cycloaddition reaction between an alkyne and an azide as dipoles to form a 1,3-triazole and was reported by HUISGEN et al. in 1965 [93]. This reaction is often referred to as the “ideal” click reaction and has the properties of being quantitative, insensitive, robust, and general. Therefore, it gained a boost of interest after the copper catalyzed version was introduced by MELDAL et al. [94, 95] and SHARPLESS et al. in 2002 [96]. HUISGEN reaction Cu (I)-catalyzed azide–alkyne cycloaddition (CuAAC) has successfully fulfilled the requirements of click chemistry as prescribed by SHARPLESS and within the past few years has become a premier component of the click chemistry paradigm. CuAAC between a terminal alkyne and an azide resulted in a large reduction in reaction time and allows the reaction to occur at RT with high yields and regioselective formation of only the 1,4-triazoles (Scheme 14), but the reaction generates a mixture of 1,4- and 1,5-disubstituted 1,2,3-triazoles regioisomers with using non-catalysed process under thermal conditions (temperature~120°C). The HUISGEN 1,3-dipolar cycloaddition was found to be compatible with various protecting groups such as acetyl and benzyl groups, both used in carbohydrate synthesis [97].



Scheme 14: CuAAC at elevated temperature or the addition of Cu (I) ions [97]

The reaction mechanism for CuAAC was proposed by SHARPLESS et al. and there was no fully elucidating mechanism until now. Scheme 15 shows the proposed catalytic cycle for coupling azido-sugar and alkyne R, which involves several postulated and transient Cu (I)-acetylide complexes, it first forms a π -complex between the Cu (I) metal and the terminal alkyne before the proton is substituted by the Cu (I) ion [92, 96].

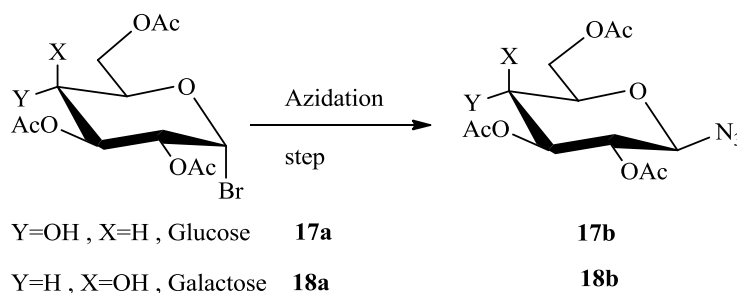


Scheme 15: Proposed catalytic cycle for azide-alkyne coupling [97]

Although a terminal alkyne having a pK_a value of ~ 25 in aqueous system, this is lowered by the initial formation of the π complex at 10 units, this allows the substitution of the proton in the aqueous system in the first place. Whether arising in the course, other intermediate steps or directly to the triazole is formed and still unclear. Calculation of F.HIMO et al. [97] appeared that the stepwise mechanism involving an unusual six-membered Cu (III)-heterocycles, is energetically more favorable than the concerted mechanism and should therefore preferably take place.

4.7.1 Synthesis of the Azide Moieties

Azidoglycoside **17b** and **18b** were formed by treatment of a widely used α -acetobromoglycoside with NaN_3 in dry DMF at RT as β -anomers in good yield (Scheme 16). This azidation step was applied according to the method of OGAWA et al. [98]. These compounds and **19** (6-Azido-6-deoxy- α -methylglucopyranosids, see Scheme 17) coupled with several terminal alkyne moieties in order to prepare a library of glyco-triazol at positions C-1 and C-6.



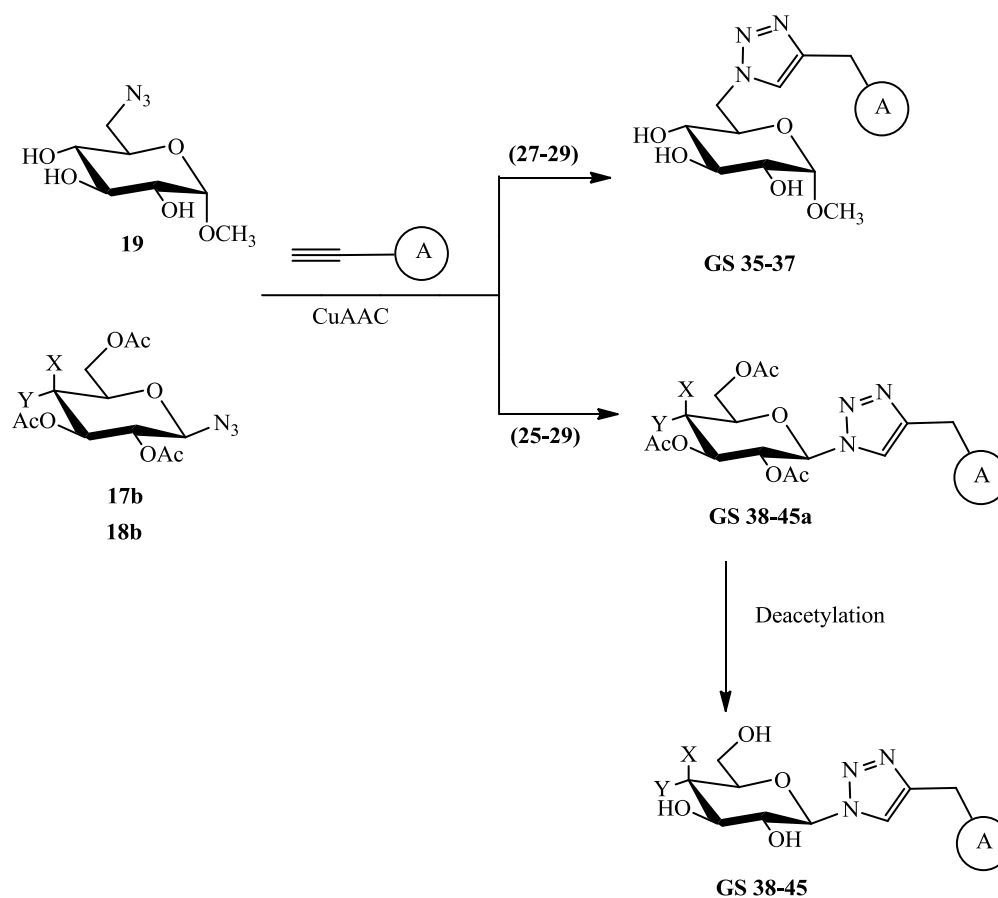
Scheme 16: synthesis of β -azidoglycoside at the position C-1

4.7.2 Synthesis of the Acetylene Derivatives

Since a number of required alkyne was not commercially available, we have been looking for a feasible pathway for alkylation of existing or commercially available scaffolds. Alkylation of *N*-3 of the DPH (hydantoin) was prepared by modifying the method of USIFOH [99]. The optimized method has been successfully applied to combine between DPH, BHP and PPZ (*N*-base bodies) and propargyl bromide solution (80 wt. % in toluene) which obtained DIH (**27**), BIP (**28**) and PPI (**29**) respectively. In addition, BIF (**25**), DIB (**26**) was used (Scheme 17). The alkylation of base body should basically run as a nucleophilic substitution between a haloalkane and a nitrogen atom. Potassium carbonate is used as base for deprotonation of the hydantoin and piperazine nitrogen in the presence propargyl bromide in DMF as solvent, then substituted a halogen atom of the reactant. All three *N*-alkynes were synthesized successfully at RT with good yields.

4.7.3 Click Reaction

This part focus on the chemical synthesis of a new class of glyco-triazole at position C-1 (Scheme 17, **GS38-45**) starting from glucose and galactose with azido group at C-1 position **17b**, **18b** respectively. In addition, azido-glycoside **19** was used to prepare glyco-triazoles at the C-6 position. Coupling of such azides to the terminal alkynes (**25-29**) with structurally diverse using CuAAC reactions gave a range of glyco-triazoles derivatives at the C-1 (**GS38-45a**) as acetylated compounds at C-1 and unprotected glyco-triazoles at position C-6 (**GS35-37**).



Scheme 17: Synthesis of perhydroxylated glyco-triazole compounds

Actually, there are several salts which contain Cu (I), for example CuI and CuOTf.C₆H₆ can be employed but sometimes generate unwanted diacetylene and bis-triazole by-products. Additionally the reaction must be run with acetonitrile as a co-solvent and requires a nitrogen base. Cu (I) can be introduced by the reduction of CuSO₄·5H₂O by sodium ascorbate. The advantage of this method is that Cu (II) salts are chemically stable, cleaner and cheaper than Cu (I) compounds [96, 100]. This catalyst mixture was added to azide and alkyne in a 2 ml Eppendorf tube, in 1 ml of dry DMF as solvent, excellent solvent

properties were shown to work in concentrated. The reaction was conducted at 70 °C for 1 h in an ultrasonic bath. After completion of the reaction, the DMF was removed from the mixture, which was practically carried out by co-evaporation with toluene. Then the remaining reactants and catalyst residues are separated by a chromatographic purification [101].

In the final step, the acetate protecting groups were removed (deacetylation step) from substituted triazole sugars with a catalytic amount of NaOMe in dry MeOH which afforded the library of perhydroxylated triazole glucopyranoside and galactopyranosid (**GS38-45**) with complete regioselectivity (β -anomers) and high yields (more than 90 %) at position C-1. In contrast, the yield of unprotected 6-azido-glucoside was not as high as protected glucoside and galactoside (60-75 %). So that, using protected sugar to couple with alkyne is much better than unprotected, due to high yields, ease of purification, less side product and a decrease in the copper ions in the final compounds. Therefore it is a very reliable and simple system that makes this the preferable route.

5 Discussion and Summary

The final compounds were synthesized for the first time as promising agents to inhibit Myt1 kinase as small molecule inhibitors, which contain a carbohydrate core, connected with linkers and *N*-containing moieties at position C-1. In addition, gluco- and galacto-azides were connected with different alkyne moieties at position C-6, and C-1 to determine the described glyco-triazoles. It might be systematically varied different groups (Fig.17) of the starting compounds and the effect will be investigated in future studies.

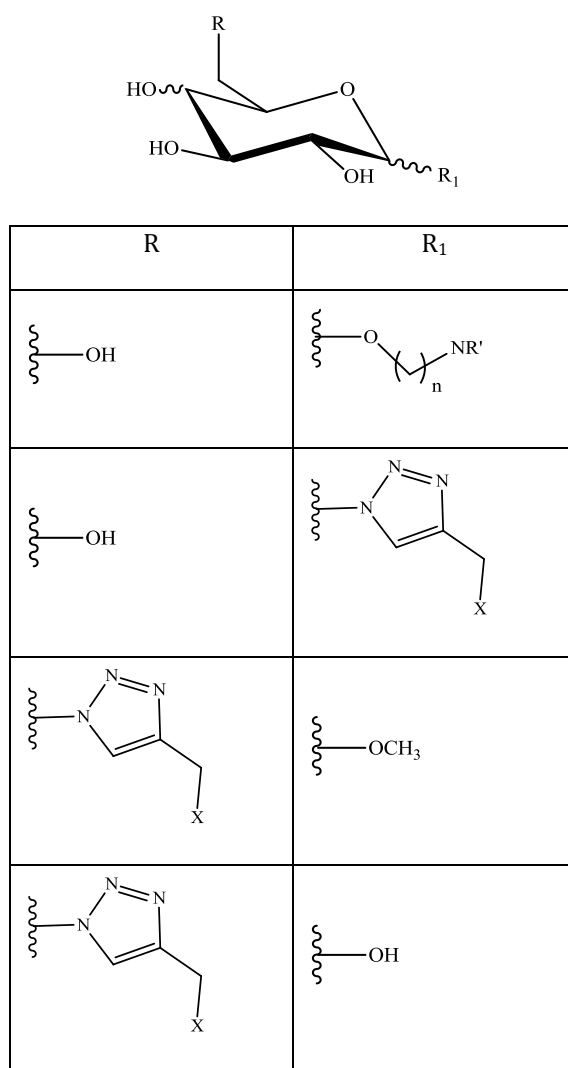


Fig.17: General structure of the final compounds, R' = Acceptors, n = Spacer groups, X = Basic moieties

We also carried out docking studies on these compounds looking for the most potent compounds allowing further insights into the inhibitor interaction of this kinase. Based on the staurosporine, which was supposed to inhibit Myt1 kinase, the docked results showed

that most of these compounds have inhibition more than staurosporine, according to the gold score and corrected gold score values.

Molecular docking indicated that selectivity towards the Myt1 kinase might be achieved by introducing bulky hydrophobic moieties (phenyl, biphenyl) with linear alkyl chain at C-1 and glyco-triazoles with several alkyne components at C-1 and C-6. Therefore, we found that the compound with butyl chain with DPH (**GS31**) is more interesting than other short chains and may be sufficiently large to fill up the hydrophobic pocket. The most interesting one with DPH was **GS37**, which has been scored highest and shows a probable good binding mode. These results showed that the DPH is more favorable than other acceptors according to scores and values. Many of the other triazole final compounds also showed good binding with ATP-binding site of Myt1 kinase, better than staurosporine itself such as **GS40**, **GS44** and **GS45**.

In total, 17 compounds were successfully synthesized and isolated. These compounds were prepared in high yields, 6 of these final compounds represent glucopyranosidyl alkyl acceptors (**GS29-34**) with different alkyl chain and acceptors system. Furthermore, 11 of the final compounds afford a series of gluco-triazoles at C-1 (**GS38-41**) and galacto-triazoles (**GS42-45**) at the same position. 1-Methyl glyco-triazoles (**GS35-37**) were also prepared but with triazole components at C-6 position.

We used a protection group strategy for synthesis of glycoside intermediates via acid catalyzed methods, and then coupled with acceptors. This pathway was succeeded remarkably better than preparing acceptor intermediates first and then coupled with a glycosyl donor. As expected removal of the protection groups worked well affording the final compounds with good yields.

For the triazole compounds, we have synthesized a small library of substrate analogues based on 1,4-disubstituted 1,2,3-triazole derivatives of glucose and galactose, modified at either the C-1 or C-6 positions. This was achieved by coupling the azide sugars with several structurally diverse terminal alkynes by using the copper (I)-catalyzed alkyne-azide cycloaddition (CuAAC) reaction, giving targets compounds in good yields and with complete regioselectivity. The synthetic route adapted to the final compounds is not known from the literature and by preventing hydroxyl protecting groups (**GS35-37**), it was significantly simplified.

We have first positive results from a binding assay; two glyco-triazole compounds were noticed in the binding assay by interaction with Myt1 kinase [61] and that is why the further development of this structure is very interesting. DAVIS et al. [102] had described the influence of how difficult it is to inhibit Myt1. Only 3 out of 72 highly optimized known kinase inhibitors (Dasatinib, EKB-596, and PD173074) showed an effect. All other compounds showed no effect, including staurosporine. According to this report, Myt1 is among the hardest to affect kinases. That is why our new compounds are very interesting as new lead structures.

Future exploration will require the biological activity of these new potential ATP-competitive compounds. The research can be continued to modify the carbohydrate scaffold, spacer group, acceptors and alkyne components for development of structure activity relationships.

6 Experimental Section

6.1 Materials and Methods

6.1.1 Chemicals and Solvents

All solvents are received from the Institute of Pharmacy, Martin-Luther-University Halle-Wittenberg, dried and distilled by standard procedures [103]. Chemicals were purchased from commercial suppliers and were used as received without further purification.

Chemicals	Company
Bortrifluorid-diethylether-complex	Aldrich
(S)-1,2-Isopropylidenglycerol	Aldrich
Sodium azide	Aldrich
Sodium hydride	Aldrich
Potassium tert-butoxide	Aldrich
Palladium hydroxide	Aldrich
Trityl chloride	Aldrich
Benzyl chloride	Fluka
3-Bromo-1-propanol, 97 %	Aldrich
1,4-Dibromobutane, 99 %	Aldrich
2-Iodoethanol, 99 %	Aldrich
1,3-Dibromopropane, 99 %	Aldrich
4-Bromo-1-butanol	Aldrich
3-Chloro-1-propanol, 98 %	Aldrich
1-Bromo-4-chlorobutane, 99 %	Aldrich
Trichloroacetonitrile	Aldrich
Copper(II) sulfate pentahydrate	Aldrich
Sodium-L-ascorbate	Aldrich
Propargyl bromide solution 80 % in toluene	Fluka

5,5-Diphenyl-2,4-imidazolidinedione	Sigma
1-Benzhydrylpiperazine, 97 %	Aldrich
1-(2-Pyrimidyl)piperazine	Aldrich
Methyl- α -D-glucopyranoside	Aldrich
1-(2-Pyrimidyl)piperazine 98 %	Aldrich
2,3,4,6-Tetra- <i>O</i> -benzyl-D-glucopyranose	Sigma
Acetobromo- α -D-galactose, 93 %	Sigma
Acetobromo- α -D-glucose, 95 %	Sigma
Methanesulfonyl chloride,	Aldrich
Tetrabutylammonium iodide, 98 %	Aldrich

6.1.2 NMR Spectroscopy

$^1\text{H-NMR}$ spectra were obtained with a Varian Gemini 2000 with 400 MHz working frequency for $^1\text{H-NMR}$ and Varian Unity Inova 500 spectrometer operating at 500 MHz for the $^1\text{H-NMR}$ and H-H-Cosy spectra. $^1\text{H-NMR}$ spectra were referenced to $\delta_{\text{H}}=7.24$ ppm for deuterated CDCl_3 and $\delta_{\text{H}}=4.87$ ppm for deuterated CD_3OD .

6.1.3 Mass Spectrometry

All the samples were measured using mass spectrometer operating in ESI mode. The samples were dissolved in a suitable solvent and injected using a syringe pump. The ionization was performed at 4.5 kV in the electrospray positive and negative mode. The inclusion of the spectra was performed with a LCQ Classic mass spectrometer from Thermo Finnigan. The device features a heated capillary (200 °C) and has a flow rate of 20 $\mu\text{l}/\text{min}$.

6.1.4 Melting Points

The determination of the melting range was performed on a Boetius hot stage microscope. The melting ranges are uncorrected values. The melting point (M.p.) was obtained for the solid compounds.

6.1.5 Chromatography

TLC

Reactions were monitored by thin layer chromatography (TLC) on pre-coated silica gel plates from Merck (E. Merck 60 F₂₅₄). The substance mixture was applied on the plate via a capillary tube and developed in separation chamber. Few drops of TEA were added to the mobile phases, which were standard eluent of the following composition:

	Eluent (EL)	Composition (v: v)
EL 1	Chloroform - methanol	50:50
EL 2	Chloroform - methanol	90:10
EL 3	Chloroform - ethyl acetate	90:10
EL 4	Acetone - heptane	35:15
EL 5	Acetonitrile - water	99:1
EL6	Chloroform - methanol	70:30
EL7	Chloroform - methanol	80:20

The compounds were detected visually under UV light at first at a wavelength of 254 nm, followed by detection of sugars with dipping in a solution of thymol-sulfuric acid (0.5 g of thymol and 5 ml of conc. H₂SO₄ in 95 ml of ethanol) and heating at 130 °C for 10 minutes, so sugars can be detected as pink spots.

Column Chromatography

Non pressure chromatography was performed on silica gel 60 from Merck with a particle size from 0.063 to 200 μ m, silica gel 60 from 0.040 to 0.063 mm for flash chromatography.

6.2 Synthetic Procedures

6.2.1 Synthesis of Benzylated Glycoside Intermediates

Synthesis of the compounds **3** was achieved by the published method and experimental data corresponding with the literature [60]. The reported yields were the best yields obtained from the respective reaction.

The glycoside compounds (**4a-d**) were synthesized by three methods, the same amounts of starting material was used. For the reaction conditions, see table 2 and 3.

Method A:

Trichloroacetimidate Method

The synthesis was carried out according to R.R. SCHMIDT et al. [28]. (0.10 g, 0.18 mmol of benzylated glucopyranose was dissolved in anhydrous DCM (5 ml) with stirring under Ar, and 0.07 g, 3.04 mmol of NaH (60 % oil suspension) and 1 ml of trichloroacetonitrile were added. The mixture was stirred at RT for 2 hrs and then halo alcohol (1.1 eq) or (S)-1,2-isopropylidenglycerol (**8a,b**) was added. Cooling to -20 °C, then BF₃·Et₂O (1 ml) was added. The mixture was stirred for further 2 hrs, washed with H₂O and extracted with DCM, filtered, dried over Na₂SO₄, and concentrated. The crude material obtained was purified by column chromatography on silica using heptane/ether or chloroform/ethyl acetate gradients with increasing polarity, concentrated to yield compounds as pale yellow oil.

Method B:

Borontrifluoride Etherate Method

These compounds were synthesized by the modified published method [80, 81]. To a solution of protected sugar in DCM (5 ml) was added at RT one portion of halo alcohol (1.1 eq) or (S)-1,2-isopropylidenglycerol (**8a,b**). The solution was stirred for 10 min under Ar, and then BF₃·Et₂O (1 ml) was added. The resulting solution was stirred for a certain time monitored by TLC. For neutralization eq TEA was added and washed with water, the organic layer was dried over Na₂SO₄, filtered and concentrated. Purification was accomplished by column chromatography using chloroform/ethyl acetate.

Method C:

PTC Method

General procedure for the synthesis of substituted glycosides, which were synthesized by the modified published method [82]. The glucopyranose was dissolved in DCM (5 ml) and washed with Ar, stirred for 10 min, and 0.07 g, 3.04 mmol of NaH (60 % oil suspension) was added and stirred for 15 min, bromo alcohol (1.1 eq) was added, stirred for 20 min. One portion of THF (5 ml) was added, stirred for a certain time controlled by TLC to obtain more product. The mixture was washed with H₂O, dried over Na₂SO₄ and concentrated under reduced pressure. The residue was purified by column chromatography (chloroform/ethyl acetate).

1-*O*-(2-Iodoethyl)-2,3,4,6-tetra-*O*-benzyl-D-glucopyranoside (4a)

Empirical Formula: C₃₆H₃₉IO₆

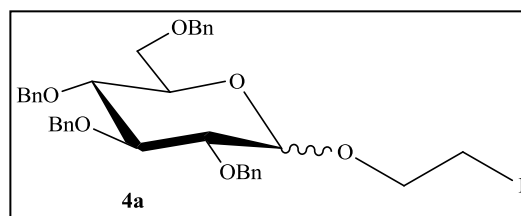
Formula Weight: 694.59 g/mol

Mass spectrum: M+Na

R_f (EL 3): 0.72

Method A: 65 %

Method B: 84 %



¹H- NMR (500 MHz, CDCl₃):

δ 7.37– 7.08 (m, 20H, *H*-Ph), 5.03 – 4.92 (m, 1H, -CH₂-Ph), 4.87 – 4.38 (m, 9H, -CH₂-Ph, *H*-1), 3.96 (t, J = 9.3 Hz, 1H, *H*-3), 3.90 – 3.40 (m, 7H, *H*-6', *H*-6, *H*-4, *H*-2, -CH₂-O-, *H*-5), 3.37 – 3.23 (m, 2H, -CH₂-I).

1-*O*-(3-Bromopropyl)-2,3,4,6-tetra-*O*-benzyl-D-glucopyranoside (4b)

Empirical Formula: C₃₇H₄₁BrO₆

Formula Weight: 661.62 g/mol

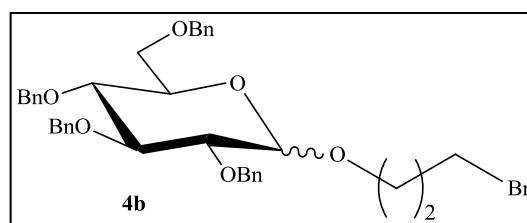
Mass spectrum: M+Na

R_f (EL 3): 0.74

Method A: 63 %

Method B: 80 %

Method C: 75 %



¹H- NMR (500 MHz, CDCl₃):

δ 7.46 – 6.89 (m, 20H, *H*-Ph), 5.01 – 4.18 (m, 9H, -CH₂-Ph, *H*-1), 4.08 – 3.16 (m, 10H, *H*-5, *H*-3, *H*-6', *H*-6, *H*-4, *H*-2, -CH₂-O-, -CH₂-Br), 2.21 – 1.91 (m, 2H, -CH₂-).

1-*O*-(4-Chlorobutyl)-2,3,4,6-tetra-*O*-benzyl-D-glucopyranoside (4c)

Empirical Formula: C₃₈H₄₃ClO₆

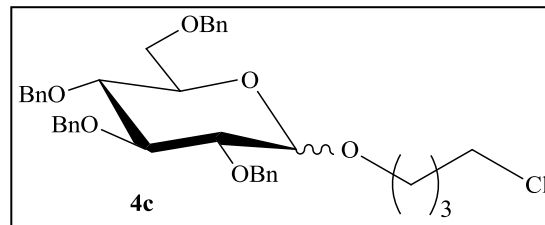
Formula Weight: 631.19 g/mol

Mass spectrum: M+Na

R_f (EL 3): 0.75

Method A: 52 %

Method B: 60 %



H- NMR (500 MHz, CDCl₃):

δ 7.31 – 7.02 (m, 20H, *H*-Ph), 4.94 – 4.36 (m, 8H, -CH₂-Ph), 4.34 – 4.26 (m, 1H, *H*-1), 4.10 – 3.79 (m, 2H, *H*-5, -CH₂-O-), 3.70 – 3.43 (m, 7H, -CH₂-O-, *H*-3, *H*-4, *H*-6', *H*-6, -CH₂-Cl), 3.42 – 3.31 (m, 1H, *H*-2), 1.87 – 1.63 (m, 4H, -CH₂-CH₂-).

1-*O*-(4-Bromobutyl)-2,3,4,6-tetra-*O*-benzyl-D-glucopyranoside (4d)

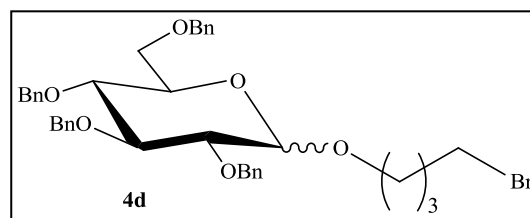
Empirical Formula: C₃₈H₄₃BrO₆

Formula Weight: 675.64 g/mol

Mass spectrum: M+Na

R_f (EL 3): 0,76

Method C: 75 %



¹H- NMR (400 MHz, CDCl₃):

δ 7.45 – 7.02 (m, 20H, *H*-Ph), 4.98 – 4.43 (m, 8H, -CH₂-Ph), 4.36 – 4.31 (m, 1H, *H*-1), 4.00 – 3.89 (m, 1H, *H*-5), 3.88 – 3.77 (m, 1H, *H*-3), 3.76 – 3.47 (m, 5H, -CH₂-O-, *H*-6', *H*-6, *H*-4), 3.46 – 3.32 (m, 3H, *H*-2, -CH₂-Br), 1.97 – 1.87 (m, 2H, -CH₂-), 1.81 – 1.70 (m, 2H, -CH₂-).

3-*O*-(6-Azido-2,3,4-tri-*O*-benzyl-D-glucosyl)-1,2-iso-propylidene-*sn*-glycerol (8a)

This compound was synthesized as published previously [60] and obtained as a white waxy substance.

Empirical Formula: C₃₃H₃₉N₃O₇

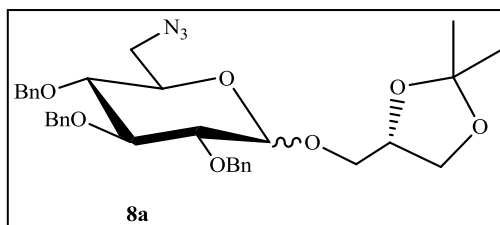
Formula Weight: 589.67 g/mol

Mass spectrum: M+Na

R_f (EL 3): 0.5

Method A: 50 %

Method B: 70 %



3-*O*-(2, 3, 4-Tetra-*O*-benzyl-D-glucosyl)-1,2-isopropylidene-*sn*-glycerol (8b)

Empirical Formula: C₄₀H₄₆O₈

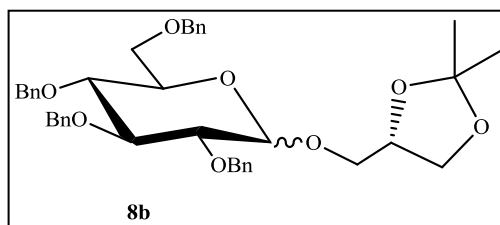
Formula Weight: 654.78 g/mol

Mass spectrum: M+Na

R_f (EL 3): 0.45

Method A: 48 %

Method B: 60 %



¹H- NMR (400 MHz, CDCl₃):

δ 7.42 – 7.07 (m, 20H, **H-Ph**), 5.01 – 4.49 (m, 8H, -CH₂-Ph), 4.49 – 4.41 (m, 1H, **H-1**), 4.38 – 4.24 (m, 1H, **sn-2**), 4.05 (dd, *J* = 8.2, 6.2 Hz, 1H, **sn-1**), 4.00 – 3.91 (m, 1H, **H-3**), 3.87 (dd, *J* = 10.1, 5.6 Hz, 1H, **sn-3**), 3.84 – 3.75 (m, 1H, **H-5**), 3.73 (dd, *J* = 8.3, 6.1 Hz, 1H, **sn-1'**), 3.67 – 3.58 (m, 1H, **sn-3'**), 3.57 – 3.50 (m, 1H, **H-4**), 3.49 – 3.26 (m, 6H, **H-2**), 1.40, 1.35, (2s, 6H, 2 x -CH₃).

6.2.2 Synthesis of Benzylated Glycopyranosidyl Alkyl Acceptors

These compounds were synthesized by the modified published method [83]. The mixture of the intermediate **4a-f** (0.20 g, 1 eq) and K_2CO_3 (3 eq), KI (1 eq) - not used with Iodoalkyl glycoside, in distilled DMF (5 ml) was washed with Ar, to the mixture a basic moiety was added (1.1 eq), stirred at RT for certain time (table 4 and 8). The reaction was periodically monitored by TLC. Ethyl acetate was added to the mixture, washed 2 times with 30 ml of H_2O , brine. The mixture was then extracted 3 times with 30 ml of ethyl acetate, the combined ethyl acetate phases were washed with water, brine, dried over Na_2SO_4 filtered and concentrated in vacuo. The residue was purified by column chromatography (chloroform/ethyl acetate) to give **9a-e** as colorless oil.

1-(Diphenylmethyl)-4-[3-(2,3,4,6-tetra-*O*-benzyl-D-glucopyranosidyl)propyl]piperazine (**9a**)

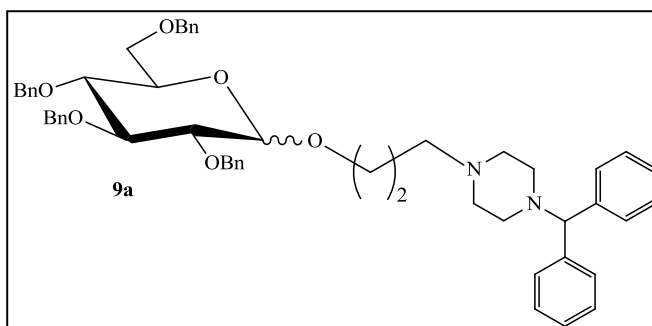
Empirical Formula: $C_{54}H_{60}N_2O_6$

Formula Weight: 833.06 g/mol

Mass spectrum: $M+Na$, $M+H$

R_f (EL 2): 0.82

Yield: 65 %



1H - NMR (500 MHz, $CDCl_3$):

δ 7.44 – 7.05 (m, 30H, *H*-Ph), 4.99 – 4.40 (m, 8H, $-CH_2$ -Ph), 4.35 (m, 1H, *H*-1), 4.18 (s, 1H, $-CH-$), 4.01 – 3.89 (m, 1H, $-CH_2$ -O-), 3.81 – 3.48 (m, 5H, $-CH_2$ -O-, *H*-3, *H*-4, *H*-6', *H*-6), 3.46 – 3.34 (m, 2H, *H*-2, *H*-5), 2.54 – 2.20 (m, 10H, $-CH_2$ -N-, 4 x $-CH_2$ -piperazine), 1.89 – 1.71 (m, 2H, $-CH_2$ -).

10-[3-(2,3,4,6-Tetra-*O*-benzyl-D-glucoopyranosidyl)propyl]-10*H*-phenothiazine-5,5-dioxide (9b)

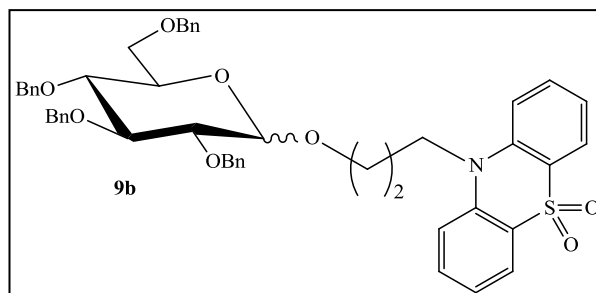
Empirical Formula: C₄₉H₄₉NO₈S

Formula Weight: 811.98 g/mol

Mass spectrum: M+Na

R_f (EL 3): 0.66

Yield: 60 %



¹H- NMR (500 MHz, CDCl₃):

δ 8.15 – 7.96 (m, 2H, *H*-4', *H*-6'), 7.56 – 7.07 (m, 26H, *H*-Ph), 4.95 – 4.74 (m, 4H, -CH₂-Ph), 4.59 – 4.41 (m, 4H, -CH₂-Ph), 4.39 – 4.31 (m, 1H, *H*-1), 4.29 – 4.20 (m, 2H, -CH₂-O), 4.06 – 3.96 (m, 1H, *H*-5), 3.84 (t, J = 9.5 Hz, 1H, *H*-3), 3.75 – 3.57 (m, 4H, *H*-6', *H*-6, -CH₂-NR), 3.53 – 3.35 (m, 2H, *H*-2, *H*-4), 2.24 – 2.14 (m, 2H, -CH₂-).

3-[3-(2,3,4,6-Tetra-*O*-benzyl-D-glucoopyranosidyl)propyl]-5,5-diphenyl-imidazolidine-2,4-dione (9c)

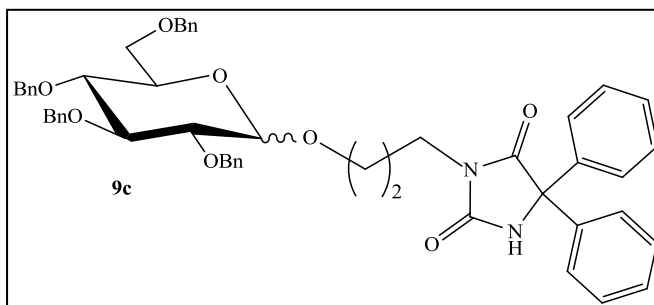
Empirical Formula: C₅₂H₅₂N₂O₈

Formula Weight: 832.97 g/mol

Mass spectrum: M+Na, M-H

R_f (EL 3): 0.45

Yield: 67 %



¹H- NMR (500 MHz, CDCl₃):

δ 7.40 – 7.03 (m, 30H, *H*-Ph), 6.31 (s, 1H, *H*-NR), 5.00 – 4.30 (m, 8H, -CH₂-Ph), 4.29 – 4.18 (m, 1H, *H*-1), 4.01 – 3.82 (m, 2H, *H*-5, *H*-3), 3.77 – 3.22 (m, 8H, *H*-4, *H*-6', *H*-6, -CH₂-O-, *H*-2, -CH₂-NR), 2.00 – 1.85 (m, 2H, -CH₂-).

3-[4-(2,3,4,6-Tetra-*O*-benzyl-D-glucopyranosidyl)butyl]-5,5-diphenyl-imidazolidine-2,4-dione (9d)

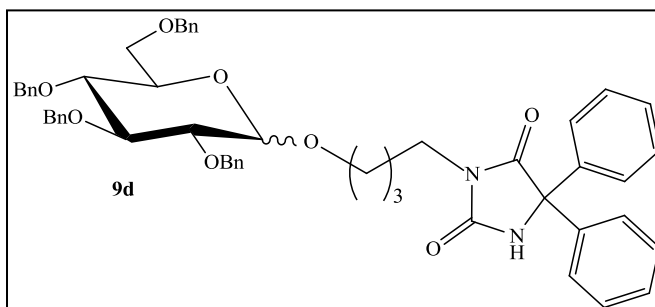
Empirical Formula: C₅₃H₅₄N₂O₈

Formula Weight: 847.0 g/mol

Mass spectrum: M+Na, M-H

R_f (EL 3): 0.45

Yield: 55 %



¹H- NMR (400 MHz, CDCl₃):

δ 7.35 – 7.02 (m, 30H, **H**-Ph), 6.20 (s, 1H, **H**-NR), 4.83 (t, J = 11.0 Hz, 2H, -**CH**₂-Ph), 4.73 (t, J = 11.6 Hz, 2H, -**CH**₂-Ph), 4.62 (d, J = 11.1 Hz, 1H, -**CH**₂-Ph), 4.54 (d, J = 12.2 Hz, 1H, -**CH**₂-Ph), 4.46 (dd, J = 11.6, 2.5 Hz, 2H, -**CH**₂-Ph), 4.32 – 4.25 (m, 1H, **H**-1), 3.93 – 3.82 (m, 1H, -**CH**₂-O-), 3.70 – 3.43 (m, 7H, **H**-3, **H**-4, **H**-6', **H**-6, -**CH**₂-O-, -**CH**₂-NR), 3.43 – 3.28 (m, 2H, **H**-2, **H**-5), 1.76 – 1.54 (m, 4H, -**CH**₂-**CH**₂-).

1-(2-Pyrimidinyl)-4-[3-(2,3,4,6-tetra-*O*-benzyl-D-glucopyranosidyl)propyl]piperazine (9e)

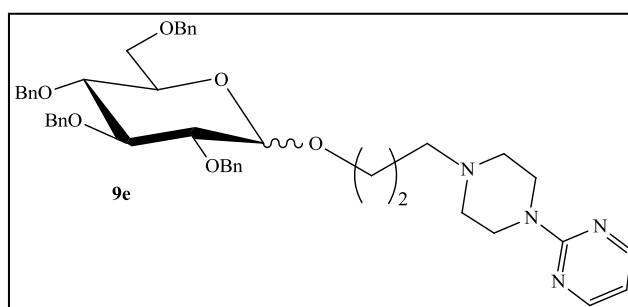
Empirical Formula: C₄₅H₅₂N₄O₆

Formula Weight: 744.91 g/mol

Mass spectrum: M+H

R_f (EL 2): 0.78

Yield: 55 %



¹H- NMR (500 MHz, CDCl₃):

δ 8.28 (dd, J = 4.7, 2.0 Hz, 2H, -**CH**-pyrimidine), 7.48 – 7.08 (m, 20H, **H**-Ph) , 6.47 (t, J = 4.8 Hz, 1H, -**CH**-pyrimidine), 5.00 – 4.42 (m, 8H, -**CH**₂-Ph), 4.41 – 4.36 (m, 1H, **H**-1), 4.05 – 3.93 (m, 1H, **H**-5), 3.90 – 3.40 (m, 11H, **H**-3, **H**-4, **H**-6, **H**-6', **H**-2, -**CH**₂-O-, 2 x **CH**₂- piperazine), 2.55 – 2.39 (m, 6H, -**CH**₂-NR, 2 x **CH**₂-piperazine), 1.92 – 1.80 (m, 2H, -**CH**₂-).

6.2.3 Synthesis of Acceptor Intermediates

Substituted BHP

General procedure for the synthesis of substituted BHP, which were synthesized by the modified published method [85]. To a solution of BHP (1.0 g, 3.96 mmol) in acetone (17 ml) 15 ml of 25 % aq. NaOH solution was added and stirred under Ar for 10 min. the spacer (1.1 eq) was added to the reaction mixture and further stirred for a certain time (see table 5) at a different temperature (RT or heating 60 °C). H₂O was added to the mixture and 25 ml of diethyl ether, dried over Na₂SO₄, filtered, concentrated and purified by column chromatography (acetone/heptane) to give the substituted BHP (**10a-c**) as yellow syrup. The same procedure was applied with using different solvents (DCM, DMF) and several bases like: NaH, Et₃N, and K₂CO₃.

1-Benzhydryl-4-(3-chloropropyl)piperazine (10a)

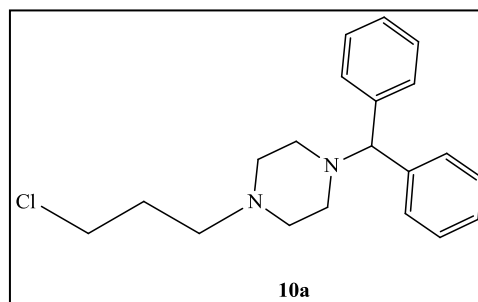
Empirical Formula: C₂₀H₂₅ClN₂

Formula Weight: 328.87 g/mol

Mass spectrum: M+H

R_f (EL 4): 0.62

Yield: 80 %



¹H- NMR (500 MHz, CDCl₃):

δ 7.42 – 7.37 (m, 4H, **H**-Ph), 7.24 (t, J = 7.6 Hz, 4H, **H**-Ph), 7.19 – 7.11 (m, 2H, **H**-Ph), 4.20 (s, 1H, -**CH**-), 3.67 (t, J = 6.1 Hz, 2H, -**CH**₂-Cl), 2.50 – 2.20 (m, 10H, -**CH**₂-NR, 4 x -**CH**₂-piperazine), 1.95 – 1.85 (m, 2H, -**CH**₂-).

1-Benzhydryl-4-(3-bromopropyl)-piperazine (10b)

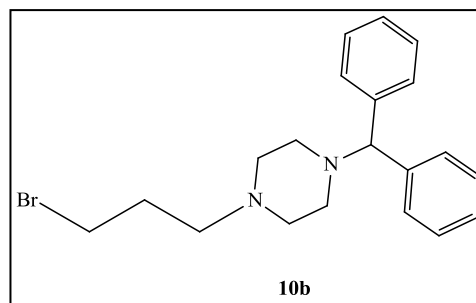
Empirical Formula: $C_{20}H_{25}BrN_2$

Formula Weight: 373.33 g/mol

Mass spectrum: M+Na

R_f (EL 4): 0.77

Yield: 80 %



¹H- NMR (500 MHz, CDCl₃):

δ 7.38 (t, J = 10.9 Hz, 4H, **H**-Ph), 7.24 (t, J = 7.5 Hz, 4H, **H**-Ph), 7.15 (t, J = 7.3 Hz, 2H, **H**-Ph), 4.51 (t, J = 8.3 Hz, 2H, -CH₂-Br), 4.20 (s, 1H, -CH-), 3.41 (t, J = 6.7 Hz, 2H, -CH₂-NR), 2.82 – 2.26 (m, 8H, 4 x -CH₂-piperazine), 2.05 – 1.94 (m, 2H, -CH₂-).

1-Benzhydryl-4-(3-hydroxypropyl)-piperazine (10c)

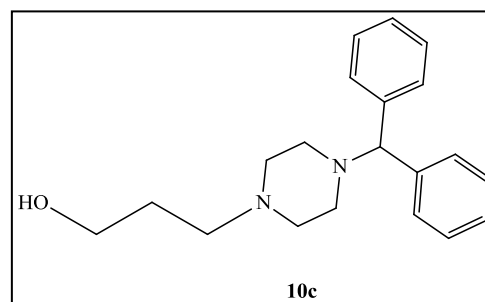
Empirical Formula: $C_{20}H_{26}N_2O$

Formula Weight: 310.43 g/mol

Mass spectrum: M+H

R_f (EL 4): 0.68

Yield: 60 %



¹H- NMR (500 MHz, CDCl₃):

δ 7.38 (t, J = 10.9 Hz, 4H, **H**-Ph), 7.24 (t, J = 7.5 Hz, 4H, **H**-Ph), 7.15 (t, J = 7.3 Hz, 2H, **H**-Ph), 4.20 (s, 1H, -CH-), 3.63 – 3.39 (m, 4H, -CH₂-NR, -CH₂-OH), 2.50 – 2.01 (m, 4H, 2 x -CH₂-piperazine), 1.86 – 1.69 (m, 4H, 2 x -CH₂-piperazine, -CH₂-).

Substituted DPH

General procedure for the synthesis of substituted DPH, which were achieved by the modified published method [86]. DPH (0.53 g, 1.93 mmol) was dissolved in DMF (20 ml), stirred, washed with Ar and (0.08 g, 3.34 mmol) of NaH (60 % oil suspension) was added. After cooling, to the mixture the spacer (1.1 eq) was added, TBAI (small amount) and the solution was further stirred at different temperature (RT or heating 55-100 °C) for certain

time (see table 6). The reaction was periodically monitored by TLC to obtain more yields. The mixture was then extracted 4 times with 50 ml of ethyl acetate, the combined organic phases were washed with 2 times with 30 ml water, brine, dried over Na_2SO_4 , filtered and concentrated in vacuo. The crude mixture was purified by column chromatography (chloroform/ethyl acetate) to give the substituted DPH (**11a-c**) as a colorless oil. **11b** was prepared also by THF and $(\text{CH}_3)_3\text{COK}$.

3-(3-Bromopropyl)-5,5-diphenyl-imidazolidine-2,4-dione (**11a**)

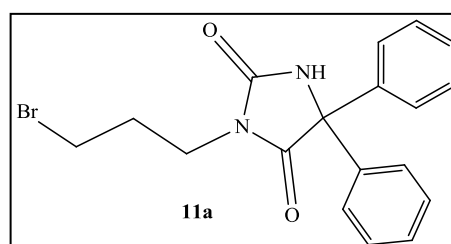
Empirical Formula: $\text{C}_{18}\text{H}_{17}\text{BrN}_2\text{O}_2$

Formula Weight: 373.24 g/mol

Mass spectrum: $\text{M}+\text{Na}$

R_f (EL 6): 0.28

Yield: 85 %



^1H -NMR (500 MHz, CDCl_3)

δ 7.42 – 7.28 (m, 10H, *H*-Ph), 6.25 (s, 1H, *H*-NR), 3.75 – 3.68 (m, 2H, $-\text{CH}_2\text{-Br}$), 3.37 – 3.30 (m, 2H, $-\text{CH}_2\text{-NR}$), 2.26 – 2.17 (m, 2H, $-\text{CH}_2\text{-}$).

3-(3-Hydroxypropyl)-5,5-diphenyl-imidazolidine-2,4-dione (**11b**)

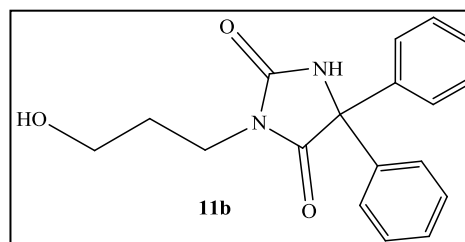
Empirical Formula: $\text{C}_{18}\text{H}_{18}\text{N}_2\text{O}_3$

Formula Weight: 310.34 g/mol

Mass spectrum: M-H

R_f (EL 6): 0.15

Yield: 85 %



^1H -NMR (500 MHz, CDCl_3):

δ 7.42 – 7.27 (m, 10H, *H*-Ph), 6.64 (s, 1H, *H*-NR), 3.78 – 3.43 (m, 4H, $-\text{CH}_2\text{-NR}$, $-\text{CH}_2\text{-OH}$), 1.85 – 1.76 (m, 2H, $-\text{CH}_2\text{-}$).

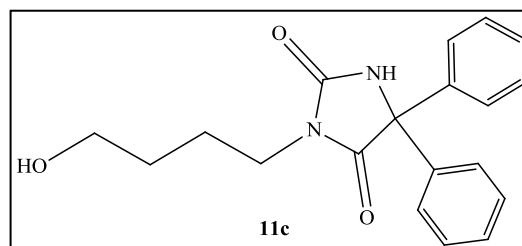
3-(4-Hydroxybutyl)-5,5-diphenyl-imidazolidine-2,4-dione (11c)Empirical Formula: C₁₉H₂₀N₂O₃

Formula Weight: 324.37 g/mol

Mass spectrum: M+Na

R_f (EL 6): 0.13

Yield: 50 %

¹H- NMR (500 MHz, CDCl₃):

δ 7.40 – 7.29 (m, 10H, *H*-Ph), 6.37 (s, 1H, *H*-NR), 3.68 – 3.56 (m, 4H, -CH₂-NR, -CH₂-OH), 1.80 – 1.68 (m, 2H, -CH₂-), 1.59 – 1.50 (m, 2H, -CH₂-).

6.2.4 Synthesis of Glycosyl Acetates

This compound was synthesized according to published method [90]. The acetylated sugar (1.0 g, 2.56 mmol) was dissolved in DMF (5 ml), washed with Ar, heated to 55 °C, hydrazine acetate (1.2 eq) was added to the mixture, stirred for 0.5 h and controlled with TLC. The mixture was diluted with 30 ml of ethyl acetate, washed 2 times with 30 ml of H₂O and brine. The organic layer was dried over Na₂SO₄, filtered and concentrated. Purification was accomplished by column chromatography (chloroform/methanol) to obtain tetraacetate sugar **12** as colorless syrup.

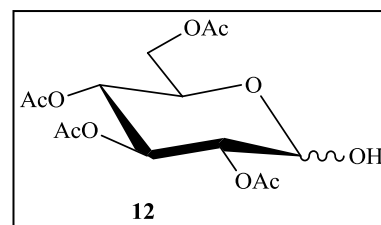
2,3,4,6-Tetra-*O*-acetyl-D-glucopyranose (12)Empirical Formula: C₁₄H₂₀O₁₀

Formula Weight: 348.30 g/ml

Mass spectrum: M+Na

R_f (EL 2): 0.66

Yield: 91 %



^1H - NMR (400 MHz, CDCl_3):

δ 5.48 (t, $J = 9.7$ Hz, 1H, **H-3**), 5.41 (d, $J = 3.6$ Hz, 1H, **H-1 α**), 5.04 (dd, $J = 9.7, 3.2$ Hz, 1H, **H-4**), 4.89 – 4.79 (m, 1H, **H-2**), 4.71 (d, $J = 8.0$ Hz, 1H, **H-1 β**), 4.26 – 4.15 (m, 2H, **H-6',H-5**), 4.14 – 4.05 (m, 1H, **H-6**), 2.05, 2.03, 1.99, 1.97 (4s, 12H, 4 **CH₃-Ac**).

6.2.5 Synthesis of Acetylated Glycoside Intermediates

Compound **12** (0.15 g, 0.43 mmol) was treated with several halo alcohol (1.1 eq) and $\text{BF}_3 \cdot \text{Et}_2\text{O}$ (1 ml) and stirred overnight by the same procedure as described above (Borontrifluoride etherate method) to give glycoside intermediate **13-15** as a yellow syrup.

1-*O*-(2-Iodoethyl)-2,3,4,6-tetra-*O*-acetyl-D-glucopyranoside (**13**)

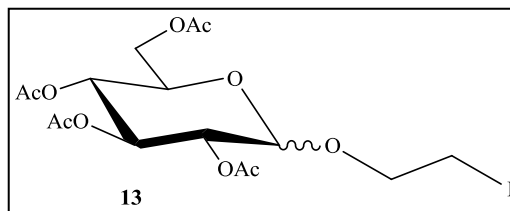
Empirical Formula: $\text{C}_{16}\text{H}_{23}\text{IO}_{10}$

Formula Weight: 502.25 g/mol

Mass spectrum: $\text{M}+\text{Na}$

R_f (EL 2): 0.80

Yield: 65 %



^1H - NMR (400 MHz, CDCl_3):

δ 5.19 (t, $J = 9.5$ Hz, 1H, **H-3**), 5.06 (t, $J = 9.7$ Hz, 1H, **H-4**), 4.99 (dd, $J = 9.6, 8.0$ Hz, 1H, **H-2**), 4.83 (dd, $J = 10.3, 3.7$ Hz, 1H, **H-1 α**), 4.54 (d, $J = 7.9$ Hz, 1H, **H-1 β**), 4.23 (dd, $J = 12.3, 4.8$ Hz, 1H, **H-6'**), 4.16 – 4.02 (m, 2H, **-CH₂-O-**, **H-6**), 3.82 – 3.71 (m, 1H, **-CH₂-O-**), 3.71 – 3.64 (m, 1H, **H-5**), 3.38 – 3.14 (m, 2H, **-CH₂I**), 2.07, 2.06, 2.00, 1.98 (4s, 12H, 4 **CH₃-Ac**).

1-*O*-(3-Bromopropyl)-2,3,4,6-tetra-*O*-acetyl-D-glucopyranoside (**14**)

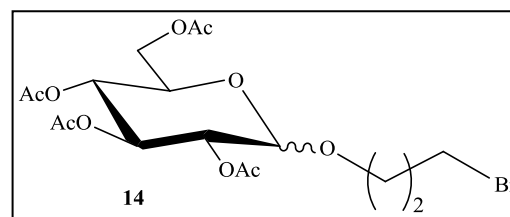
Empirical Formula: $\text{C}_{17}\text{H}_{25}\text{BrO}_{10}$

Formula Weight: 469.27 g/mol

Mass spectrum: $\text{M}+\text{Na}$

R_f (EL 2): 0.78

Yield: 60 %



^1H - NMR (400 MHz, CDCl_3):

δ 5.18 (t, $J = 9.5$ Hz, 1H, **H-3**), 5.04 (t, $J = 9.6$ Hz, 1H, **H-4**), 4.95 (dd, $J = 9.6, 8.0$ Hz, 1H, **H-2**), 4.85 (dd, $J = 10.3, 3.8$ Hz, 1H, **H-1 α**), 4.48 (d, $J = 8.0$ Hz, 1H, **H-1 β**), 4.28 – 4.19 (m, 1H, **H-6'**), 4.15 – 4.05 (m, 1H, **H-6**), 3.77 (t, $J = 6.6, 5.7$ Hz, 2H, $-\text{CH}_2\text{O}-$), 3.71 – 3.60 (m, 1H, **H-5**), 3.51 (t, $J = 6.6$ Hz, 2H, $-\text{CH}_2\text{-Br}$), 2.17 – 1.94 (m, 14H, 4 $\text{CH}_3\text{-Ac}$, $-\text{CH}_2-$).

1-*O*-(3-Chloropropyl)-2,3,4,6-tetra-*O*-acetyl-D-glucopyranoside (**15**)

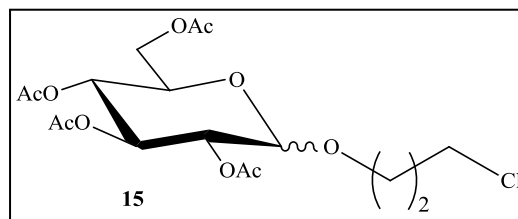
Empirical Formula: $\text{C}_{17}\text{H}_{25}\text{ClO}_{10}$

Formula Weight: 424.82 g/mol

Mass spectrum: $\text{M}+\text{Na}$

R_f (EL 2): 0.79

Yield: 45 %



^1H - NMR (400 MHz, CDCl_3):

δ 6.25 (d, $J = 3.7$ Hz, 1H, **H-1 α**), 5.79 (d, $J = 8.3$ Hz, 1H, **H-1 β**), 5.50 – 5.34 (m, 1H, **H-3**), 5.31 – 5.18 (m, 1H, **H-4**), 5.06 – 4.94 (m, 1H, **H-2**), 4.91 – 4.53 (m, 1H, **H-5**), 4.31 – 3.97 (m, 3H, **H-6'**, **H-6**, $-\text{CH}_2\text{-O}-$), 3.97 – 3.80 (m, 1H, $-\text{CH}_2\text{-O}-$), 3.76 – 3.51 (m, 2H, $-\text{CH}_2\text{-Cl}$), 2.21 – 1.90 (m, 14H, 4 $\text{CH}_3\text{-Ac}$, $-\text{CH}_2-$).

6.2.6 Synthesis of Acetylated Glycopyranosidyl Alkyl Acceptors

Compounds **13-15** (0.20 g, 1 eq) were treated (see table 8) with several basic moieties (1.1 eq) by the same procedure as described above (**9a-f**) to give compound **16a-f** as colorless syrup.

3-[2-(2,3,4,6-Tetra-*O*-acetyl-D-glucopyranosidyl)ethyl]-5,5-diphenyl-imidazolidine-2,4-dione (16a)

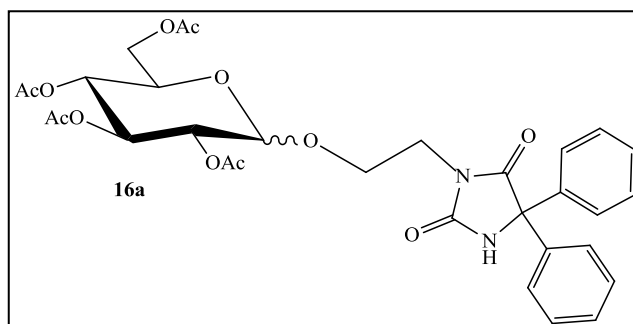
Empirical Formula: $C_{31}H_{34}N_2O_{12}$

Formula Weight: 626.60 g/mol

Mass spectrum: M+Na, M-H

R_f (EL 2): 0.78

Yield: 88 %



¹H- NMR (400 MHz, CDCl₃):

δ 7.86 (s, 1H, *H*-NR), 7.50 – 6.96 (m, 10H, *H*-Ph), 5.08 – 4.98 (m, 1H, *H*-3), 4.95 – 4.75 (m, 3H, *H*-4, *H*-2, *H*-1α), 4.35 (d, J = 7.9 Hz, 1H, *H*-1β), 4.03 – 3.95 (m, 1H, *H*-6'), 3.94 – 3.83 (m, 1H, *H*-6), 3.74 – 3.53 (m, 4H, -CH₂-O-, -CH₂-NR), 3.51 – 3.39 (m, 1H, *H*-5), 1.94, 1.90, 1.87, 1.82 (4s, 12H, 4 CH₃-Ac).

3-[3-(2,3,4,6-Tetra-*O*-acetyl-D-glucopyranosidyl)propyl]-5,5-diphenyl-imidazolidine-2,4-dione (16b)

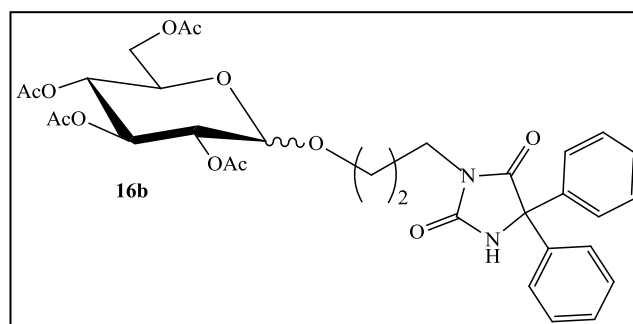
Empirical Formula: $C_{32}H_{36}N_2O_{12}$

Formula Weight: 640.63 g/mol

Mass spectrum: M+Na, M-H

R_f (EL 2): 0.84

Yield: 75 %



¹H- NMR (400 MHz, CDCl₃):

δ 7.86 (s, 1H, *H*-NR), 7.49 – 7.10 (m, 10H, *H*-Ph), 5.06 (t, J = 9.5 Hz, 1H, *H*-3), 5.00 – 4.88 (m, 1H, *H*-4), 4.83 – 4.79 (m, 1H, *H*-2), 4.78 – 4.74 (m, 1H, *H*-1α), 4.31 (d, J = 8.0 Hz, 1H, *H*-1β), 4.19 – 4.08 (m, 1H, *H*-6'), 4.05 – 3.87 (m, 1H, *H*-6), 3.83 – 3.71 (m, 1H, -CH₂-O-), 3.66 – 3.32 (m, 4H, -CH₂-O-, -CH₂-NR, *H*-5), 2.06 – 1.63 (m, 14H, 4 CH₃-Ac, -CH₂-).

1-(2-Pyrimidinyl)-4-[3-(2,3,4,6-tetra-*O*-acetyl-D-glucopyranosidyl)propyl]piperazine (16c)

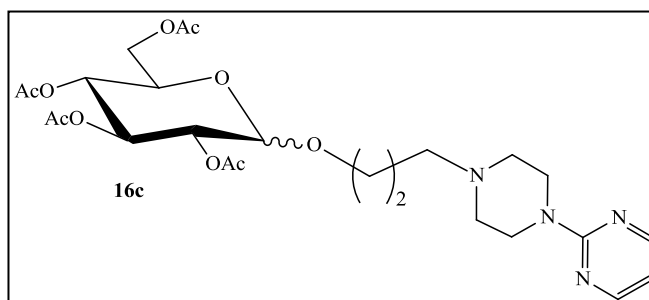
Empirical Formula: C₂₅H₃₆N₄O₁₀

Formula Weight: 552.57 g/mol

Mass spectrum: M+Na, M+H

R_f (EL 7): 0.83

Yield: 73 %



¹H- NMR (400 MHz, CDCl₃):

δ 8.36 – 8.18 (m, 2H, 2 x -*CH*-pyrimidine), 6.55 – 6.43 (m, 1H, -*CH*-pyrimidine), 5.48 – 5.42 (m, 1H, *H*-3), 5.09 – 4.91 (m, 2H, *H*-4, *H*-2), 4.84 (dd, J = 10.2, 3.7 Hz, 1H, *H*-1α), 4.49 (d, J = 7.9 Hz, 1H, *H*-1β), 4.30 – 4.19 (m, 1H, *H*-6'), 4.16 – 4.00 (m, 2H, *H*-6, *H*-5), 3.95 – 3.71 (m, 5H, -*CH*₂-O-, 2 x -*CH*₂-piperazine), 3.54 – 3.38 (m, 1H, -*CH*₂-O-), 2.64 – 2.35 (m, 6H, -*CH*₂-NR, 2 x -*CH*₂-piperazine), 2.06, 2.04, 2.01, 1.98 (4s, 12H, 4 *CH*₃-Ac), 1.90 – 1.78 (m, 2H, -*CH*₂-).

1-(Diphenylmethyl)-4-[3-(2,3,4,6-tetra-*O*-acetyl-D-glucopyranosidyl)propyl]piperazine (16d)

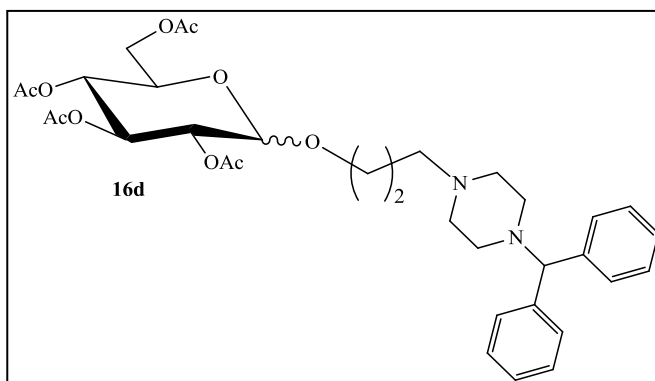
Empirical Formula: C₃₄H₄₄N₂O₁₀

Formula Weight: 640.72 g/mol

Mass spectrum: M+H

R_f (EL 3): 0.70

Yield: 68 %



¹H- NMR (400 MHz, CDCl₃):

δ 7.38 (d, J = 7.9 Hz, 4H, *H*-Ph), 7.24 (t, J = 7.9, 7.3 Hz, 4H, *H*-Ph), 7.15 (d, J = 7.3 Hz, 2H, *H*-Ph), 5.43 (t, J = 9.8 Hz, 1H, *H*-3), 5.16 (t, J = 9.5 Hz, 1H, *H*-4), 5.10 – 4.90 (m, 2H, -*CH*-, *H*-2), 4.83 (dd, J = 10.2, 3.7 Hz, 1H, *H*-1α), 4.46 (d, J = 7.9 Hz, 1H, *H*-1β), 4.30 – 4.15 (m, 2H, *H*-6'), 4.13 – 3.94 (m, 2H, *H*-6, *H*-5), 3.77 – 3.36 (m, 2H, -*CH*₂-O-), 2.61 –

2.28 (m, 6H, $-\text{CH}_2\text{-NR}$, 2 x $-\text{CH}_2\text{-piperazine}$), 2.06, 2.02, 2.01, 1.98 (4s, 12H, 4 $\text{CH}_3\text{-Ac}$), 1.86 – 1.70 (m, 2H, $-\text{CH}_2\text{-}$).

10-[3-(2,3,4,6-Tetra-*O*-acetyl-D-glucopyranosidyl)propyl]-10*H*-phenothiazine-5,5-dioxide (16e)

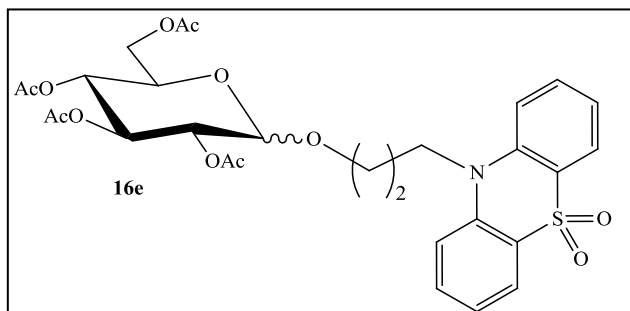
Empirical Formula: $\text{C}_{29}\text{H}_{33}\text{NO}_{12}\text{S}$

Formula Weight: 619.63 g/mol

Mass spectrum: $\text{M}+\text{Na}$

R_f (EL 2): 0.80

Yield: 65 %



^1H - NMR (500 MHz, CDCl_3):

δ 8.12 – 8.00 (m, 2H, $\text{H-4}'$, $\text{H-6}'$), 7.75 – 7.57 (m, 2H, $\text{H-2}'$, $\text{H-8}'$), 7.49 – 7.33 (m, 2H, $\text{H-2}'$, $\text{H-8}'$), 7.30 – 7.14 (m, 3H, $\text{H-1}'$, $\text{H-9}'$), 5.24 – 5.11 (m, 1H, H-3), 5.10 – 4.94 (m, 2H, H-4 , H-2), 4.88 (dd, $J = 3.6, 10.2$ Hz, 1H, $\text{H-1}\alpha$), 4.46 (d, $J = 7.9$ Hz, 1H, $\text{H-1}\beta$), 4.34 – 4.03 (m, 4H, $-\text{CH}_2\text{-O-}$, $\text{H-6}'$, H-6), 4.02 – 3.89 (m, 1H, $-\text{CH}_2\text{-N-}$), 3.72 – 3.51 (m, 2H, H-5 , $-\text{CH}_2\text{-NR}$), 2.21 – 2.10 (m, 2H, $-\text{CH}_2\text{-}$), 2.05, 2.01, 1.99, 1.97 (4s, 12H, 4 $\text{CH}_3\text{-Ac}$).

3-[4-(2,3,4,6-Tetra-*O*-acetyl-D-glucopyranosidyl)butyl]-5,5-diphenyl-imidazolidine-2,4-dione (16f)

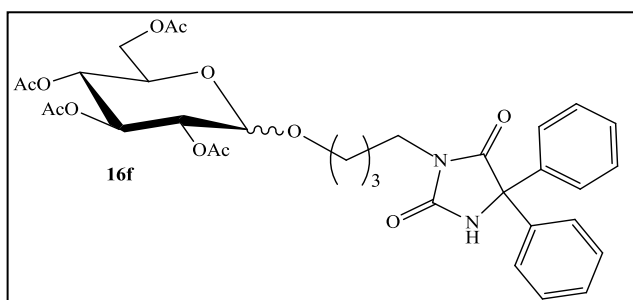
Empirical Formula: $\text{C}_{33}\text{H}_{38}\text{N}_2\text{O}_{12}$

Formula Weight: 654.66 g/mol

Mass spectrum: $\text{M}+\text{Na}$, M-H

R_f (EL 2): 0.84

Yield: 55 %



^1H - NMR (400 MHz, CDCl_3):

δ 7.88 (s, 1H, H-NR), 7.37 – 6.93 (m, 10H, H-Ph), 5.07 (t, $J = 9.5$ Hz, 1H, H-3), 5.01 – 4.89 (m, 1H, H-4), 4.83 (dd, $J = 9.5, 8.0$ Hz, 1H, H-2), 4.74 (dd, $J = 10.2, 3.7$ Hz, 1H, $\text{H-1}\alpha$), 4.33 (d, $J = 8.0$ Hz, 1H, $\text{H-1}\beta$), 4.18 – 4.07 (m, 1H, $\text{H-6}'$), 4.04 – 3.92 (m, 1H, H-6),

3.64 – 3.24 (m, 5H, $-\text{CH}_2\text{-O-}$, $-\text{CH}_2\text{-NR}$, $H-5$), 1.95, 1.90, 1.87, 1.84 (4s, 12H, 4 $\text{CH}_3\text{-Ac}$), 1.67 – 1.37 (m, 4H, $-\text{CH}_2\text{-CH}_2\text{-}$).

6.2.7 Synthesis of Perhydroxylated Compounds

Two methods were used to prepare the final compounds **GS29-34**:

Catalytically hydrogenation step:

The benzylated glucopyranosidyl alkyl acceptor **9a-f** (120 mg) was dissolved in 50 ml of methanol/ethyl acetate, 1:1 (v/v), Pd/C (60 mg, 5 wt %) and HCOOH (0.5 ml) was added. The hydrogenation was carried out in a hydrogenation apparatus at a pressure of 3 bar and RT. After 24 hrs, the hydrogenation was stopped, Pd/C was filtered off and the solvent removed on a rotary evaporator. The residue was subjected to column chromatography on silica gel with chloroform/methanol to yield the final compound as a white paste-like substance.

Deacetylation step:

The acetylated glucopyranosidyl alkyl acceptor **16a-f** (160 mg) was dissolved in methanol (20 ml) under Ar, 80 μL of sodium methoxide (0.1 M in methanol) was added and after 10 hrs another 40 μL . Another amount (20 μL) was added dependent on the TLC until it showed that most of starting material was converted. The mixture was then filtered and concentrated in vacuo. The residue was purified by column chromatography (chloroform/methanol). The resulting product was obtained in quantitative yields (see table 9).

3-[2-(D-Glucopyranosidyl)ethyl]-5,5-diphenyl-imidazolidine-2,4-dione (**GS29**)

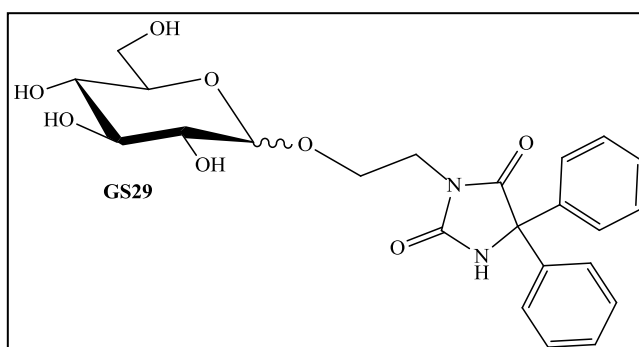
Empirical Formula: $\text{C}_{23}\text{H}_{26}\text{N}_2\text{O}_8$

Formula Weight: 458.46 g/mol

Mass spectrum: $\text{M}+\text{Na}$, $\text{M}-\text{H}$

R_f (EL 7): 0.46

Yield: 86 %



¹H- NMR (400 MHz, CDCl₃):

δ 7.46 – 7.29 (m, 10H, **H-Ph**), 4.81 (d, J = 3.8 Hz, 1H, **H-1α**), 4.27 (d, J = 7.8 Hz, 1H, **H-1β**), 4.16 – 4.04 (m, 1H, **-CH₂-O-**), 3.96 – 3.61 (m, 4H, **-CH₂-O-**, **H-6'**, **H-6**, **H-5**), 3.57 (dd, J = 11.9, 5.8 Hz, 1H, **-CH₂-NR**), 3.40 – 3.30 (m, 1H, **-CH₂-NR**), 3.29 – 3.19 (m, 2H, **H-3**, **H-4**), 3.19 – 3.09 (m, 1H, **H-2**).

3-[3-(D-Glucopyranosidyl)propyl]-5,5-diphenyl-imidazolidine-2,4-dione (GS30)

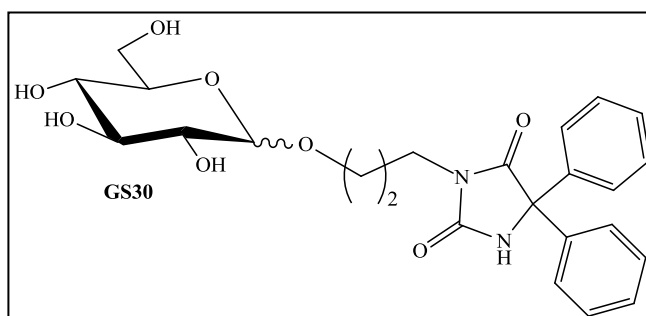
Empirical Formula: C₂₄H₂₈N₂O₈

Formula Weight: 472.48 g/mol

Mass spectrum: M+Na, M-H

R_f (EL 7): 0.30

Yield: 82 %



¹H- NMR (400 MHz, CDCl₃):

δ 7.50 – 7.30 (m, 10H, **H-Ph**), 4.78 (d, J = 3.8 Hz, 1H, **H-1α**), 4.22 (d, J = 7.8 Hz, 1H, **H-1β**), 3.98 – 3.90 (m, 1H, **-CH₂-O-**), 3.88 (dd, J = 11.9, 2.1 Hz, 1H, **H-6'**), 3.83 – 3.66 (m, 4H, **H-6**, **H-5**, **-CH₂-O-**, **-CH₂-NR**), 3.65 – 3.55 (m, 1H, **-CH₂-NR**), 3.32 – 3.21 (m, 2H, **H-3**, **H-4**), 3.21 – 3.13 (m, 1H, **H-2**), 2.05 – 1.91 (m, 2H, **-CH₂-**).

3-[4-(D-Glucopyranosidyl)butyl]-5,5-diphenyl-imidazolidine-2,4-dione (GS31)

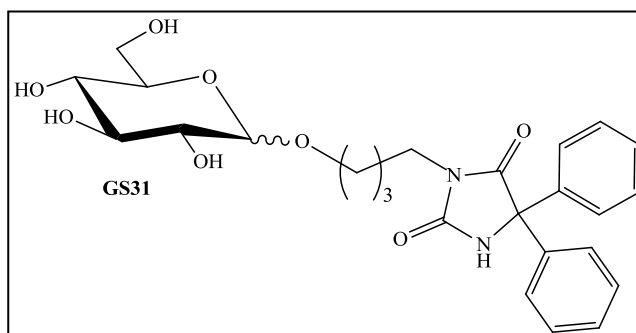
Empirical Formula: C₂₅H₃₀N₂O₈

Formula Weight: 486.51 g/mol

Mass spectrum: M+Na, M-H

R_f (EL 7): 0.50

Yield: 80 %



¹H- NMR (400 MHz, CDCl₃):

δ 7.48 – 7.33 (m, 10H, **H-Ph**), 4.79 (d, J = 3.8 Hz, 1H, **H-1α**), 4.26 (d, J = 7.8 Hz, 1H, **H-1β**), 3.99 – 3.91 (m, 1H, **-CH₂-O-**), 3.87 (dd, J = 11.9, 2.3 Hz, 1H, **H-6'**), 3.82 – 3.76 (m,

1H, **H-6**), 3.74 – 3.48 (m, 5H, -CH₂-O-, -CH₂-NR, **H-5**), 3.37 – 3.25 (m, 2H, **H-3**, **H-4**), 3.20 (m, 1H, **H-2**), 1.84 – 1.74 (m, 2H, -CH₂-), 1.70 – 1.58 (m, 2H, -CH₂-).

1-(Diphenylmethyl)-4-[3-(D-glucopyranosidyl)propyl]piperazine (GS32)

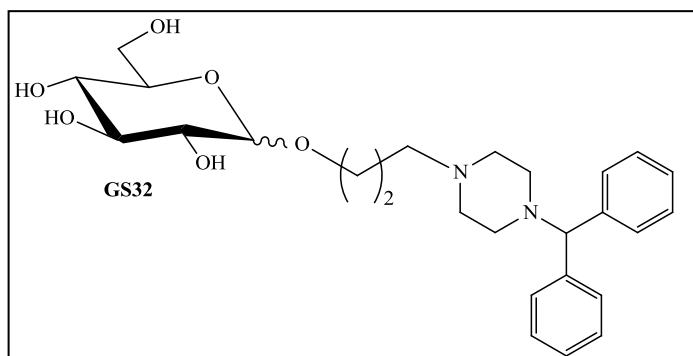
Empirical Formula: C₂₆H₃₆N₂O₆

Formula Weight: 472.57 g/mol

Mass spectrum: M+Na, M+H

R_f (EL 2): 0.34

Yield: 84 %



¹H- NMR (400 MHz, CDCl₃):

δ 7.47 (d, J = 7.5 Hz, 4H, **H-Ph**), 7.31 (t, J = 7.6 Hz, 4H, **H-Ph**), 7.21 (t, J = 7.4 Hz, 2H, **H-Ph**), 4.81 (d, J = 3.8 Hz, 1H, **H-1α**), 4.31 – 4.24 (m, 2H, **H-1β**, -CH-), 4.02 – 3.92 (m, 1H, -CH₂-O-), 3.92 – 3.79 (m, 2H, **H-6'**, **H-6**), 3.74 – 3.47 (m, 3H, **H-5**, -CH₂-NR), 3.39 – 3.32 (m, 1H, **H-3**), 3.32 – 3.26 (m, 1H, **H-4**), 3.20 (m, 1H, **H-2**), 2.75 – 2.39 (m, 8H, 2 x -CH₂-piperazine), 1.97 – 1.78 (m, 2H, -CH₂-).

1-(2-Pyrimidinyl)-4-[3-(D-glucopyranosidyl)propyl]piperazine (GS33)

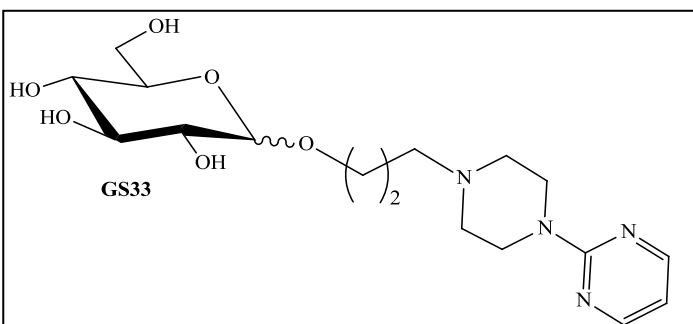
Empirical Formula: C₁₇H₂₈N₄O₆

Formula Weight: 384.42 g/mol

Mass spectrum: M+H, M-H

R_f (EL 7): 0.26

Yield: 82 %



¹H- NMR (500 MHz, CDCl₃):

δ 8.36 (d, J = 4.5 Hz, 2H, 2 x -CH-pyrimidine), 6.64 (t, J = 4.5 Hz, 1H, -CH-pyrimidine), 4.83 (d, J = 3.7 Hz, 1H, **H-1α**), 4.31 (d, J = 7.8 Hz, 1H, **H-1β**), 4.04 – 3.97 (m, 1H, -CH₂-O-), 3.94 – 3.81 (m, 7H, 2 x -CH₂-piperazine, -CH₂-O-, **H-6'**, **H-6**), 3.78 – 3.50 (m, 3H, -CH₂-N, **H-5**), 3.39 – 3.28 (m, 2H, **H-3**, **H-4**), 3.22 (m, 1H, **H-2**), 2.72 – 2.54 (m, 4H, 2 x -CH₂-piperazine), 2.00 – 1.85 (m, 2H, -CH₂-).

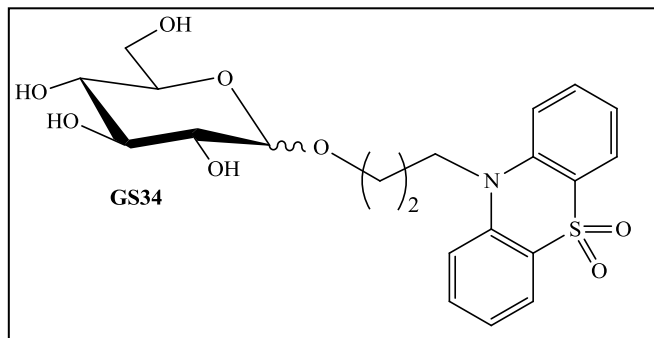
10-[3-(D-Glucopyranosidyl)propyl]-10*H*-phenothiazine-5,5-dioxide (GS34)Empirical Formula: C₂₁H₂₅NO₈S

Formula Weight: 451.49 g/mol

Mass spectrum: M+Na

R_f (EL 7): 0.50

Yield: 79 %

¹H- NMR (500 MHz, CDCl₃):

δ 8.07 (d, J = 7.6 Hz, 2H, **H-4'**, **H-6'**), 7.82 – 7.72 (m, 4H, **H-2'**, **H-3'**, **H-7'**, **H-8'**), 7.40 – 7.32 (m, 2H, **H-1'**, **H-9'**), 4.83 (d, J = 3.7 Hz, 1H, **H-1 α**), 4.59 – 4.51 (m, 1H, **-CH₂-O-**), 4.31 (d, J = 7.8 Hz, 1H, **H-1 β**), 4.13 – 3.99 (m, 1H, **-CH₂-O-**), 3.99 – 3.81 (m, 2H, **H-6'**, **H-6**), 3.81 – 3.51 (m, 3H, **-CH₂-NR**, **H-5**), 3.51 – 3.17 (m, 3H, **H-3**, **H-4**, **H-2**), 2.31 – 2.04 (m, 2H, **-CH₂-**).

6.2.8 Synthesis of Azidoglucosides and Azidogalactosides

These compounds were synthesized by the published method [98]. A mixture of Acetobromo- α -D-glucose or galactose (1.0 g, 2.43 mmol) and NaN₃ (0.32 g, 4.92 mmol) in DMF (5 ml) was stirred for 10 min at RT. The mixture was diluted with ethyl acetate, washed 3 times with 50 ml H₂O and brine. The organic layer was dried over Na₂SO₄, filtered and concentrated in vacuo. Purification was accomplished by column chromatography (chloroform/ethyl acetate) to obtain azido sugar **17b**, **18b** as white solids.

1-Azido-2,3,4,6-tetra-*O*-acetyl- β -D-glucose (17b)Empirical Formula: C₁₄H₁₉N₃O₉

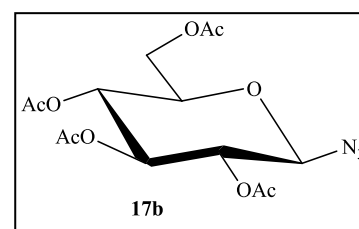
Formula Weight: 373.31 g/mol

Mass spectrum: M+Na

R_f (EL 3): 0.36

Yield: 91 %

M.p.: 120-124 °C



^1H - NMR (400 MHz, CDCl_3):

δ 5.20 (dd, $J = 9.9, 9.4$ Hz, 1H, **H-3**), 5.09 (t, $J = 9.7$ Hz, 1H, **H-4**), 4.94 (dd, $J = 9.4, 9.0$ Hz, 1H, **H-2**), 4.63 (d, $J = 8.9$ Hz, 1H, **H-1 β**), 4.26 (dd, $J = 12.5, 4.8$ Hz, 1H, **H-6'**), 4.15 (dd, $J = 12.5, 2.3$ Hz, 1H, **H-6**), 3.78 (ddd, $J = 10.0, 4.8, 2.3$ Hz, 1H, **H-5**), 2.15, 2.07, 2.01, 1.99 (s, 12H, 4 x CH_3 Ac).

1-Azido-2,3,4,6-tetra-*O*-acetyl- β -D-galactose (**18b**)

Empirical Formula: $\text{C}_{14}\text{H}_{19}\text{N}_3\text{O}_9$

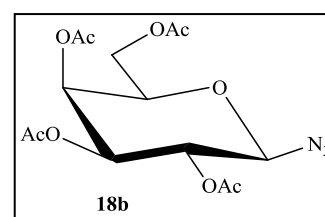
Formula Weight: 373.31 g/mol

Mass spectrum: $\text{M}+\text{Na}$

R_f (EL 3): 0.35

Yield: 80 %

M.p.: 80-85 $^\circ\text{C}$



^1H - NMR (400 MHz, CDCl_3):

δ 5.40 (dd, $J = 3.3, 1.1$ Hz, 1H, **H-4**), 5.14 (dd, $J = 10.4, 8.8$ Hz, 1H, **H-2**), 5.01 (dd, $J = 10.4, 3.4$ Hz, 1H, **H-3**), 4.57 (d, $J = 8.7$ Hz, 1H, **H-1 β**), 4.21 – 4.07 (m, 2H, **H-6'**, **H-6**), 4.02 – 3.96 (m, 1H, **H-5**), 2.15, 2.07, 2.04 1.97 (s, 12H, 4 x CH_3 Ac).

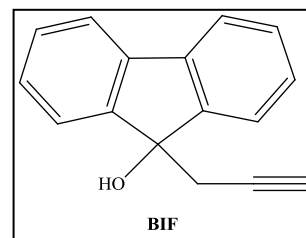
6.2.9 Synthesis of Terminal Acetylenes

These compounds were synthesized by the modified published method [99]. To a solution of basic moiety (1.0 g) in DMF (10 ml) K_2CO_3 (2 eq), propargyl bromide (1.1 eq) and KI (1.3 eq) were added. The resulting mixture was stirred for 24 hrs under Ar, periodically monitored by TLC. The crude residue was extracted 3 times with 30 ml of ethyl acetate, the combined organic phases were washed 2 times with 30 ml water, brine, dried over Na_2SO_4 , filtered and concentrated in vacuo. The residue was subjected to column chromatography with chloroform/ethyl acetate to yield the terminal alkyne as a solid substance. BIF and DIP were prepared by the procedure in Ref.[61].

9-(Prop-2-ynyl)-9H-fluoren-9-ol (BIF)

Empirical formula: $C_{16}H_{12}O$

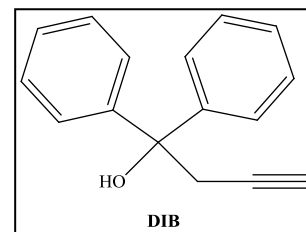
Formula Weight: 220.27 g/mol



1,1-Diphenylbut-3-in-1-ol (DIB)

Empirical formula: $C_{16}H_{12}O$

Formula Weight: 220.27 g/mol



5,5-Diphenyl-3-(prop-2-ynyl)-imidazolidine-2,4-dione (DIH)

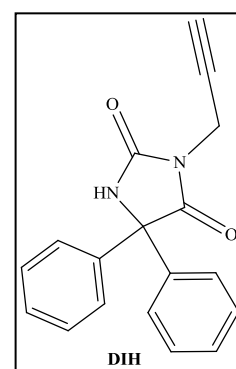
Empirical Formula: $C_{18}H_{14}N_2O_2$

Formula Weight: 290.31 g/mol

Mass spectrum: $M+Na$, $M-H$

R_f (EL 2): 0.75

Yield: 78 %



1H - NMR (400 MHz, $CDCl_3$):

δ 7.35 – 7.09 (m, 10H, **H-Ph**), 6.14 (s, 1H, **H-NR**), 4.23 (dd, $J = 13.3, 2.5$ Hz, 2H, **-CH₂-**), , 2.13 (dt, $J = 7.8, 2.5$ Hz, 1H, **-CH-**).

1-Benzhydryl-4-(prop-2-ynyl)-piperazine (BIP)

Empirical Formula: $C_{20}H_{22}N_2$

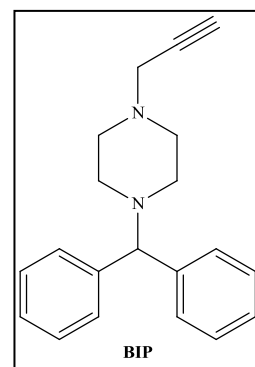
Formula Weight: 290.40 g/mol

Mass spectrum: $M+H$

R_f (EL 2): 0.75

Yield: 85 %

M.p.: 85-89 °C



¹H- NMR (500 MHz, CD₃OD):

δ 7.45 (d, *J* = 7.7 Hz, 4H, **H-Ph**), 7.30 (t, *J* = 7.7 Hz, 4H, **H-Ph**), 7.27 – 7.15 (m, 2H, **H-Ph**), 4.27 (s, 1H, **-CH-**), 3.39 – 3.27 (m, 6H, 2 x **-CH₂-piperazine**, **-CH₂-**), 2.81 – 2.33 (m, 5H, 2 x **-CH₂-piperazine**, **-CH-**).

2-[4-(Prop-2-ynyl)-piperazine-1-yl]-pyrimidine (PIP)

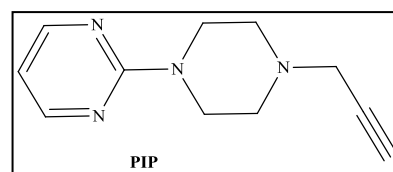
Empirical Formula: C₁₁H₁₄N₄

Formula Weight: 202.25 g/mol

Mass spectrum: M+H, M-H

R_f (EL 2): 0.70

Yield: 70 %



¹H- NMR (400 MHz, CD₃OD):

δ 8.36 (d, *J* = 4.5 Hz, 2H, 2 x **-CH-pyrimidine**), 6.63 (dd, *J* = 5.1, 4.5 Hz, 1H, **-CH-pyrimidine**), 3.88 (t, *J* = 5.1 Hz, 4H, 2 x **-CH₂-piperazine**), 3.40 (d, *J* = 2.5 Hz, 2H, **-CH₂-**), 2.74 (t, *J* = 2.5 Hz, 1H, **-CH-**), 2.67 (dd, *J* = 5.7, 5.1 Hz, 4H, 2 x **-CH₂-piperazine**).

6.2.10 Synthesis of Acetylated Gluco- and Galactotriazole Derivatives

These compounds were synthesized by published method [101]. A mixture of sugar derivatives containing azide group at C-1 or C-6 (0.20 g) was dissolved in DMF (1 ml) in a 2 ml Eppendorf tube and one of the acetylene derivatives (1.1 eq) was added. Then sodium ascorbate (0.1 eq) and CuSO₄·5H₂O (0.03 eq) were added. The tube was sealed and stirred for 1 hr at 70 °C in an ultrasonic bath. The reaction mixture was transferred to a round bottom flask and co-evaporated with toluene on a rotary evaporator. The residue was purified by column chromatography with (acetonitrile/water) to yield **GS (35-37)**, **GS (38-45a)** as unprotected final compound, acetylated glyco-triazoles, respectively.

1-(2-Pyrimidinyl)-4-[(1-methyl-6-deoxy- α -D-glucopyranosid-6-yl)-(1*H*-1,2,3-triazol-4-yl)methyl]piperazine (GS35)

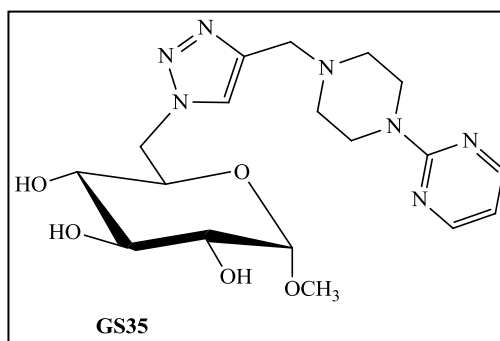
Empirical Formula: C₁₈H₂₇N₇O₅

Formula Weight: 421.45 g/mol

Mass spectrum: M+H

R_f (EL 6): 0.50

Yield: 65 %



¹H- NMR (500 MHz, CD₃OD):

δ 8.34 (d, $J = 4.8$ Hz, 2H, 2 x -CH-pyrimidine), 8.02 (s, 1H, 1H, triazol-H), 6.62 (t, $J = 4.8$ Hz, 1H, -CH-pyrimidine), 4.90 (dd, $J = 14.3, 2.4$ Hz, 1H, **H-6'**), 4.67 (d, $J = 3.7$ Hz, 1H, **H-1 α**), 4.57 (dd, $J = 14.2, 8.3$ Hz, 1H, **H-6**), 3.94 – 3.86 (m, 1H, **H-5**), 3.86 – 3.81 (m, 4H, 2 x -CH₂-piperazine), 3.80 (s, 2H, -CH₂-), 3.68 (t, $J = 9.2$ Hz, 1H, **H-3**), 3.43 (dd, $J = 9.7, 3.8$ Hz, 1H, **H-2**), 3.23 – 3.17 (m, 1H, **H-4**), 3.14 (s, 3H, -O-CH₃), 2.61 – 2.55 (m, 4H, 2 x -CH₂-piperazine).

1-Benzhydryl-4-[(1-methyl-6-deoxy- α -D-glucopyranosid-6-yl)-(1*H*-1,2,3-triazol-4-yl)methyl]piperazine (GS36)

Empirical Formula: C₂₇H₃₅N₅O₅

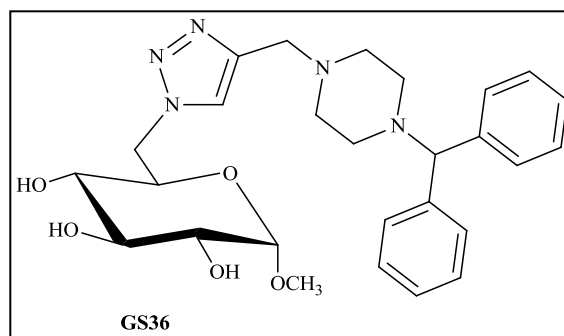
Formula Weight: 509.59 g/mol

Mass spectrum: M+Na, M-H

R_f (EL 6): 0.45

Yield: 65 %

M.p.: 143-147 °C



¹H- NMR (500 MHz, CD₃OD):

δ 7.91 (s, 1H, triazol-H), 7.39 (d, $J = 7.3$ Hz, 4H, **H-Ph**), 7.24 (t, $J = 7.6$ Hz, 4H, **H-Ph**), 7.14 (t, $J = 7.3$ Hz, 2H, **H-Ph**), 4.82 (dd, $J = 14.2, 2.3$ Hz, 1H, **H-6'**), 4.63 (d, $J = 3.7$ Hz, 1H, **H-1 α**), 4.50 (dd, $J = 14.3, 8.2$ Hz, 1H, **H-6**), 4.21 (s, 1H, -CH-), 3.89 – 3.82 (m, 1H, **H-**

5), 3.64 (t, $J = 9.2$ Hz, 1H, **H-3**), 3.38 (dd, $J = 9.7, 3.7$ Hz, 1H, **H-2**), 3.17 – 3.13 (m, 1H, **H-4**), 3.12 (s, 3H, -O-**CH**₃), 2.69 (m, 4H, 2 x -**CH**₂-piperazine), 2.56 – 2.31 (m, 4H, 2 x -**CH**₂-piperazine).

4-[(1-Methyl-6-deoxy- α -D-glucopyranosid-6-yl)-(1H-1,2,3-triazol-4-yl)methyl]-5,5-diphenyl-imidazolidine-2,4-dione (GS37)

Empirical Formula: C₂₅H₂₇N₅O₇

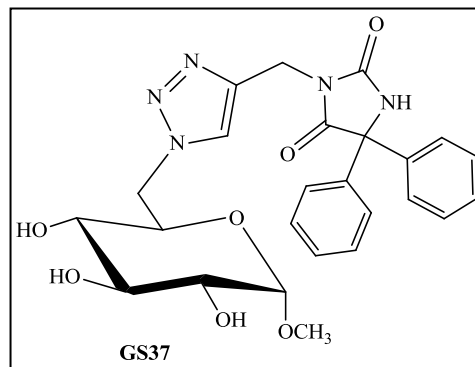
Formula Weight: 509.51 g/mol

Mass spectrum: M+H, M-H

R_f (EL 6): 0.52

Yield: 75 %

M.p.: 145-150 °C



¹H- NMR (500 MHz, CD₃OD):

δ 8.02 (s, 1H, triazol-**H**), 7.92 (s, 1H, **H-NR**), 7.48 – 7.32 (m, 10H, **H-Ph**), 4.93 – 4.82 (m, 1H, **H-6'**), 4.54 (d, $J = 3.7$ Hz, 1H, **H-1 α**), 4.47 (dd, $J = 14.2, 8.6$ Hz, 1H, **H-6**), 3.81 – 3.72 (m, 1H, **H-5**), 3.60 (t, $J = 9.2$ Hz, 1H, **H-3**), 3.36 (m, 1H, **H-2**), 3.13 (dd, $J = 9.9, 8.8$ Hz, 1H, **H-4**), 3.03 (s, 3H, -O-**CH**₃), 2.92 (d, $J = 13.1$ Hz, 2H, -**CH**₂-).

1-(2-Pyrimidinyl)-4-[1-(2,3,4,6-tetra-O-acetyl- β -D-glucopyranosid-1-yl)-(1H-1,2,3-triazol-4-yl)methyl]piperazine (GS38a)

Empirical Formula: C₂₅H₃₃N₇O₉

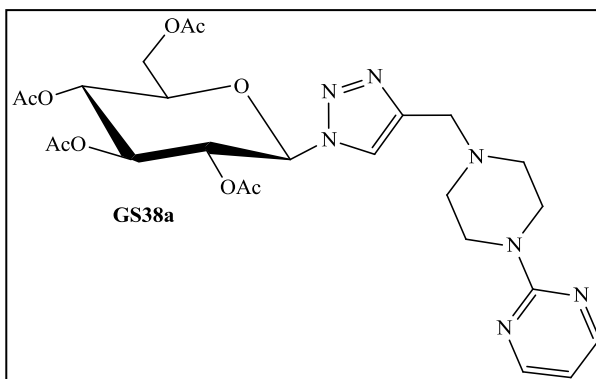
Formula Weight: 575.57 g/mol

Mass spectrum: M+Na, M+H

R_f (EL 5): 0.32

Yield: 71 %

M.p.: 168-173 °C



¹H- NMR (500 MHz, CDCl₃):

δ 8.27 (d, *J* = 4.7 Hz, 2H, 2 x -CH-pyrimidine), 7.73 (s, 1H, triazol-H), 6.45 (t, *J* = 4.7 Hz, 1H, -CH-pyrimidine), 5.84 (d, *J* = 9.2 Hz, 1H, H-1β), 5.44 – 5.36 (m, 2H, H-2, H-3), 5.26 – 5.17 (m, 1H, H-4), 4.30 (dd, *J* = 12.6, 5.0 Hz, 1H, H-6'), 4.14 (dd, *J* = 12.6, 2.0 Hz, 1H, H-6), 4.02 – 3.94 (m, 1H, H-5), 3.86 – 3.78 (m, 4H, 2 x -CH₂-piperazine), 3.71 (d, *J* = 3.6 Hz, 2H, -CH₂-), 2.53 (t, *J* = 5.1 Hz, 4H, 2 x -CH₂-piperazine), 2.07, 2.05, 2.01, 1.83 (4s, 12H, 4 CH₃-Ac).

1-(Diphenylmethyl)-4-[1-(2,3,4,6-tetra-*O*-acetyl-β-D-glucopyranosid-1-yl)-(1*H*-1,2,3-triazol-4-yl)methyl]piperazine (GS39a)

Empirical Formula: C₃₄H₄₁N₅O₉

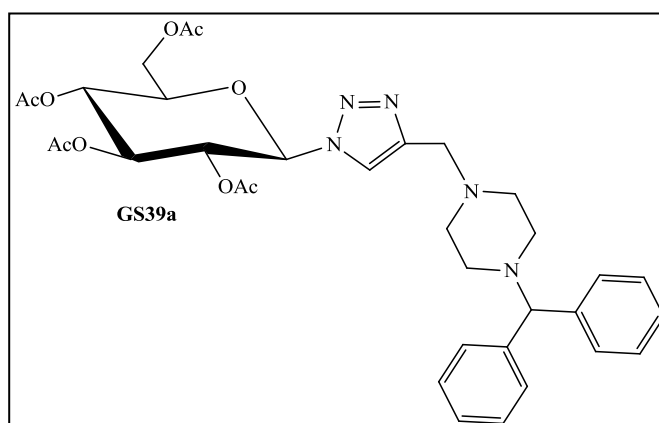
Formula Weight: 663.71 g/mol

Mass spectrum: M+Na, M+H

R_f (EL 2): 0.40

Yield: 70 %

M.p.: 206-210 °C



¹H- NMR (500 MHz, CDCl₃):

δ 7.68 (s, 1H, triazol-H), 7.38 (d, *J* = 8.0 Hz, 4H, H-Ph), 7.28 – 7.21 (m, 4H, H-Ph), 7.15 (t, *J* = 7.3 Hz, 2H, H-Ph), 5.83 (d, *J* = 8.9 Hz, 1H, H-1β), 5.44 – 5.31 (m, 2H, H-2, H-3), 5.21 (t, *J* = 9.5 Hz, 1H, H-4), 4.29 (dd, *J* = 12.6, 5.0 Hz, 1H, H-6'), 4.22 (s, 1H, -CH-), 4.13 (dd, *J* = 12.6, 2.0 Hz, 1H, H-6), 4.01 – 3.94 (m, 1H, H-5), 3.68 (s, 2H, -CH₂-), 2.62 – 2.32 (m, *J* = 44.3 Hz, 8H, 4 x -CH₂-piperazine), 2.08, 2.06, 2.01, 1.84 (4s, 12H, 4 CH₃-Ac).

9-[1-(2,3,4,6-Tetra-*O*-acetyl- β -D-glucopyranosid-1-yl)-(1*H*-1,2,3-triazol-4-yl)methyl]-9*H*-fluoren-9-ol (GS40a)

Empirical Formula: C₃₀H₃₁N₃O₁₀

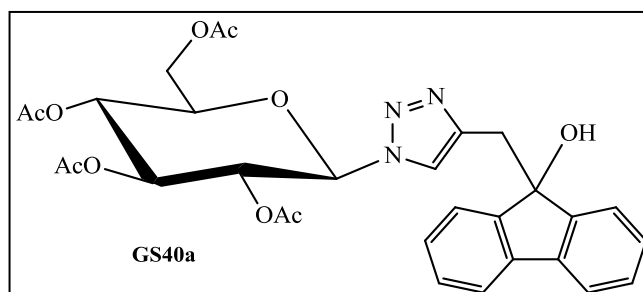
Formula Weight: 593.58 g/mol

Mass spectrum: M+Na

R_f (EL 5): 0.86

Yield: 62 %

M.p.: 207-211 °C



¹H- NMR (500 MHz, CDCl₃):

δ 7.65 (d, J = 7.5 Hz, 2H, **H-Ph**), 7.58 (d, J = 7.4 Hz, 2H, **H-Ph**), 7.36 – 7.29 (m, 2H, **H-Ph**), 7.28 – 7.23 (m, 3H, **H-Ph**, triazol-**H**), 5.16 (t, J = 9.7 Hz, 1H, **H-4**), 5.04 (t, J = 9.8 Hz, 1H, **H-3**), 4.89 (t, J = 9.1 Hz, 1H, **H-2**), 4.59 (d, J = 8.9 Hz, 1H, **H-1 β**), 4.20 (dd, J = 12.5, 4.8 Hz, 1H, **H-6'**), 4.10 (dd, J = 12.5, 2.3 Hz, 1H, **H-6**), 3.78 – 3.70 (m, 1H, **H-5**), 2.84 (d, J = 2.6 Hz, 2H, -**CH₂-**), 2.03, 2.01, 1.96, 1.94 (4s, 12H, 4 **CH₃-Ac**).

2-[1-(2,3,4,6-Tetra-*O*-acetyl- β -D-glucopyranosid-1-yl)-(1*H*-1,2,3-triazol-4-yl)methyl]-1,1-diphenylethanol (GS41a)

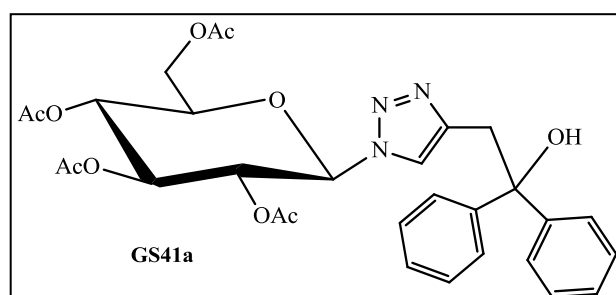
Empirical Formula: C₃₀H₃₃N₃O₁₀

Formula Weight: 595.59 g/mol

Mass spectrum: M+Na

R_f (EL 2): 0.76

Yield: 65 %



¹H- NMR (500 MHz, CD₃OD):

δ 7.88 (s, 1H, triazol-**H**), 7.40 – 7.33 (m, 4H, **H-2',H-6'**), 7.27 – 7.21 (m, 4H, **H-3',H-5'**), 7.20 – 7.14 (m, 2H, **H-4'**), 5.18 – 5.12 (m, 1H, **H-3**), 5.03 (t, J = 9.8 Hz, 1H, **H-4**), 4.92 – 4.83 (m, 1H, **H-2**), 4.58 (d, J = 8.9 Hz, 1H, **H-1 β**), 4.20 (dd, J = 12.5, 4.8 Hz, 1H, **H-6'**),

4.09 (dd, $J = 12.5, 2.3$ Hz, 1H, **H-6**), 3.76 – 3.67 (m, 1H, **H-5**), 3.08 (d, $J = 2.6$ Hz, 2H, -**CH₂-**), 2.01, 2.00, 1.95, 1.93 (4s, 12H, 4 **CH₃-Ac**).

1-(2-Pyrimidinyl)-4-[1-(2,3,4,6-tetra-*O*-acetyl- β -D-galactopyranosid-1-yl)-(1*H*-1,2,3-triazol-4-yl)methyl]piperazine (GS42a)

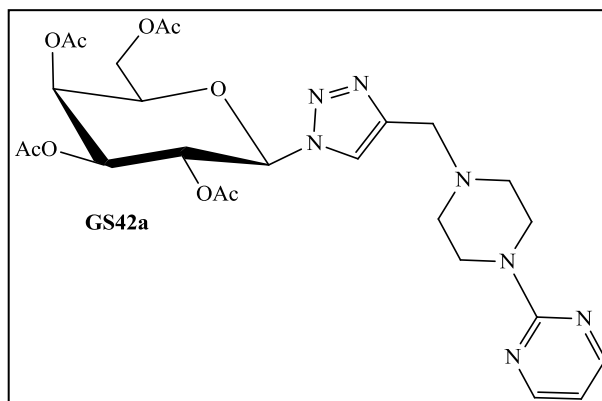
Empirical Formula: C₂₅H₃₃N₇O₉

Formula Weight: 575.57 g/mol

Mass spectrum: M+Na, M+H

R_f (EL 5): 0.23

Yield: 72 %



¹H- NMR (500 MHz, CDCl₃):

δ 8.27 (d, $J = 4.7$ Hz, 2H, 2 x -**CH**-pyrimidine), 7.79 (s, 1H, triazol-**H**), 6.45 (t, $J = 4.7$ Hz, 1H, -**CH**-pyrimidine), 5.81 (d, $J = 9.3$ Hz, 1H, **H-1 β**), 5.52 (dd, $J = 12.1, 6.6$ Hz, 2H, **H-2, H-4**), 5.22 (dd, $J = 10.3, 3.4$ Hz, 1H, **H-3**), 4.27 – 4.08 (m, 3H, **H-6'**, **H-6, H-5**), 3.83 (s, 4H, 2 x -**CH₂**-piperazine), 2.53 (s, 4H, 2 x -**CH₂**-piperazine), 2.20, 2.03, 1.99, 1.84 (4s, 12H, 4 **CH₃-Ac**).

1-(Diphenylmethyl)-4-[1-(2,3,4,6-tetra-*O*-acetyl- β -D-galactopyranosid-1-yl)-(1*H*-1,2,3-triazol-4-yl)methyl]piperazine (GS43a)

Empirical Formula: C₃₄H₄₁N₅O₉

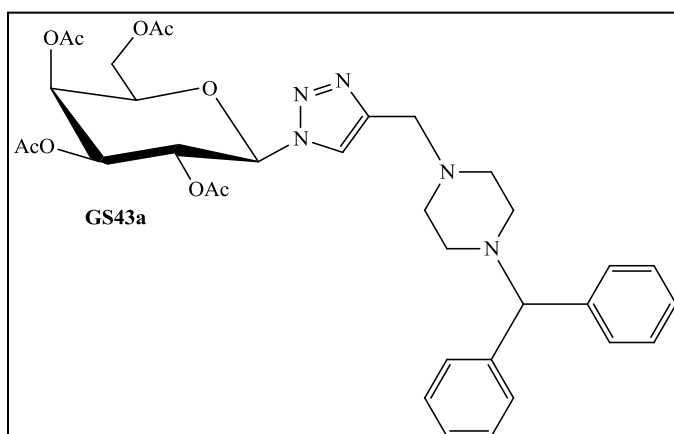
Formula Weight: 663.71 g/mol

Mass spectrum: M+Na

R_f (EL 5): 0.42

Yield: 74 %

M.p.: 193-198 °C



¹H- NMR (500 MHz, CDCl₃):

δ 7.73 (s, 1H, triazol-**H**), 7.40 – 7.34 (m, 4H, **H-Ph**), 7.24 (m, 4H, **H-Ph**), 7.14 (t, $J = 7.3$ Hz, 2H, **H-Ph**), 5.78 (d, $J = 9.3$ Hz, 1H, **H-1 β**), 5.56 – 5.50 (m, 1H, **H-4**), 5.48 (d, $J = 9.4$

Hz, 1H, **H-2**), 5.21 (dd, $J = 10.3, 3.4$ Hz, 1H, **H-3**), 4.25 – 4.07 (m, 4H, **H-6'**, **H-6**, **H-5**, -**CH-**), 3.68 (s, 2H, -**CH₂-**), 2.63 – 2.29 (m, 8H, 4 x -**CH₂-**piperazine), 2.20, 2.02, 1.98, 1.84 (4s, 12H, 4 **CH₃-Ac**).

1-(2,3,4,6-Tetra-*O*-acetyl- β -D-galactopyranosid-1-yl)-(1*H*-1,2,3-triazol-4-yl)methyl]-5,5-diphenyl-imidazolidine-2,4-dione (GS44a)

Empirical Formula: C₃₂H₃₃N₅O₁₁

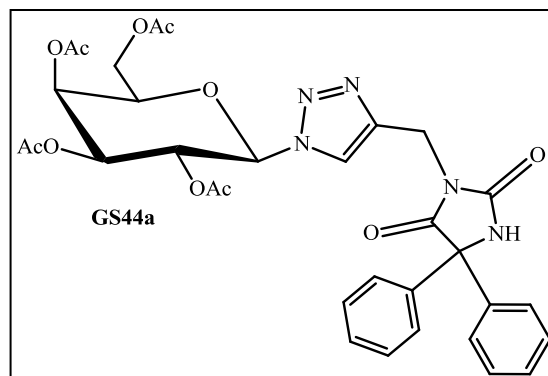
Formula Weight: 663.63 g/mol

Mass spectrum: M+Na, M-H

R_f (EL 5): 0.82

Yield: 73 %

M.p.: 180-185 °C



¹H- NMR (500 MHz, CDCl₃):

δ 7.92 (s, 1H, , triazol-**H**), 7.82 (s, 1H, **H-NR**), 7.36 – 7.21 (m, 10H, **H-Ph**), 5.78 (d, $J = 9.3$ Hz, 1H, **H-1 β**), 5.46 (dd, $J = 11.3, 8.3$ Hz, 2H, **H-2**, **H-4**), 5.19 (dd, $J = 10.3, 3.4$ Hz, 1H, **H-3**), 4.79 (d, $J = 2.8$ Hz, 2H, -**CH₂-**), 4.20 – 4.15 (m, 1H, **H-6'**), 4.14 – 4.08 (m, 1H, **H-5**), 4.04 (dd, $J = 11.4, 6.8$ Hz, 1H, **H-6**), 2.14, 1.96, 1.93, 1.71 (4s, 12H, 4 **CH₃-Ac**).

9-[1-(2,3,4,6-Tetra-*O*-acetyl- β -D-galactopyranosid-1-yl)-(1*H*-1,2,3-triazol-4-yl)methyl]-9*H*-fluoren-9-ol (GS45a)

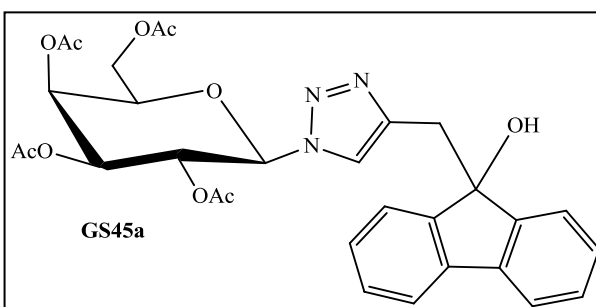
Empirical Formula: C₃₀H₃₁N₃O₁₀

Formula Weight: 593.58 g/mol

Mass spectrum: M+Na

R_f (EL 5): 0.88

Yield: 64 %



¹H- NMR (500 MHz, CDCl₃):

δ 7.57 (t, $J = 7.1$ Hz, 2H, **H-Ph**), 7.39 (s, 1H, triazol-**H**), 7.35 – 7.28 (m, 2H, **H-Ph**), 7.28 – 7.16 (m, 4H, **H-Ph**), 5.77 (d, $J = 9.3$ Hz, 1H, **H-1 β**), 5.49 (d, $J = 2.7$ Hz, 1H, **H-4**), 5.47 –

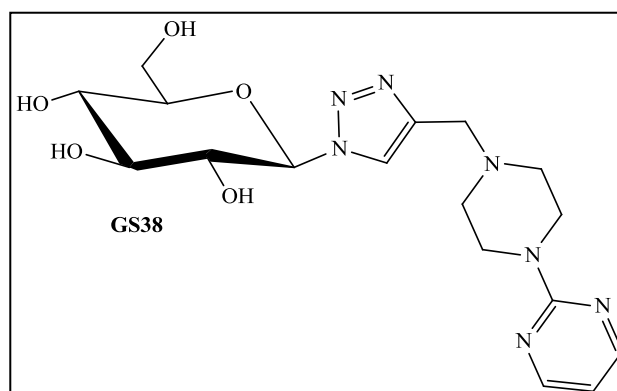
5.40 (m, 1H, **H-2**), 5.20 (dd, $J = 10.3, 3.3$ Hz, 1H, **H-3**), 4.22 – 4.05 (m, 3H, **H-6'**, **H-6**, **H-5**), 3.38 (s, 2H, $-\text{CH}_2-$), 2.18, 2.01, 1.98, 1.87 (4s, 12H, 4 CH_3 -Ac).

6.2.11 Synthesis of Gluco- and Galactotriazol Derivatives

Compounds **GS (38-45)** were treated with sodium methoxide by the same procedure as described above (deacetylation step).

1-(2-Pyrimidinyl)-4-[1-(β -D-glucopyranosid-1-yl)-(1*H*-1,2,3-triazol-4-yl)methyl]piperazine (**GS38**)

Empirical Formula: $\text{C}_{20}\text{H}_{22}\text{N}_2$
 Formula Weight: 407.42 g/mol
 Mass spectrum: $\text{M}+\text{Na}$, $\text{M}-\text{H}$
 R_f (EL 7): 0.28
 Yield: 94 %
 M.p.: 225-228 °C



^1H - NMR (500 MHz, CD_3OD):

δ 8.35 (d, $J = 4.8$ Hz, 2H, 2 x $-\text{CH}$ -pyrimidine), 8.18 (s, 1H, triazol-**H**), 6.62 (t, $J = 4.8$ Hz, 1H, $-\text{CH}$ -pyrimidine), 5.64 (d, $J = 9.2$ Hz, 1H, **H-1 β), 3.97 – 3.89 (m, 2H, **H-2**, **H-4**), 3.88 – 3.82 (m, 4H, 2 x $-\text{CH}_2$ -piperazine), 3.79 (s, 2H, $-\text{CH}_2-$), 3.76 (dd, $J = 12.2, 5.5$ Hz, 1H, **H-3**), 3.65 – 3.57 (m, 3H, **H-6'**, **H-6**, **H-5**), 3.56 – 3.51 (m, 1H, **H-4**), 2.65 – 2.58 (m, 4H, 2 x $-\text{CH}_2$ -piperazine).**

1-(Diphenylmethyl)-4-[1-(β -D-glucopyranosid-1-yl)-(1*H*-1,2,3-triazol-4-yl)methyl]piperazine (GS39)

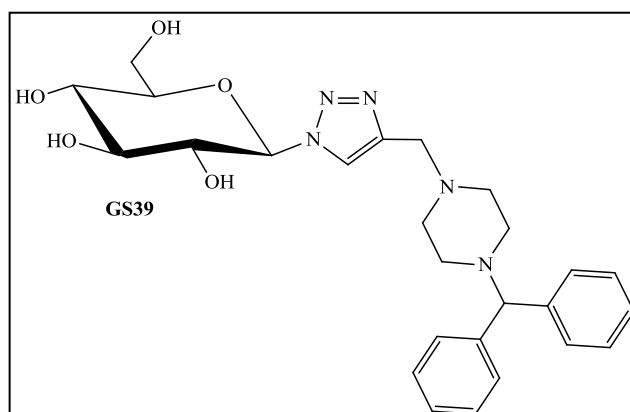
Empirical Formula: C₂₆H₃₃N₅O₅

Formula Weight: 495.57 g/mol

Mass spectrum: M+Na, M-H

R_f (EL 1): 0.85

Yield: 93 %



¹H- NMR (500 MHz, CD₃OD):

δ 8.12 (s, 1H, triazol-**H**), 7.44 (d, $J = 7.6$ Hz, 4H, **H-Ph**), 7.28 (t, $J = 7.6$ Hz, 4H, **H-Ph**), 7.18 (t, $J = 7.4$ Hz, 2H, **H-Ph**), 5.63 (d, $J = 9.2$ Hz, 1H, **H-1 β**), 4.25 (s, 1H, -**CH-**), 3.96 – 3.88 (m, 2H, **H-2**, **H-4**), 3.78 – 3.69 (m, 3H, -**CH**₂-, **H-3**), 3.64 – 3.57 (m, 2H, **H-6'**, **H-6**), 3.56 – 3.50 (m, 1H, **H-5**), 2.71 – 2.35 (m, 8H, 4 x -**CH**₂-piperazine).

9-[1-(β -D-Glucopyranosid-1-yl)-(1*H*-1,2,3-triazol-4-yl)methyl]-9*H*-fluoren-9-ol (GS40)

Empirical Formula: C₂₂H₂₃N₃O₆

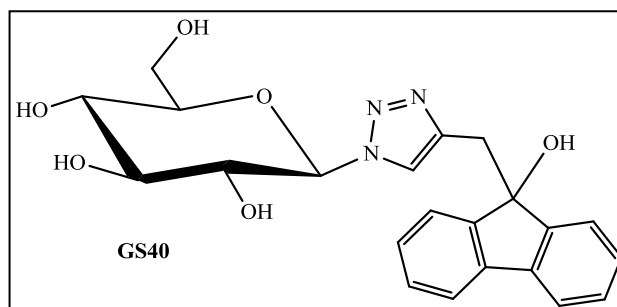
Formula Weight: 425.43 g/mol

Mass spectrum: M+Na

R_f (EL 1): 0.87

Yield: 91 %

M.p.: 185-190 °C



¹H- NMR (500 MHz, CD₃OD):

δ 7.66 (d, $J = 8.2$ Hz, 2H, **H-Ph**), 7.51 (s, 1H, triazol-**H**), 7.38 (dd, $J = 14.5, 7.2$ Hz, 4H, **H-Ph**), 7.33 – 7.26 (m, 2H, **H-Ph**), 5.49 (d, $J = 9.2$ Hz, 1H, **H-1 β**), 3.90 (dd, $J = 12.2, 1.9$ Hz, 1H, **H-6'**), 3.81 (t, $J = 9.2$ Hz, 1H, **H-2**), 3.72 (dd, $J = 12.2, 5.5$ Hz, 1H, **H-6**), 3.59 – 3.47 (m, 3H, **H-3**, **H-4**, **H-5**), 3.46 (d, $J = 3.8$ Hz, 2H, -**CH**₂-).

2-[1-(β-D-Glucopyranosid-1-yl)-(1*H*-1,2,3-triazol-4-yl)methyl]-1,1-diphenylethanol (GS41)

Empirical Formula: C₂₂H₂₅N₃O₆

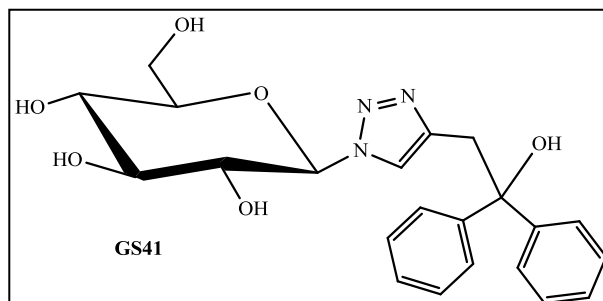
Formula Weight: 427.45 g/mol

Mass spectrum: M+Na, M-H

R_f (EL 2): 0.34

Yield: 93 %

M.p.: 140-155 °C



¹H- NMR (500 MHz, CD₃OD):

δ 7.51 (dd, *J* = 4.5, 3.6 Hz, 5H, triazol-*H*, *H*-2', *H*-6'), 7.31 (t, *J* = 7.8, 2.2 Hz, 4H, *H*-3', *H*-5'), 7.25 – 7.20 (m, 2H, *H*-4'), 5.48 (d, *J* = 9.2 Hz, 1H, *H*-1β), 3.89 (dd, *J* = 12.2, 1.9 Hz, 1H, *H*-6'), 3.83 – 3.77 (m, 3H, -CH₂-, *H*-2), 3.71 (dd, *J* = 12.2, 5.4 Hz, 1H, *H*-6), 3.58 – 3.52 (m, 2H, *H*-3, *H*-5), 3.51 – 3.45 (m, 1H, *H*-4).

1-(2-Pyrimidinyl)-4-[1-(β-D-galactopyranosid-1-yl)-(1*H*-1,2,3-triazol-4-yl)methyl]piperazine (GS42)

Empirical Formula: C₁₇H₂₅N₇O₅

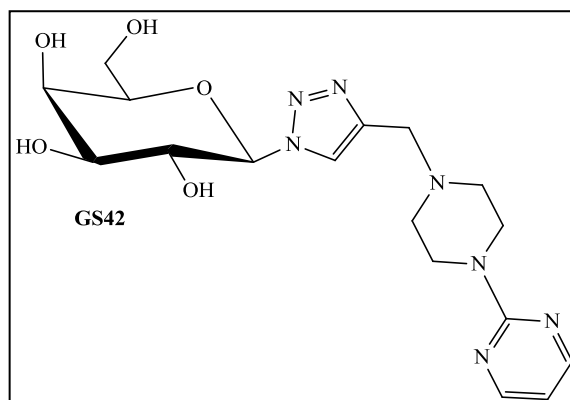
Formula Weight: 407.42 g/mol

Mass spectrum: M+Na, M-H

R_f (EL 1): 0.50

Yield: 93 %

M.p.: 214-218 °C



¹H- NMR (500 MHz, CD₃OD):

δ 8.34 (d, *J* = 4.8 Hz, 2H, 2 x -CH-pyrimidine), 8.22 (s, 1H, triazol-*H*), 6.62 (t, *J* = 4.8 Hz, 1H, -CH-pyrimidine), 5.61 (d, *J* = 9.2 Hz, 1H, *H*-1β), 4.25 – 4.14 (m, 1H, *H*-2), 4.02 (d, *J* = 2.9 Hz, 1H, *H*-4), 3.91 – 3.83 (m, 5H, *H*-6', 2 x -CH₂-piperazin), 3.83 – 3.75 (m, 4H, *H*-6, *H*-5, -CH₂-), 3.74 (dd, *J* = 9.5, 3.3 Hz, 1H, *H*-3), 2.66 – 2.58 (m, 4H, 2 x -CH₂-piperazin).

1-(Diphenylmethyl)-4-[1-(β -D-galactopyranosid-1-yl)-(1H-1,2,3-triazol-4-yl)methyl]piperazine (GS43)

Empirical Formula: $C_{26}H_{33}N_5O_5$

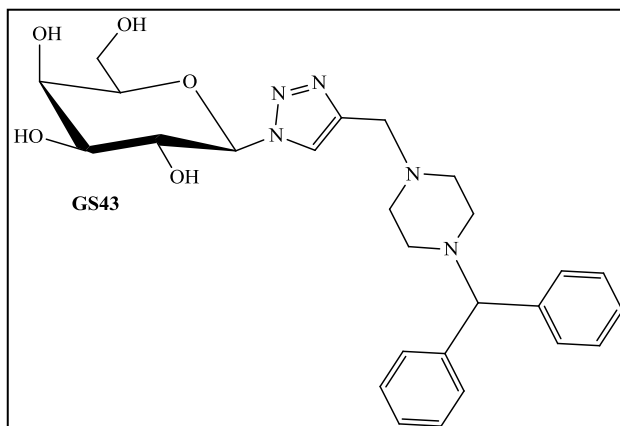
Formula Weight: 495.57 g/mol

Mass spectrum: M+Na, M-H

R_f (EL 1): 0.85

Yield: 92 %

¹H- NMR (400 MHz, CD₃OD):



δ 8.16 (s, 1H, triazol-**H**), 7.43 (d, $J = 7.2$ Hz, 4H, **H-Ph**), 7.27 (t, $J = 7.6$ Hz, 4H, **H-Ph**), 7.21 – 7.14 (m, 2H, **H-Ph**), 5.60 (d, $J = 9.2$ Hz, 1H, **H-1 β), 4.19 (t, $J = 9.3$ Hz, 1H, **H-2**), 4.02 (d, $J = 2.8$ Hz, 1H, -**CH**-), 3.90 – 3.84 (m, 1H, **H-4**), 3.84 – 3.69 (m, 6H, **H-5**, **H-6'**, **H-6**, **H-3**, -**CH**₂-), 2.51 (m, $J = 52.4$ Hz, 8H, 4 x -**CH**₂-piperazine).**

[1-(β -D-Galactopyranosid-1-yl)-(1H-1,2,3-triazol-4-yl)methyl]-5,5-diphenyl-imidazolidine-2,4-dione (GS44)

Empirical Formula: $C_{24}H_{25}N_5O_7$

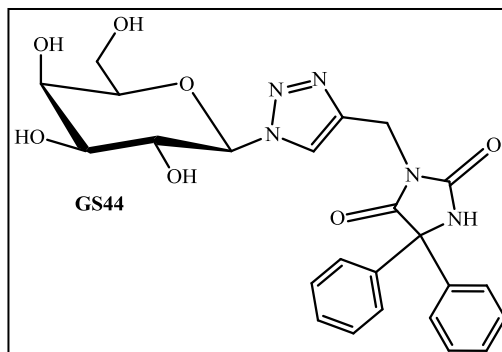
Formula Weight: 495.48 g/mol

Mass spectrum: M+Na, M-H

R_f (EL 1): 0.85

Yield: 94 %

¹H- NMR (400 MHz, CD₃OD):



δ 8.22 (s, 1H, triazol-**H**), 7.44 – 7.33 (m, 10H, **H-Ph**), 5.60 (d, $J = 9.2$ Hz, 1H, **H-1 β), 4.88 (s, 2H, -**CH**₂-), 4.18 (t, $J = 9.3$ Hz, 1H, **H-2**), 4.05 – 3.98 (m, 1H, **H-4**), 3.93 – 3.70 (m, 4H, **H-6**, **H-6'**, **H-5**, **H-3**).**

**9-[1-(β -D-Galactopyranosid-1-yl)-(1*H*-1,2,3-triazol-4-yl)methyl]-9*H*-fluoren-9-ol
(GS45)**

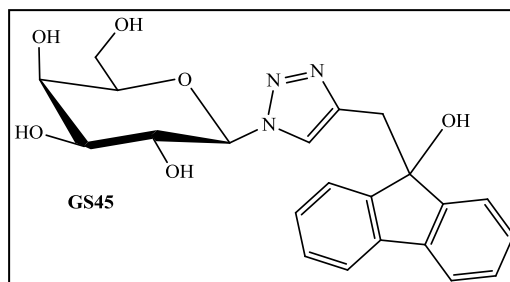
Empirical Formula: C₂₂H₂₃N₃O₆

Formula Weight: 425.43 g/mol

Mass spectrum: M+Na, M-H

R_f (EL 2): 0.90

Yield: 91 %



¹H- NMR (400 MHz, CD₃OD):

δ 7.68 – 7.64 (m, 2H, **H-Ph**), 7.62 (s, 1H, triazol-**H**), 7.40 – 7.34 (m, 4H, **H-Ph**), 7.33 – 7.26 (m, 2H, **H-Ph**), 5.46 (d, $J = 9.2$ Hz, 1H, **H-1 β**), 4.10 (t, $J = 9.4$ Hz, 1H, **H-2**), 3.99 (d, $J = 3.2$ Hz, 1H, **H-4**), 3.86 – 3.80 (m, 1H, **H-6'**), 3.80 – 3.73 (m, 2H, **H-6**, **H-5**), 3.68 (dd, $J = 9.5, 3.3$ Hz, 1H, **H-3**), 3.45 (s, 2H, **-CH₂-**).

7 Bibliography

1. Hanahan, D., Weinberg, R.A., *The hallmarks of cancer*. Cell, 2000, 100 (1), p. 57.
2. Kawabe, T., *G2 checkpoint abrogators as anticancer drugs*. Mol. Cancer Ther., 2004, 3 (4), p. 513.
3. Schermuly, R.T., Dony, E., Ghofrani, H.A., Pullamsetti, S., Savai, R., Roth, M., Sydykov, A., Lai, Y.J., Weissmann, N., Seeger, W., Grimminger, F., *Reversal of experimental pulmonary hypertension by PDGF inhibition*. J. Clin. Invest., 2005, 115 (10), p. 2811.
4. Nakajima, H., Nakajima, H., Toyoshima-Morimoto, F., Taniguchi, E., Nishida, E., *Identification of a consensus motif for Plk (Polo-like kinase) phosphorylation reveals Myt1 as a Plk1 substrate*. J. Biol. Chem., 2003, 278 (28), p. 25277.
5. Mueller, P.R., Coleman, T.R., Kumagai, A., Dunphy, W.G., *Myt1: a membrane-associated inhibitory kinase that phosphorylates Cdc2 on both threonine-14 and tyrosine-15*. Science, 1995, 270 (5233), p. 86.
6. Nakajima, H., Yonemura, S., Murata, M., Nakamura, N., Piwnicka-Worms, H., Nishida, E., *Myt1 protein kinase is essential for Golgi and ER assembly during mitotic exit*. J. Cell Biol., 2008. 181 (1), p. 89.
7. Wang, Y., Decker, S.J., Sebolt-Leopold, J., *Knockdown of Chk1, Wee1 and Myt1 by RNA interference abrogates G2 checkpoint and induces apoptosis*. Cancer Biol. Ther., 2004, 3 (3), p. 305.
8. Choi, H.S., Bode, A.M., Shim, J.H., Lee, S.Y., Dong, Z., *c-Jun N-terminal kinase 1 phosphorylates Myt1 to prevent UVA-induced skin cancer*. Mol. Cell Biol., 2009. 29 (8), p. 2168.
9. Tan, X., Zhai, Y., Chang, W., Hou, J., He, S., Lin, L., Yu, Y., Xu, D., Xiao, J., Ma, L., Wang, G., Cao, T., Cao, G., *Global analysis of metastasis-associated gene expression in primary cultures from clinical specimens of clear-cell renal-cell carcinoma*. Int. J. Cancer, 2008. 123 (5), p. 1080.
10. Bryan, B.A., Dyson, O.F., Akula, S.M., *Identifying cellular genes crucial for the reactivation of Kaposi's sarcoma-associated herpesvirus latency*. J. Gen. Virol., 2006. 87 (Pt 3), p. 519.
11. Vawter, M.P., Harvey, P.D. DeLisi, L.E., *Dysregulation of X-linked gene expression in Klinefelter's syndrome and association with verbal cognition*. Am. J. Med. Genet B Neuropsychiatr Genet, 2007, 144B (6), p. 728.
12. Hashimoto, O., Shinkawa, M., Torimura, T., Nakamura, T., Selvendiran, K., Sakamoto, M., Koga, H., Ueno, T., Sata, M., *Cell cycle regulation by the Wee1 inhibitor PD0166285, pyrido [2,3-d] pyrimidine, in the B16 mouse melanoma cell line*. BMC. Cancer, 2006, 6, p. 292.

13. Hirai, H., Iwasawa, Y., Okada, M., Arai, T., Nishibata, T., Kobayashi, M., Kimura, T., Kaneko, N., Ohtani, J., Yamanaka, K., Itadani, H., Takahashi-Suzuki, I., Fukasawa, K., Oki, H., Nambu, T., Jiang, J., Sakai, T., Arakawa, H., Sakamoto, T., Sagara, T., Yoshizumi, T., Mizuarai, S., Kotani, H., *Small-molecule inhibition of Wee1 kinase by MK-1775 selectively sensitizes p53-deficient tumor cells to DNA-damaging agents*. *Mol. Cancer Ther.*, 2009, 8 (11), p. 2992.
14. Rajeshkumar, N.V., De Oliveira, E., Ottenhof, N., Watters, J., Brooks, D., Demuth, T., Shumway, S.D., Mizuarai, S., Hirai, H., Maitra, A., Hidalgo, M., *MK-1775, a potent Wee1 Inhibitor, synergizes with gemcitabine to achieve tumor regressions, selectively in p53-deficient pancreatic cancer xenografts*. *Clin. Cancer Res.*, 2011, 17 (9), p. 2799.
15. De Witt Hamer, P.C., Mir, S.E., Noske, D., Van Noorden, C.J.F., Wuerdinger, T., *WEE1 kinase targeting combined with DNA-damaging cancer therapy catalyzes mitotic catastrophe*. *Clin. Cancer Res.*, 2011, 17 (13), p. 4200.
16. Zhou, B.N., Tang, S., Johnson, R.K., Mattern, M.P., Lazo, J.S., Sharlow, E.R., Harich, K., Kingston, D.G.I., *New glycolipid inhibitors of Myt1 kinase*. *Tetrahedron*, 2005, 61 (4), p. 883.
17. Kristjansdottir, K., *A fluorescence polarization assay for native protein substrates of kinases I*. *Anal. Biochem.*, 2003, 316 (1), p. 41.
18. Manning, G., *Genomic overview of protein kinases*. *WormBook*, 2005, p. 1.
19. Manning, G., Whyte, D.B., Martinez, R., Hunter, T., Sudarsanam, S., *The protein kinase complement of the human genome*. *Science*, 2002, 298 (5600), p. 1912.
20. Liu, F., Stanton, J.J., Wu, Z., Piwnicka-Worms, H., *The human Myt1 kinase preferentially phosphorylates Cdc2 on threonine 14 and localizes to the endoplasmic reticulum and Golgi complex*. *Mol. Cell Biol.*, 1997, 17 (2), p. 571.
21. Pardee, A.B., *G1 events and regulation of cell proliferation*. *Science*, 1989, 246 (4930), p. 603.
22. Reactome pathway database: *Cell cycle checkpoints*. Accessed on 14.03.2012, available online at: http://www.reactome.org/entitylevelview/pathwaybrowser.html#db=gk_current&focus_species_id=48887&focus_pathway_id=69620&id=69620.
23. Booher, R.N., Holman, P.S., Fattaey, A., *Human Myt1 is a cell cycle-regulated kinase that inhibits Cdc2 but not Cdk2 activity*. *J. Biol. Chem.*, 1997, 272 (35), p. 22300.
24. Gabrielli, B.G., De Souza, C.P., Tonks, I.D., Clark, J.M., Hayward, N.K., Ellem, K.A., *Cytoplasmic accumulation of cdc25B phosphatase in mitosis triggers centrosomal microtubule nucleation in HeLa cells*. *J. Cell Sci.*, 1996, 109 (Pt 5), p. 1081.
25. Boutros, R., Lobjois, V., Ducommun, B., *CDC25 phosphatases in cancer cells: key players? Good targets?*. *Nat. Rev. Cancer*, 2007, 7 (7), p. 495.

26. Yang, J., Bardes, E.S., Moore, J.D., Brennan, J., Powers, M.A., Kornbluth, S., *Control of cyclin B1 localization through regulated binding of the nuclear export factor CRM1*. *Genes Dev.*, 1998, 12 (14), p. 2131.
27. Squire, C.J., Dickson, J.M., Ivanovic, I., Baker, E.N., *Structure and inhibition of the human cell cycle checkpoint kinase, Wee1A kinase: an atypical tyrosine kinase with a key role in CDK1 regulation*. *Structure*, 2005, 13 (4), p. 541.
28. Rohe, A., Erdmann, F., Bassler, C., Wichapong, K., Sippl, W., Schmidt, M., *In vitro and in silico studies on substrate recognition and acceptance of human PKMYT1, a Cdk1 inhibitory kinase*. *Bioorg. Med. Chem. Lett.*, 2012, 22 (2), p. 1219.
29. Barr, F.A., Sillje, H.H., Nigg, E.A., *Polo-like kinases and the orchestration of cell division*. *Nat. Rev. Mol. Cell Biol.*, 2004, 5 (6), p. 429.
30. Reactome Pathway database: *Cell cycle, M., Mitotic G2-G2/M phases; G2/M-Transition; Polo -like kinase mediated events [Homo sapiens]*. Accessed on 13.03. 2012, available online at http://www.reactome.org/entitylevelview/pathway_browser.html#db=gk_current&focus_species_id=48887&focus_pathway_id=453274&id=156711.
31. McGowan, C.H., Russell, P., *Human Wee1 kinase inhibits cell division by phosphorylating p34cdc2 exclusively on Tyr15*. *EMBO J.*, 1993, 12 (1), p. 75.
32. Watanabe, N., Broome, M., Hunter, T., *Regulation of the human WEE1Hu CDK tyrosine 15-kinase during the cell cycle*. *EMBO J.*, 1995, 14 (9), p. 1878.
33. Owens, L., Simanski, S., Squire, C., Smith, A., Cartzendafner, J., Cavett, V., Caldwell Busby, J., Sato, T., Ayad, N.G., *Activation domain-dependent degradation of somatic Wee1 kinase*. *J. Biol. Chem.*, 2010, 285 (9), p. 6761.
34. Enders, G.H., *Gauchos and ochos: a Wee1-Cdk tango regulating mitotic entry*. *Cell Div.*, 2010, 5, p. 12.
35. Li, C., Andrade, M., Dunbrack, R., Enders, G.H., *A bifunctional regulatory element in human somatic Wee1 mediates cyclin A/Cdk2 binding and Crm1-dependent nuclear export*. *Mol. Cell Biol.*, 2010, 30 (1), p. 116.
36. Touny, L.H., Banerjee, P.P., *Identification of both Myt-1 and Wee-1 as necessary mediators of the p21-independent inactivation of the cdc-2/cyclin B1 complex and growth inhibition of TRAMP cancer cells by genistein*. *Prostate*, 2006, 66 (14), p. 1542.
37. Wells, N.J., Watanabe, N., Tokusumi, T., Jiang, W., Verdecia, M.A., Hunter, T., *The C-terminal domain of the Cdc2 inhibitory kinase Myt1 interacts with Cdc2 complexes and is required for inhibition of G(2)/M progression*. *J. Cell Sci.*, 1999, 112 (Pt 19), p. 3361.
38. Liu, F., Rothblum-Oviatt, C., Ryan, C.E., Piwnicka-Worms, H., *Overproduction of human Myt1 kinase induces a G2 cell cycle delay by interfering with the intracellular trafficking of Cdc2-cyclin B1 complexes*. *Mol. Cell Biol.*, 1999, 19 (7), p. 5113.

39. Matsuura, I., Wang, J.H., *Demonstration of cyclin-dependent kinase inhibitory serine / threonine kinase in bovine thymus*. J. Biol. Chem., 1996, 271 (10), p. 5443.
40. Inoue, D., Sagata, N., *The Polo-like kinase Plx1 interacts with and inhibits Myt1 after fertilization of Xenopus eggs*. EMBO J., 2005, 24 (5), p. 1057.
41. Blasina, A., de Weyer, I.V., Laus, M.C., Luyten, W.H., Parker, A.E., McGowan, C.H., *A human homologue of the checkpoint kinase Cds1 directly inhibits Cdc25 phosphatase*. Curr. Biol., 1999, 9 (1), p. 1.
42. Chaikuad, A., Eswaran, J., Fedorov, O., Cooper, C., Kroeler, T., Vollmar, M., Krojer, T., Berridge, G., Muniz, J.R.C., Pike, A.C.W., von Delft, F., Weigelt, J., Arrowsmith, C.H., Edwards, A.M., Bountra, C., Knapp, S., *Human protein kinase Myt1*. Accessed on 12/03/2012, available online at: http://www.thesgc.org/structures/structure_description/3P1A/.
43. Krishnamurty, R., Maly, D.J., *Biochemical mechanisms of resistance to small-molecule protein kinase inhibitors*. ACS Chem. Biol., 2010, 5 (1), p. 121.
44. Levitzki, A., Gazit, A., *Tyrosine kinase inhibition: an approach to drug development*. Science, 1995, 267 (5205), p. 1782.
45. Hanks, S.K., Quinn, A.M., Hunter, T., *The protein kinase family: conserved features and deduced phylogeny of the catalytic domains*. Science, 1988, 241 (4861), p. 42.
46. Lee, J.C., Adams, J.L., *Inhibitors of serine/threonine kinases*. Curr. Opin. Biotechnol., 1995, 6 (6), p. 657.
47. Morphy, R., *Selectively nonselective kinase inhibition: striking the right balance*. J. Med. Chem., 2010, 53 (4), p. 1413.
48. Liu, Y., Gray, N.S. *Rational design of inhibitors that bind to inactive kinase conformations*. Nat. Chem. Biol., 2006, 2 (7), p. 358.
49. Schermuly, R.T., Dony, E., Ghofrani, H.A., Pullamsetti, S., Savai, R., Roth, M., Sydykov, A., Lai, Y.J., Weissmann, N., Seeger, W., Grimminger, F., *Reversal of experimental pulmonary hypertension by PDGF inhibition*. J. Clin. Invest., 2005, 115 (10), p. 2811.
50. [Http://www.ema.europa.eu/docs/en_gb/document_library/epar_-_summary_for_the_public/human/000709/wc500056993.pdf](http://www.ema.europa.eu/docs/en_gb/document_library/epar_-_summary_for_the_public/human/000709/wc500056993.pdf). (Online)
51. Hantschel, O., Rix, U., Superti-Furga, G., *Target spectrum of the BCR-ABL inhibitors imatinib, nilotinib and dasatinib*. Leuk Lymphoma, 2008, 49 (4), p. 615.
52. Weisberg, E., Manley, P.W., Cowan-Jacob, S.W., Hochhaus, A., Griffin, J.D., *Second generation inhibitors of BCR-ABL for the treatment of imatinib-resistant chronic myeloid leukaemia*. Nat. Rev. Cancer, 2007, 7(5), p. 345.
53. Jonsson, S., Olsson, B., Ohlsson, C., Lorentzon, M., Mellstrom, D., Wadenvik, H., *Increased cortical bone mineralization in imatinib treated patients with chronic myelogenous leukemia*. Haematologica, 2008, 93 (7), p. 1101.

54. DeAngelo, D.J., Attar, E.C., *Use of dasatinib and nilotinib in imatinib-resistant chronic myeloid leukemia: translating preclinical findings to clinical practice*. Leuk Lymphoma, 2010, 51 (3), p. 363.
55. Leijen, S., Beijnen, J.H., Schellens, J.H., *Abrogation of the G2 checkpoint by inhibition of Wee-1 kinase results in sensitization of p53-deficient tumor cells to DNA-damaging agents*. Curr. Clin. Pharmacol., 2010, 5 (3), p. 186.
56. Bridges, K.A., Hirai, H., Buser, C.A., Brooks, C., Liu, H., Buchholz, T.A., Molkenhine, J.M., Mason, K.A., Meyn, R.E., *MK-1775, a novel Wee1 kinase inhibitor, radiosensitizes p53-defective human tumor cells*. Clin. Cancer. Res., 2011, 17 (17), p. 5638.
57. Patent, *Myt1 kinase inhibitors*, US 6391894 (B1) 2002.
58. Patent, *Myt1 kinase inhibitors*, WO 0164680 (A1) 2001.
59. Patent, *Myt1 kinase inhibitors*, WO 0033837 (A2) 2000.
60. Gollner, C., Philipp, C., Dobner, B., Sippl, W., Schmidt, M., *First total synthesis of 1,2-dipalmitoyl-3-(N-palmitoyl-6'-amino-6'-deoxy-alpha-D-glucosyl)-sn-glycerola glycolipid of a marine alga with a high inhibitor activity against human Myt1-kinase*. Carbohydr. Res., 2009, 344 (13), p. 1628.
61. Sauer, B., *Etablierung einer neuen klasse ATP-kompetitiver hemmstoffe der PKMYT1*, Department of Medicinal Chemistry, Martin-Luther-University Halle-Wittenberg, 2012.
62. Meutermans, W., Le, G.T., Becker, B., *Carbohydrates as scaffolds in drug discovery*. Chem. Med. Chem., 2006, 1 (11), p. 1164.
63. McMurry, J., *Organic Chemistry, Cornell University*, 7th Ed, 2008
64. Lech, A.M.M., *Principles and Application*, Prentice Hall, 2001.
65. Höltje, H., Sippl, W., Rognan, D., Folkers, G., *Molecular modelling. Basic principles and applications*. Wiley-VCH, Weinheim, 3rd Ed, 2008.
66. Jones, G., Willett, P., Glen, R.C., Leach, A.R., Taylor, R., *Development and validation of a genetic algorithm for flexible docking*. J. Mol. Biol., 1997, 267 (3), p. 727.
67. Jones, G., Willett, P., Glen, R.C., *A genetic algorithm for flexible molecular overlay and pharmacophore elucidation*. J. Comput. Aided. Mol. Des., 1995, 9 (6), p. 532.
68. Verdonk, M.L., Cole, J.C., Hartshorn, M.J., Murray, C.W., Taylor, R.D., *Improved protein-ligand docking using GOLD*. Proteins, 2003, 52 (4), p. 609.
69. Jones, G., Willett, P., Glen, R.C., *Molecular recognition of receptor sites using a genetic algorithm with a description of desolvation*. J. Mol. Biol., 1995, 245 (1), p. 43.

70. Wichapong, K., Lawson, M., Pianwanit, S., Kokpol, S., Sippl, W., *Postprocessing of protein-ligand docking poses using linear response MM-PB/SA: application to Wee1 kinase inhibitors*. J. Chem. Inf. Model., 2010, 50 (9), p. 1574.
71. Wichapong, K., Lindner, M., Pianwanit, S., Kokpol, S., Sippl, W., *Receptor-based 3D-QSAR studies of checkpoint Wee1 kinase inhibitors*. Eur. J. Med. Chem., 2009, 44 (4), p. 1383.
72. Robina, I., Lopez-Barba, E. Fuentes, J., *Fatty acylamino-trisaccharides. Synthesis and some stereochemical properties*. Tetrahedron, 1996, 52 (32), p. 10771.
73. Eby, R., Schuerch, C., *Use of 1-O-tosyl-D-glucopyranose derivatives in α -D-glucoside synthesis*. Carbohydr. Res., 1974, 34 (1), p. 79.
74. Weijers, C.A., Franssen, M.C., Visser, G.M., *Glycosyltransferase-catalyzed synthesis of bioactive oligosaccharides*. Biotechnol. Adv., 2008, 26 (5), p. 436.
75. Schmidt, R.R., Castro-Palomino, J.C., Retz, O., *New aspects of glycoside bond formation*. Pure. Appl. Chem., 1999, 71 (5), p. 729.
76. Schmidt, R.R., Michel, J., *Simple syntheses of α - and β -O-glycosyl imidates; preparation of glycosides and disaccharides*. Angew. Chem., 1980, 92 (9), p. 763.
77. Urban, F.J., Moore, B.S., Breitenbach, R., *Synthesis of tigogenyl β -O-cellobioside heptaacetate and glycoside tetraacetate via Schmidt's trichloroacetimidate method; some new observations*. Tetrahedron Lett., 1990, 31 (31), p. 4421.
78. Schmidt, R.R., *New Methods for the Synthesis of Glycosides and Oligosaccharides-Are There Alternatives to the Koenigs-Knorr Method? [New Synthetic Methods (56)]*. Angew. Chem., Int. Ed. Engl., 1986, 25 (3), p. 212.
79. Schmidt, R.R., Michel, J., *Facile synthesis of α - and β -O-glycosyl imidates; preparation of glycosides and disaccharides*. Angew. Chem., Int. Ed. Engl., 1980, 19, p. 731.
80. Qiu, D.X., Wang, Y.F., Caj, H.S., *Studies on Glycosides VI. Facile Synthesis of Alkyl α - and β -D-Glucopyranosides*. Synth. Commun., 1989, 19 (20), p. 3453.
81. Deng, S., Gangadharmath, U., Chang, C.W., *Sonochemistry: a powerful way of enhancing the efficiency of carbohydrate synthesis*. J. Org. Chem., 2006, 71 (14), p. 5179.
82. Adinolfi, M., Adinolfi, M., Barone, G., Iadonisi, A., Schiattarella, M., *Efficient activation of glycosyl N-(phenyl)trifluoroacetimidate donors with ytterbium(III) triflate in the glycosylation reaction*. Tetrahedron Lett., 2002, 43 (32), p. 5573.
83. Sadashiva, C.T., Narendra Sharath Chandra, J.N., Ponnappa, K.C., Veerabasappa Gowda, T., Rangappa, K.S., *Synthesis and efficacy of 1-[bis(4-fluorophenyl)-methyl]piperazine derivatives for acetylcholinesterase inhibition, as a stimulant of central cholinergic neurotransmission in Alzheimer's disease*. Bioorg. Med. Chem. Lett., 2006, 16 (15), p. 3932.

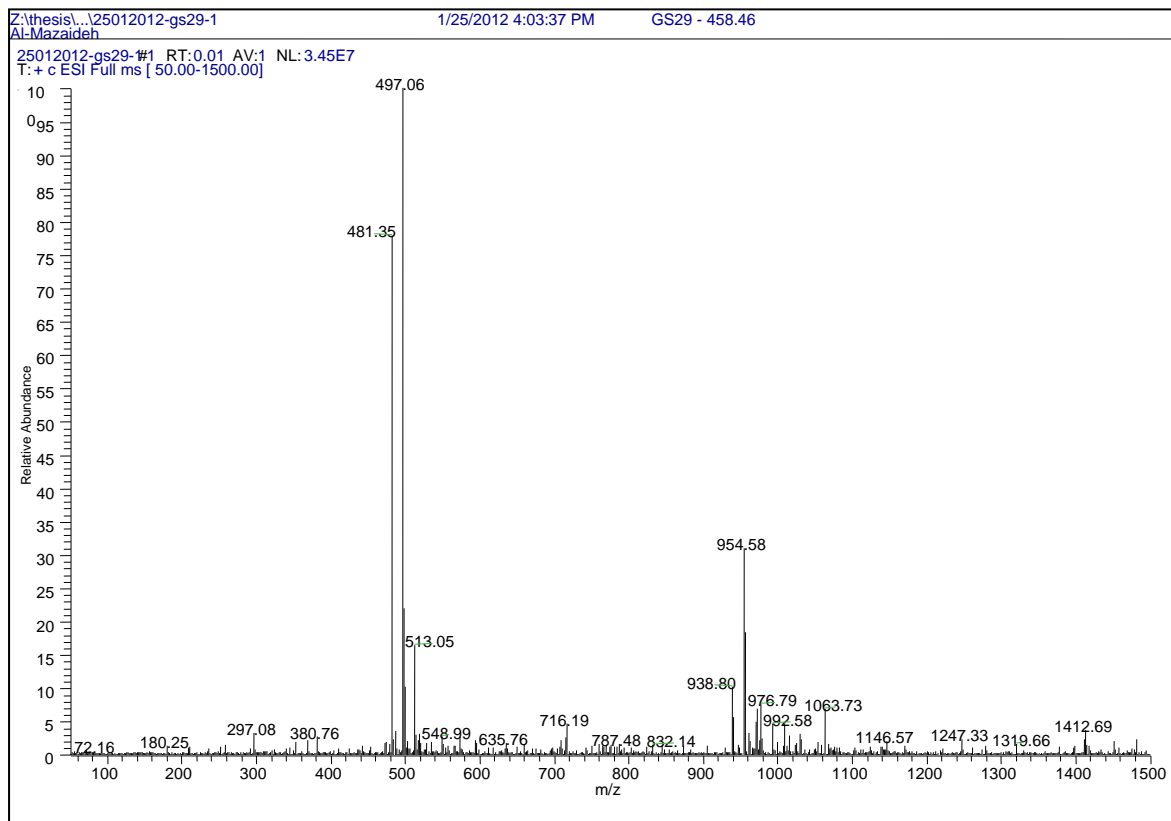
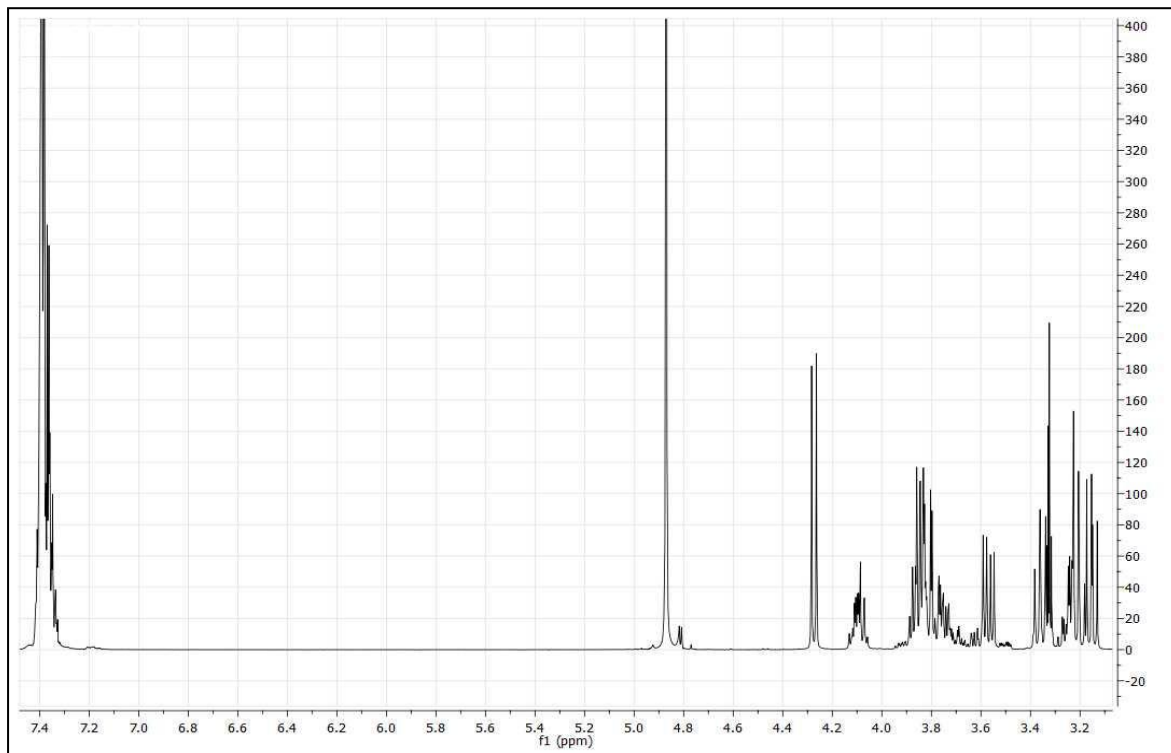
84. Schmolka, S.J., Zimmer, H., *N-Dimethylaminopropylation in a solid-liquid two-phase system: synthesis of chlorpromazine, its analogs, and related compounds*, Synthesis, 1984 (1), p. 29.
85. Komissarenko, N.A., *Synthesis of 1- ω -(benzhydrylpiperayin-1-)alkyljindoles, 9-13-(4-benzhydrylpiperazin-1-yl)propyl)carbazole and its derivatives and their antiallergic activity*. Khim. Farm. Zh., 1990. 24 (10), p. 751
86. Kosasayama, A., Konno, T., Higashi, K., Ishikawa, F., *Cyclic Guanidines. V., Cyclic Guanidines. V. Synthesis of Hypoglycemic 2,2- and 3,3-Diphenylimidazo [1,2-a] [1,3]-diazacycloalkane Derivatives*. Chem. pharm. bull., 1979. 27 (4), p. 848
87. Bieg, T., Szeja, W., *Removal of O-benzyl protective groups by catalytic transfer hydrogenation*. Synthesis, 1985 (1), p. 76.
88. Dobbelaar, P.H., Marzabadi, C.H., *Povarov reactions of exo-glycols: preparation of C-linked, quinoline analogs*. Tetrahedron, 2011, 67 (48), p. 9273.
89. Excoffier, G., Gagnare, D., Utile, J.P , *Synthesis of oligosaccharides on polymeric supports. V. Selective cleavage by hydrazine of the anomeric acetyl groups of acetylated glycosyl residues*. Carbohydr. Res., 1975, 39 (2), p. 368.
90. Herzner, H., Eberling, J., Schultz, M., Zimmer, J., Kunz, H., *Oligosaccharide Synthesis via Electrophile-Induced Activation of Glycosyl-N-Allylcarbamates*. J. carbohydr. chem., 1998, 17 (4), p. 759.
91. Kolb, H.C., Finn, M.G. Sharpless, K.B., *Click chemistry: diverse chemical function from a few good reactions*. Angew. Chem., Int. Ed. Engl., 2001, 40 (11), p. 2004.
92. Binder, W.H., Sachsenhofer, R., *'Click' chemistry in polymer and materials science*. Macromol. Rapid. Commun., 2007, 28 (1), p. 15.
93. Huisgen, R., Szeimies, G. Moebius, L., *1,3-Dipolar cycloadditions. XXXII. Kinetics of the addition of organic azides to carbon-carbon multiple bonds*. Chem. Ber., 1967, 100 (8), p. 2494.
94. Meldal, M., Tornøe, C.W., *Cu-catalyzed azide-alkyne cycloaddition*. Chem. Rev., 2008, 108 (8), p. 2952.
95. Tornøe, C.W., Christensen, C., Meldal, M., *Peptidotriazoles on solid phase: [1,2,3]-triazoles by regioselective copper(I)-catalyzed 1,3-dipolar cyclo- additions of terminal alkynes to azides*. J. Org. Chem., 2002, 67 (9), p. 3057.
96. Rostovtsev, V.V., Green, L.G., Fokin, V.V., Sharpless, K.B., *A stepwise huisgen cycloaddition process: copper(I)-catalyzed regioselective "ligation" of azides and terminal alkynes*. Angew. Chem. , Int. Ed. Engl., 2002, 41 (14), p. 2596.
97. Himo, F., Lovell, T., Hilgraf, R., Rostovtsev, V.V., Noodleman, L., Sharpless, K. B., Fokin, V.V., *Copper(I)-Catalyzed Synthesis of Azoles. DFT Study Predicts Unprecedented Reactivity and Intermediates*. J. Am. Chem. Soc., 2005, 127 (1), p. 210.

98. Ogawa, T., Nakabayashi, S., Shibata, S., *Synthetic studies on cell surface glycans. Part XVIII. Synthetic studies on nephritogenic glycosides. Synthesis of N-(β -L-aspartyl)- α -D-glucopyranosylamine.* Agric. Biol. Chem., 1983, 47 (2), p. 281.
99. Usifoh, C.O., *Anticonvulsant activity of reaction products of 5,5-diphenylhydantoin with substituted methylene bromides.* Arch. Pharm. (Weinheim), 2001, 334 (11), p. 366.
100. Dedola, S., Nepogodiev, S.A., Field, R.A., *Recent applications of the Cu(I)-catalysed Huisgen azide-alkyne 1,3-dipolar cycloaddition reaction in carbohydrate chemistry.* Org. Biomol. Chem., 2007, 5(7), p. 1006.
101. Carvalho, I., Andrade, P., Campo, V.L., Guedes, P.M.M., Sesti-Costa, R., Silva, J. S., Schenkman, S., Dedola, S., Hill, L., Rejzek, M., Nepogodiev, S.A., Field, R.A., *'Click chemistry' synthesis of a library of 1,2,3-triazole-substituted galactose derivatives and their evaluation against Trypanosoma cruzi and its cell surface trans-sialidase.* Bioorg. Med. Chem., 2010, 18 (7), p. 2412.
102. Davis, M.I., Hunt, J.P., Herrgard, S., Ciceri, P., Wodicka, L.M., Pallares, G., Hocker, M., Treiber, D.K., Zarrinkar, P.P., *Comprehensive analysis of kinase inhibitor selectivity.* Nat. Biotechnol., 2011, 29 (11), p. 1046.
103. Becker, H.G.O., Berger, W., Domscke, G., *Organikum*, Deutscher Verlag der Wissenschaften, 1974.

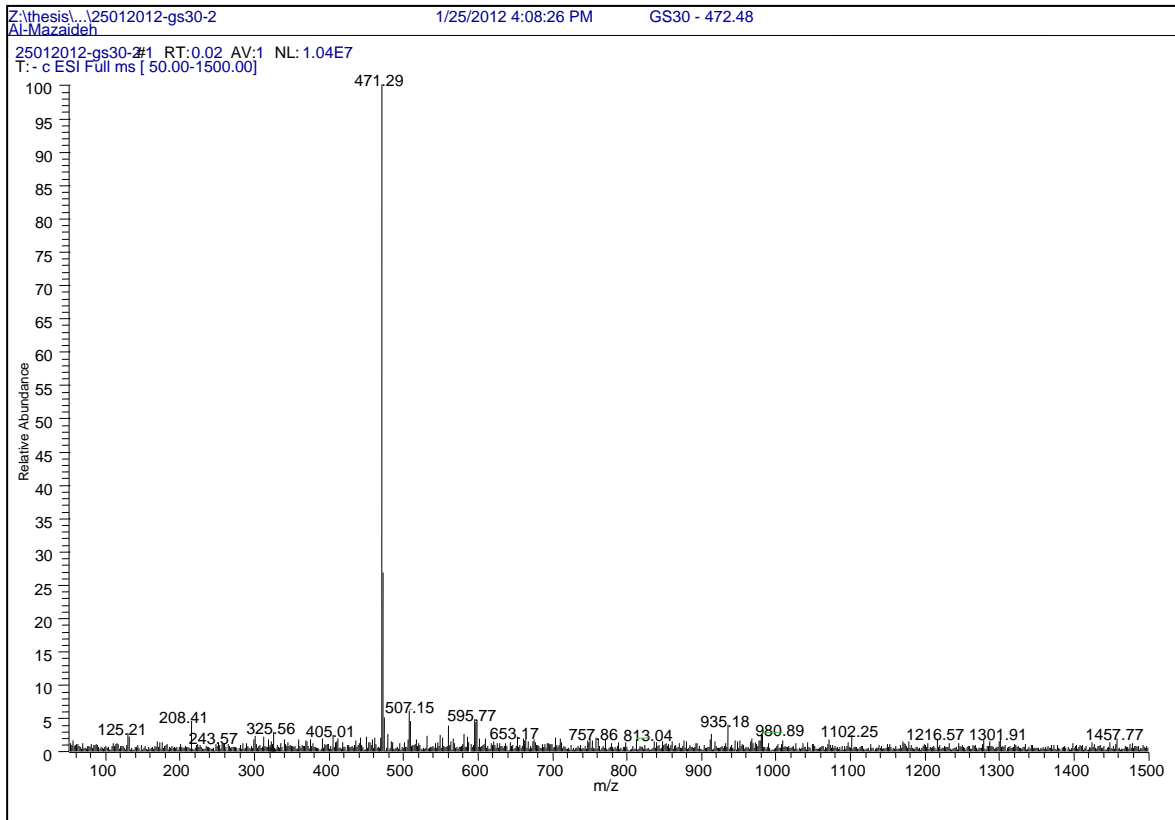
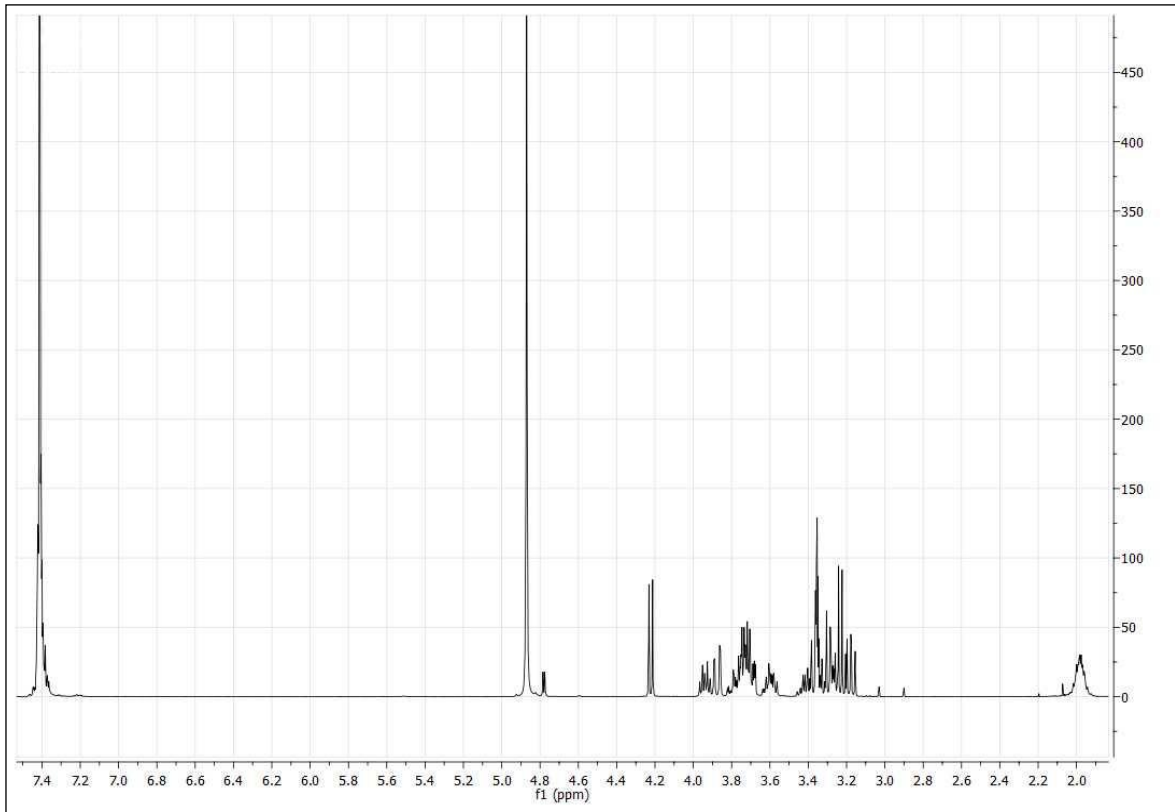
8 Appendix

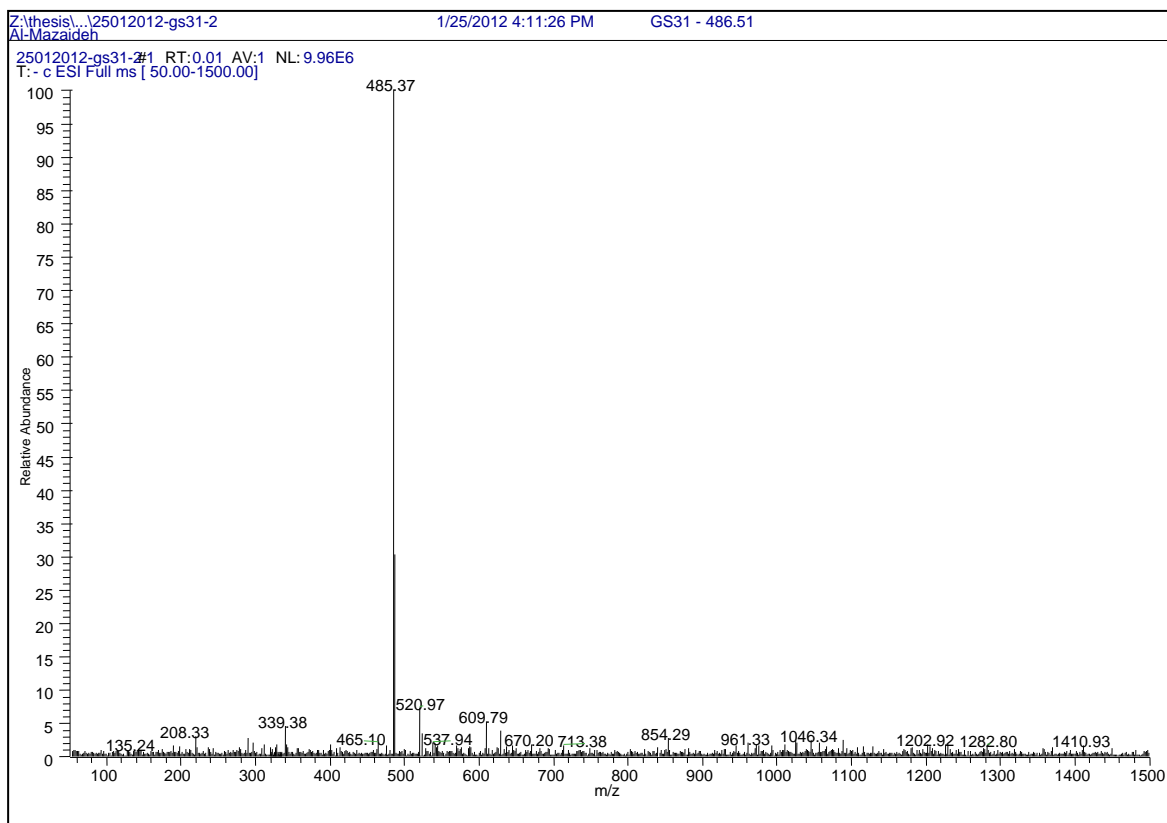
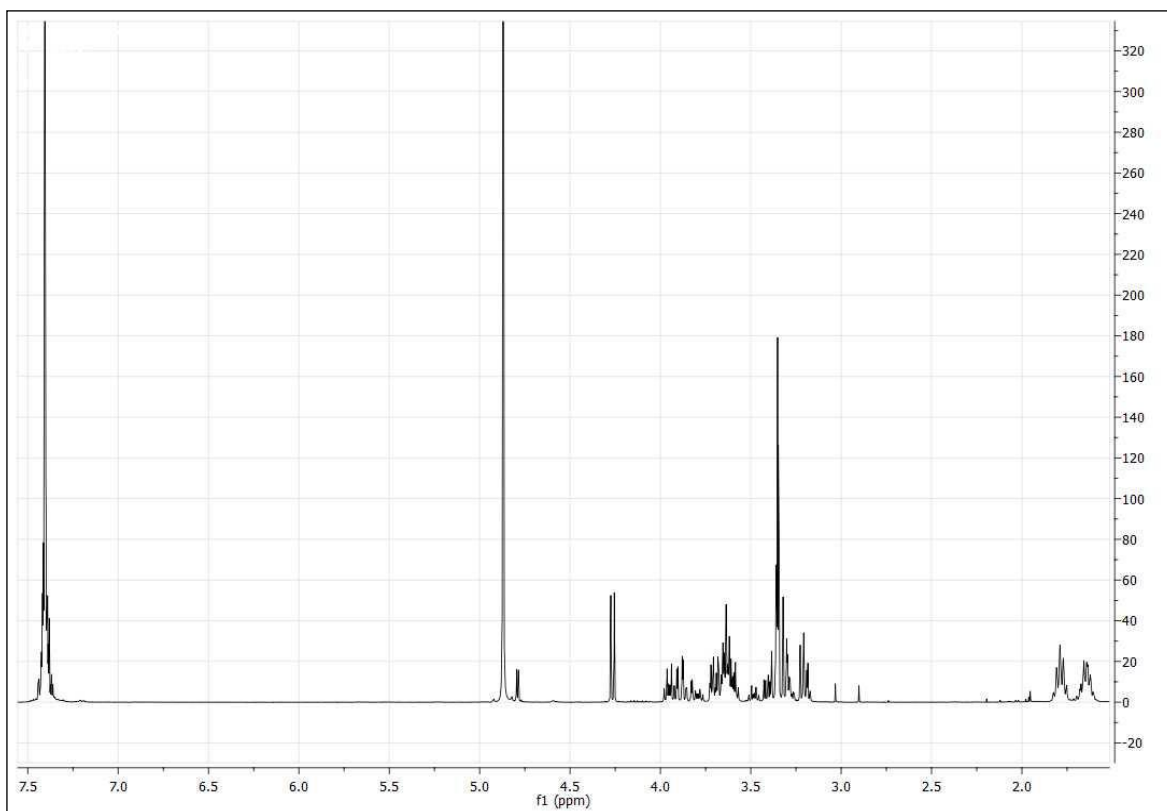
¹H-NMR spectra and ESI mass spectra of final compounds.

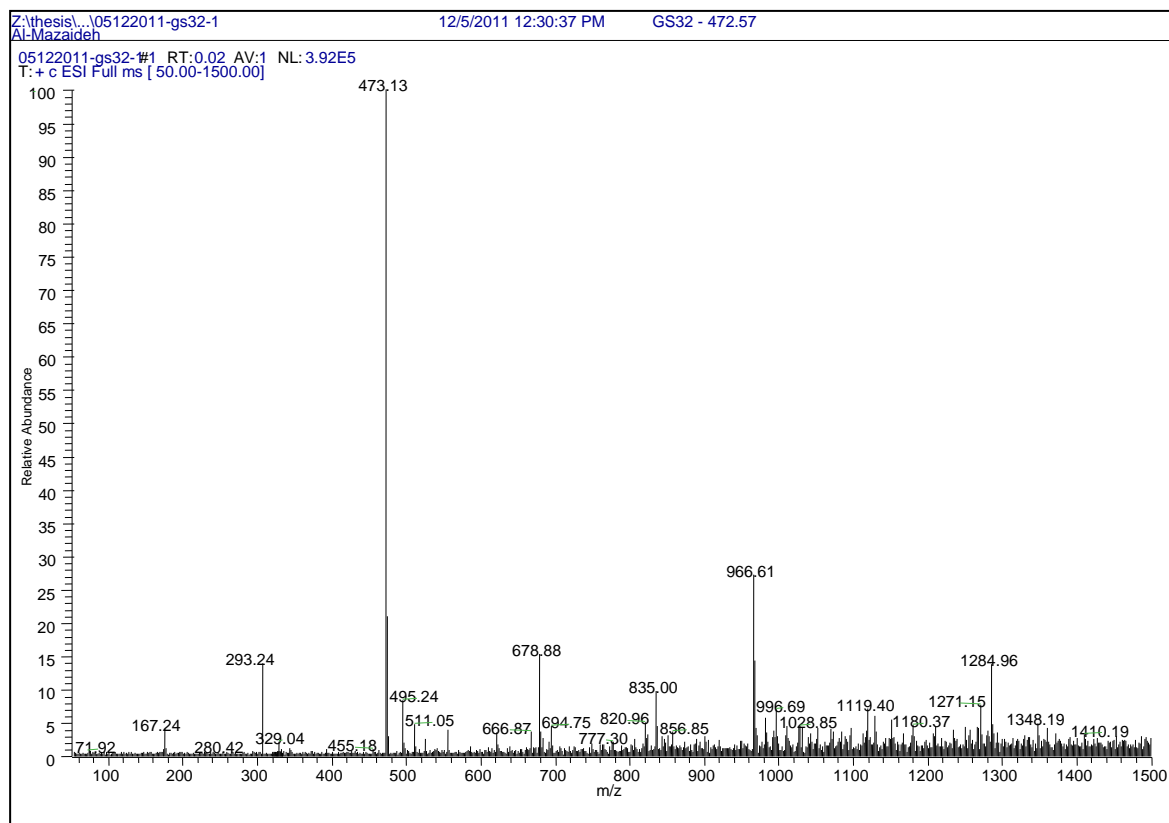
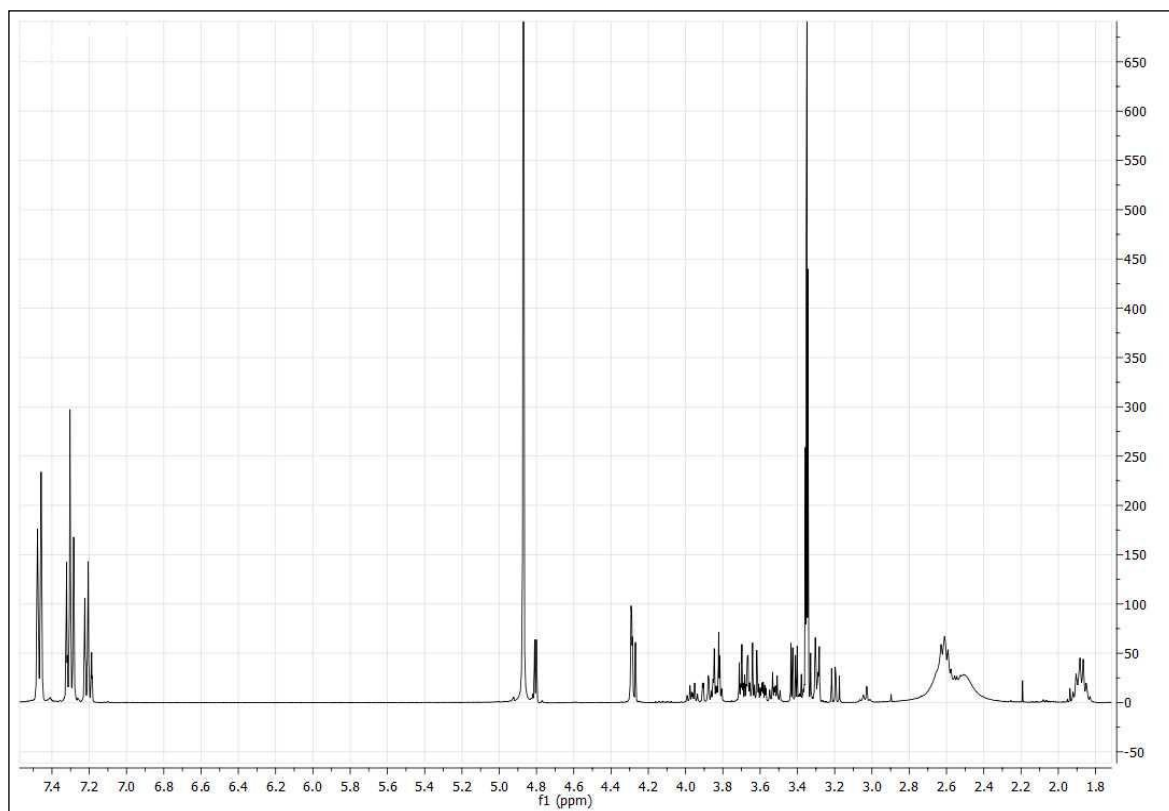
3-[2-(D-Glucopyranosidyl)ethyl]-5,5-diphenyl-imidazolidine-2,4-dione (GS29)

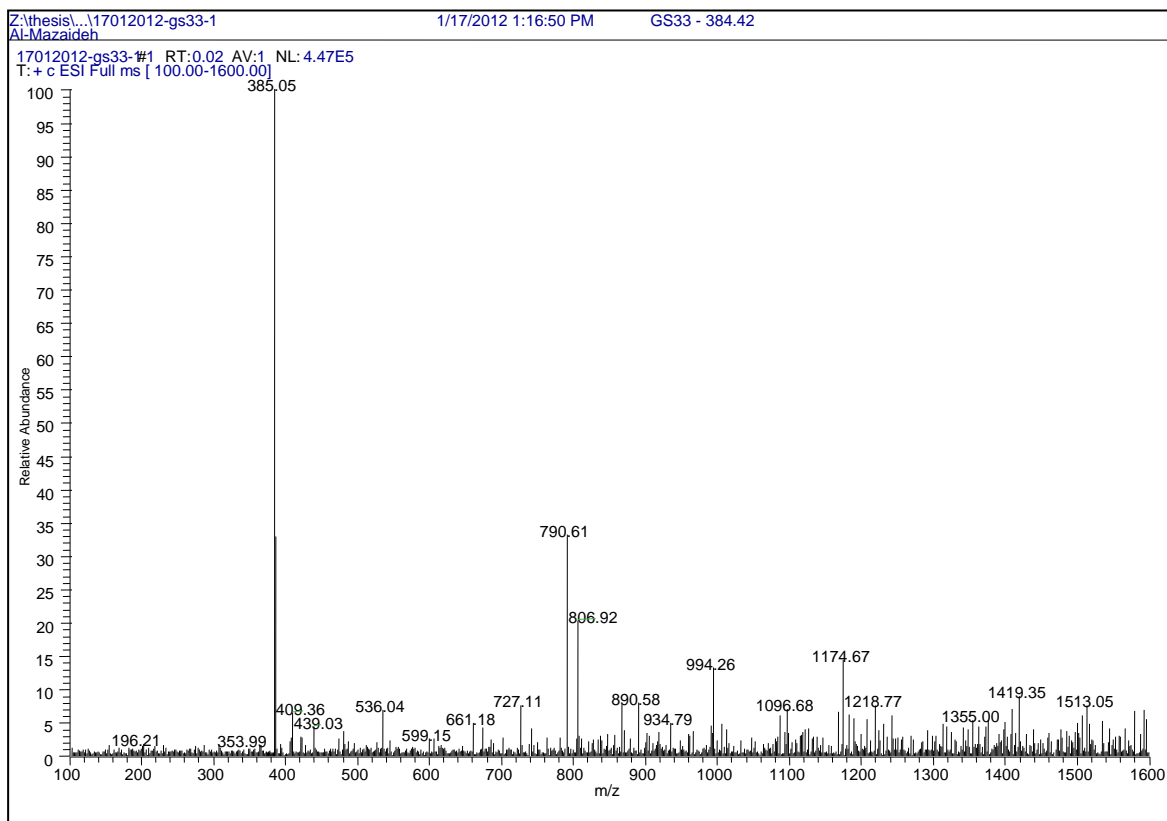
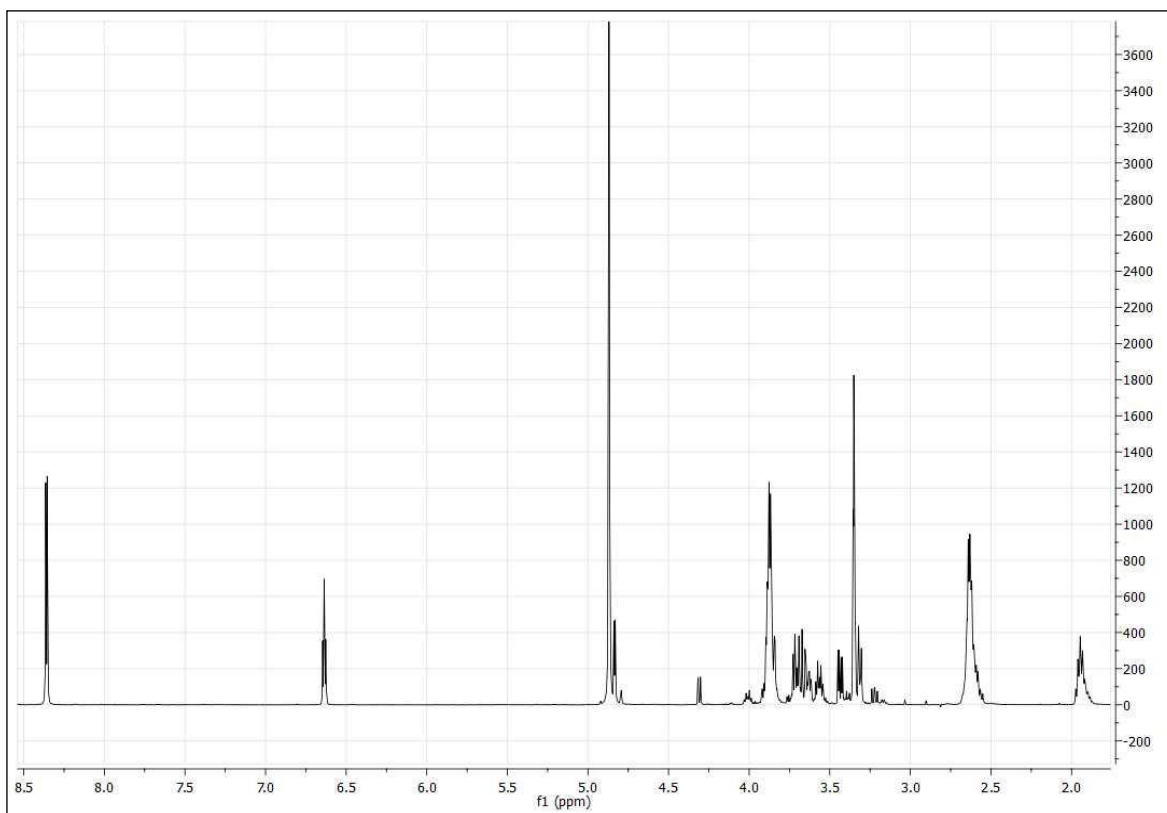


3-[3-(D-Glucoopyranosidyl)propyl]-5,5-diphenyl-imidazolidine-2,4-dione (GS30)

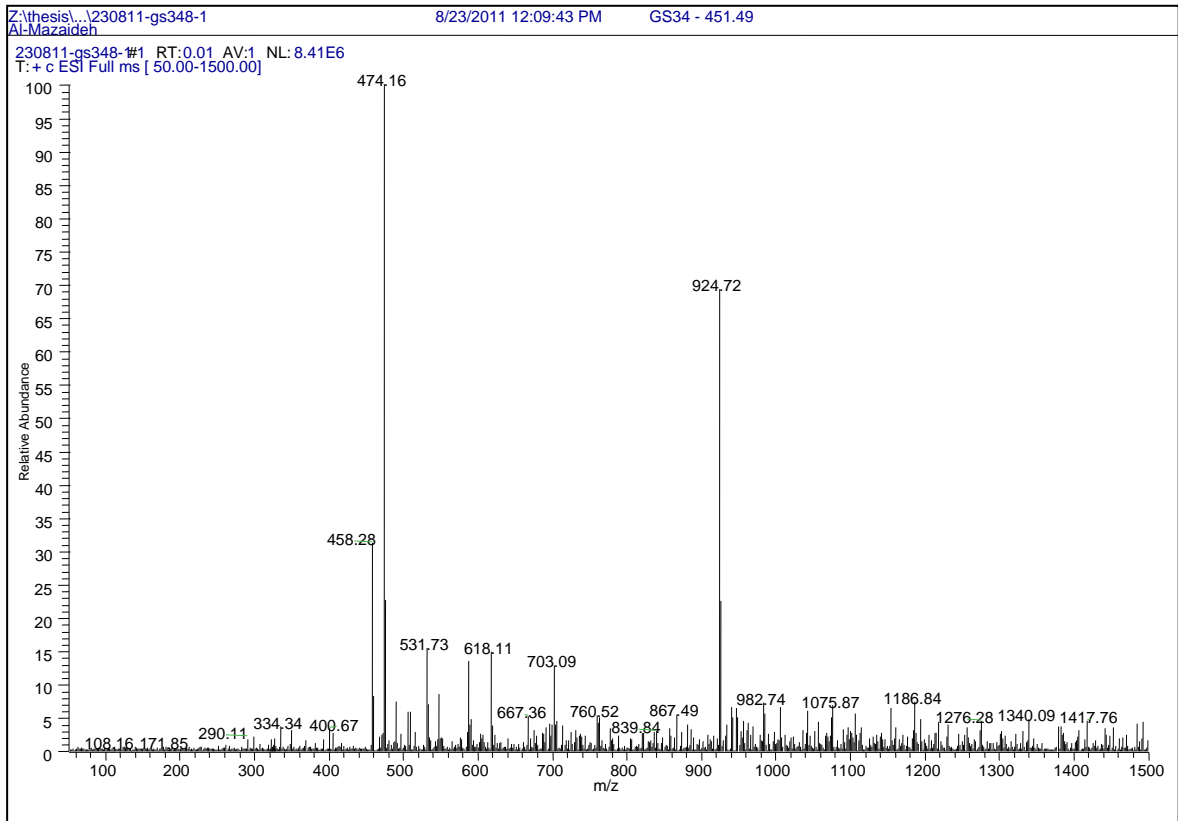
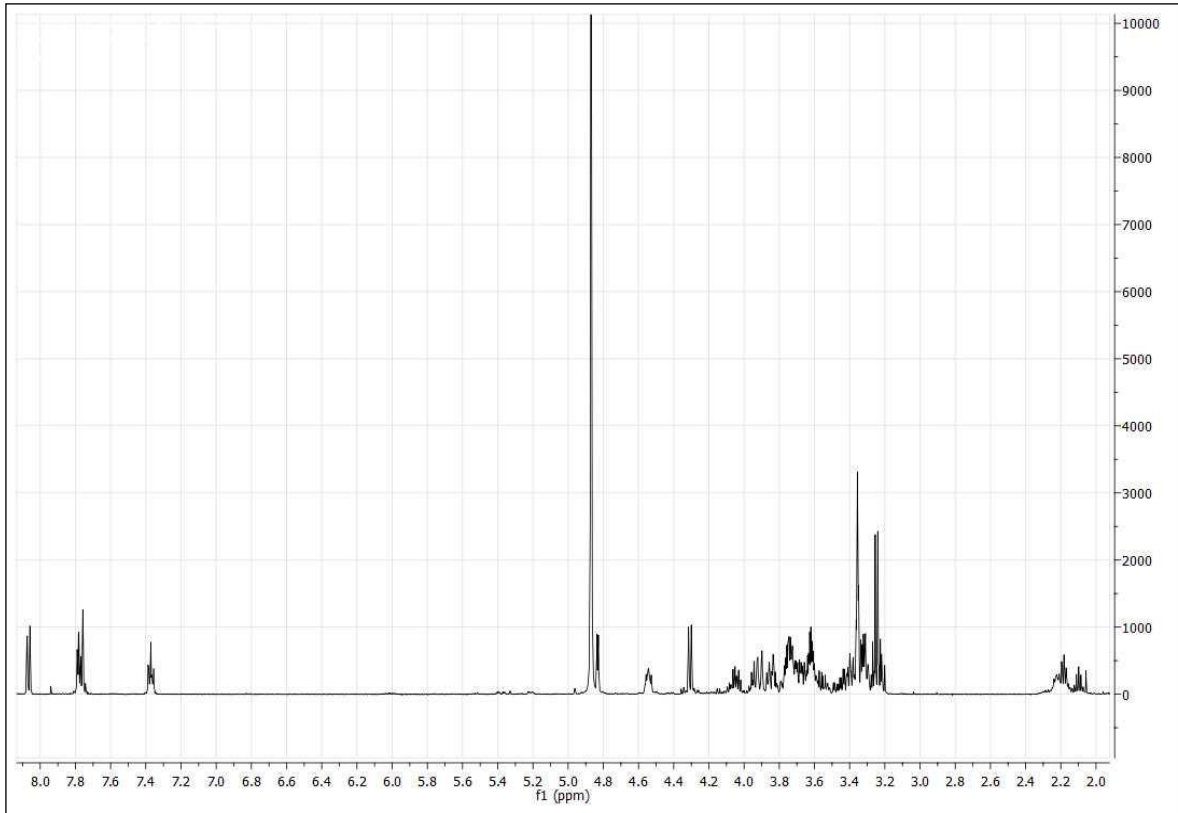


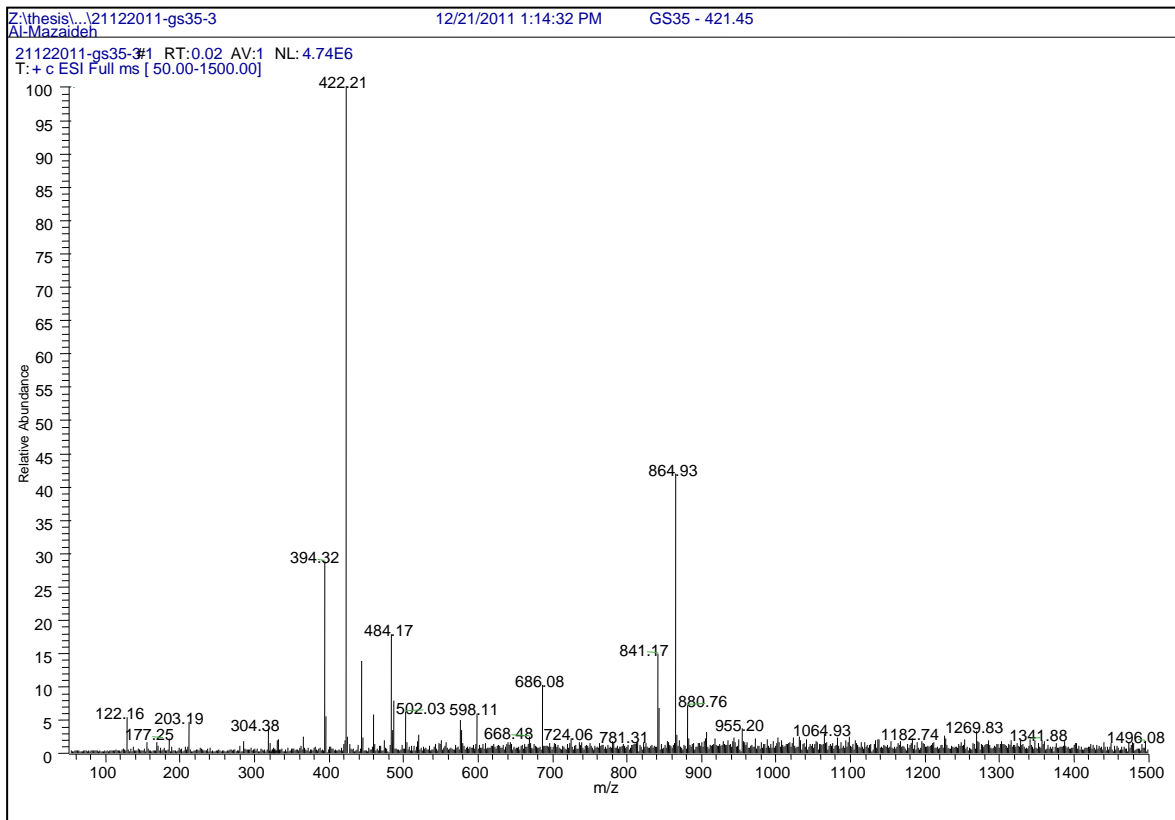
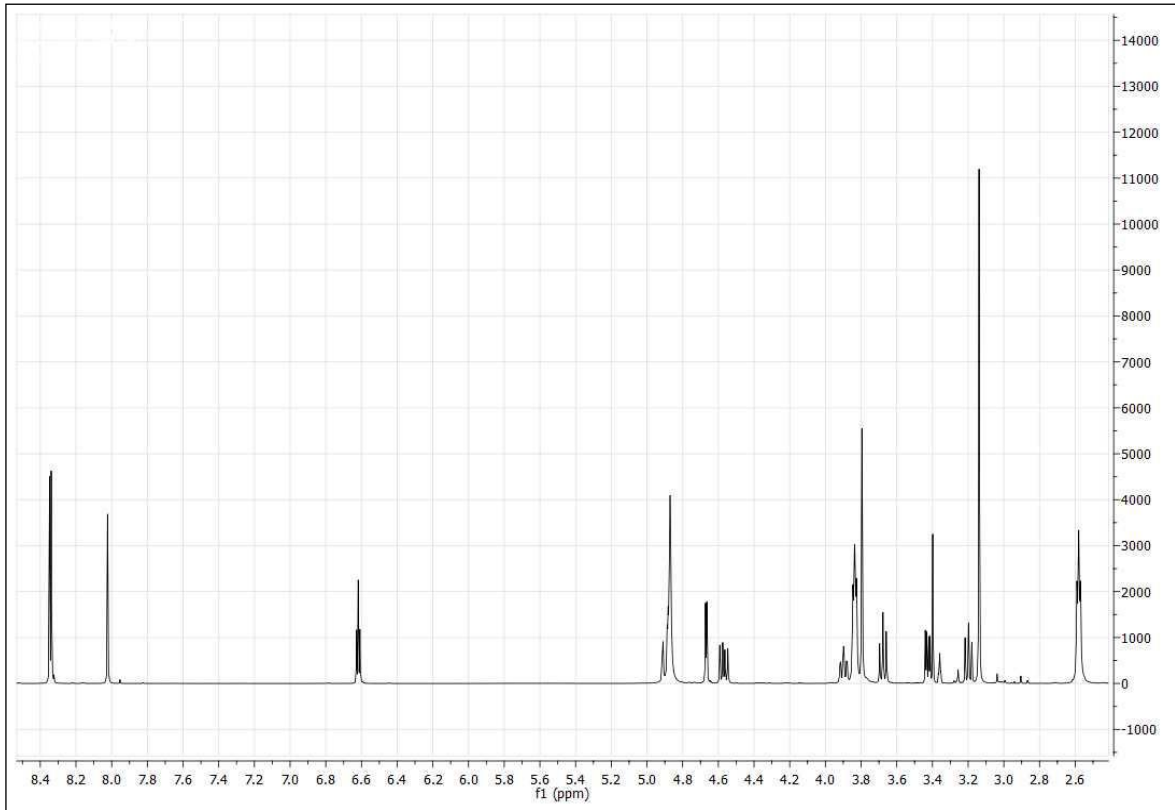
3-[4-(D-Glucopyranosidyl)butyl]-5,5-diphenyl-imidazolidine-2,4-dione (GS31)

1-(Diphenylmethyl)-4-[3-(D-glucopyranosidyl)propyl]piperazine (GS32)

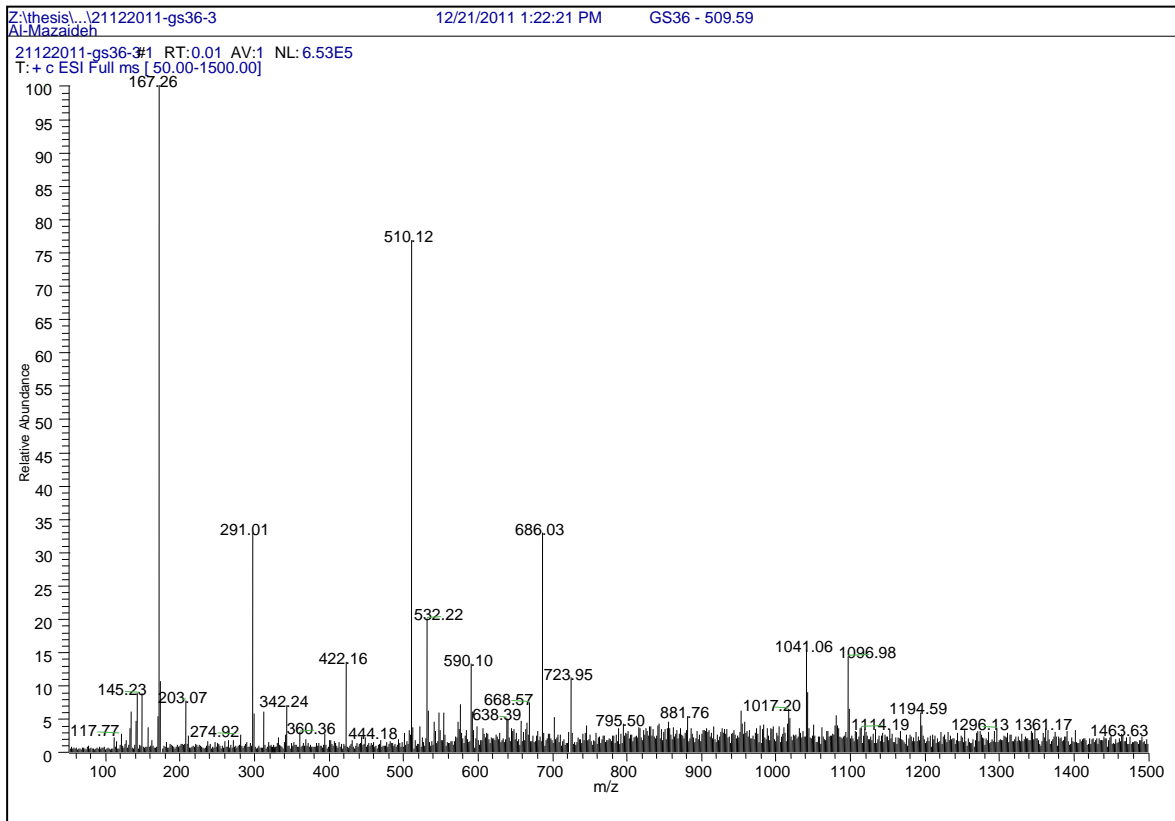
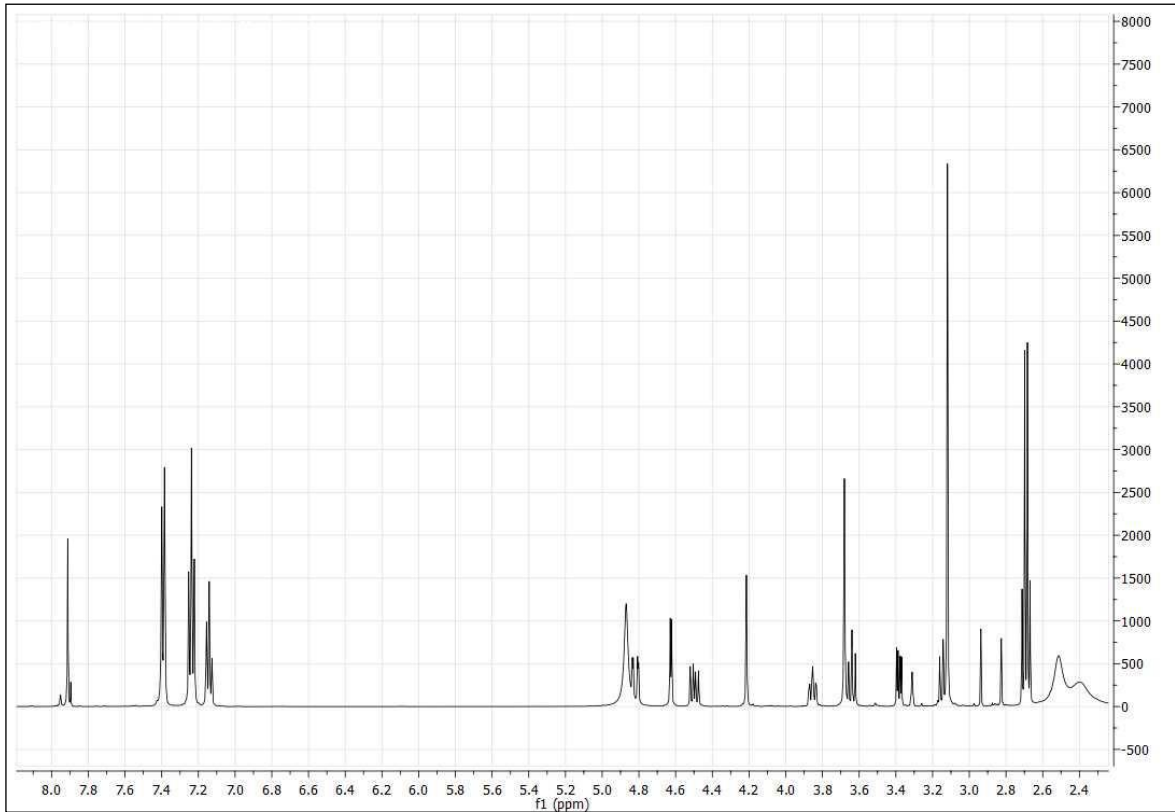
1-(2-Pyrimidinyl)-4-[3-(D-glucopyranosidyl)propyl]piperazine (GS33)

10-[3-(D-Glucopyranosidyl)propyl]-10H-phenothiazine-5,5-dioxide (GS34)

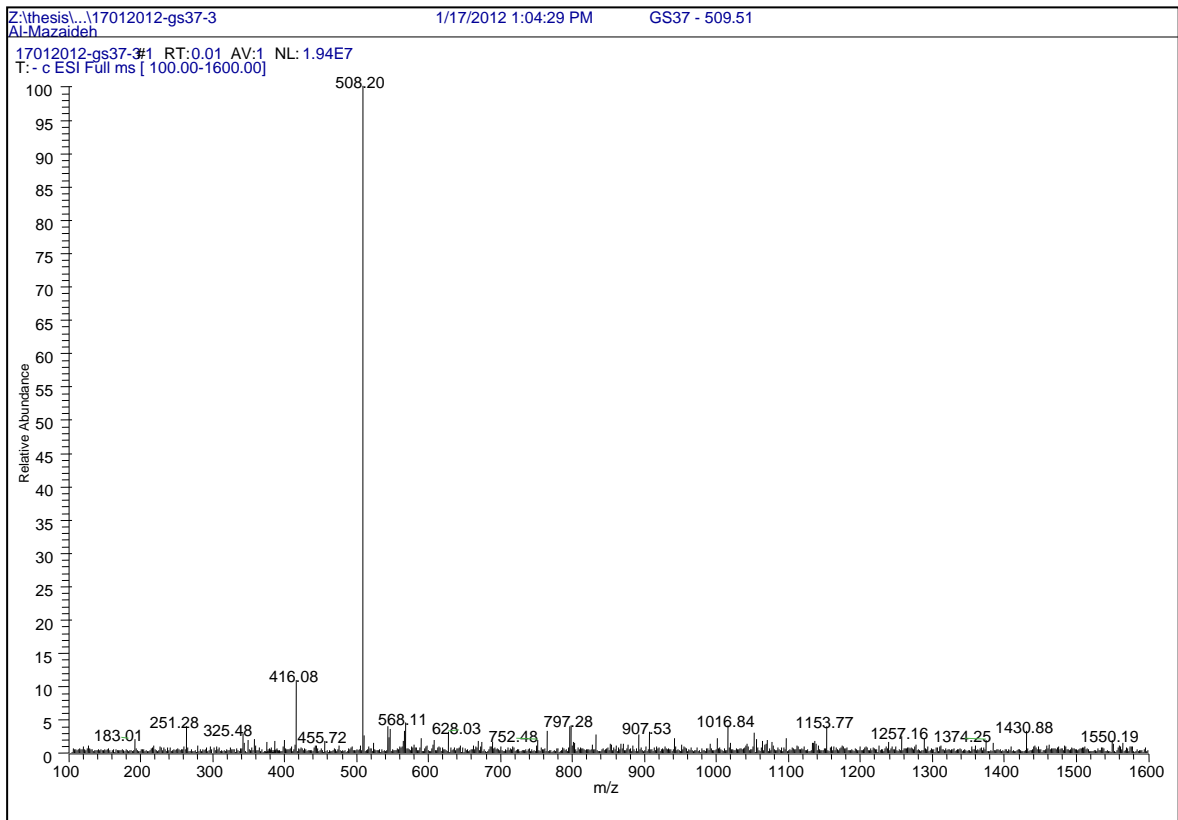
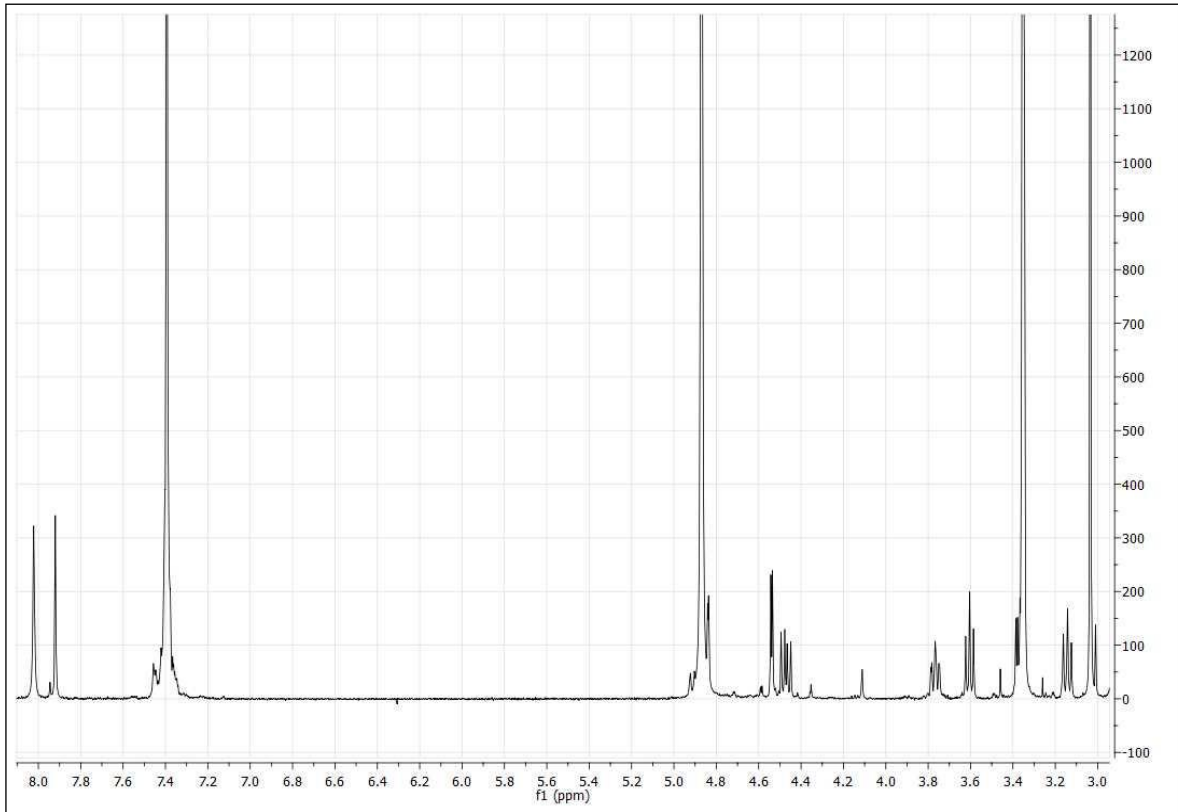


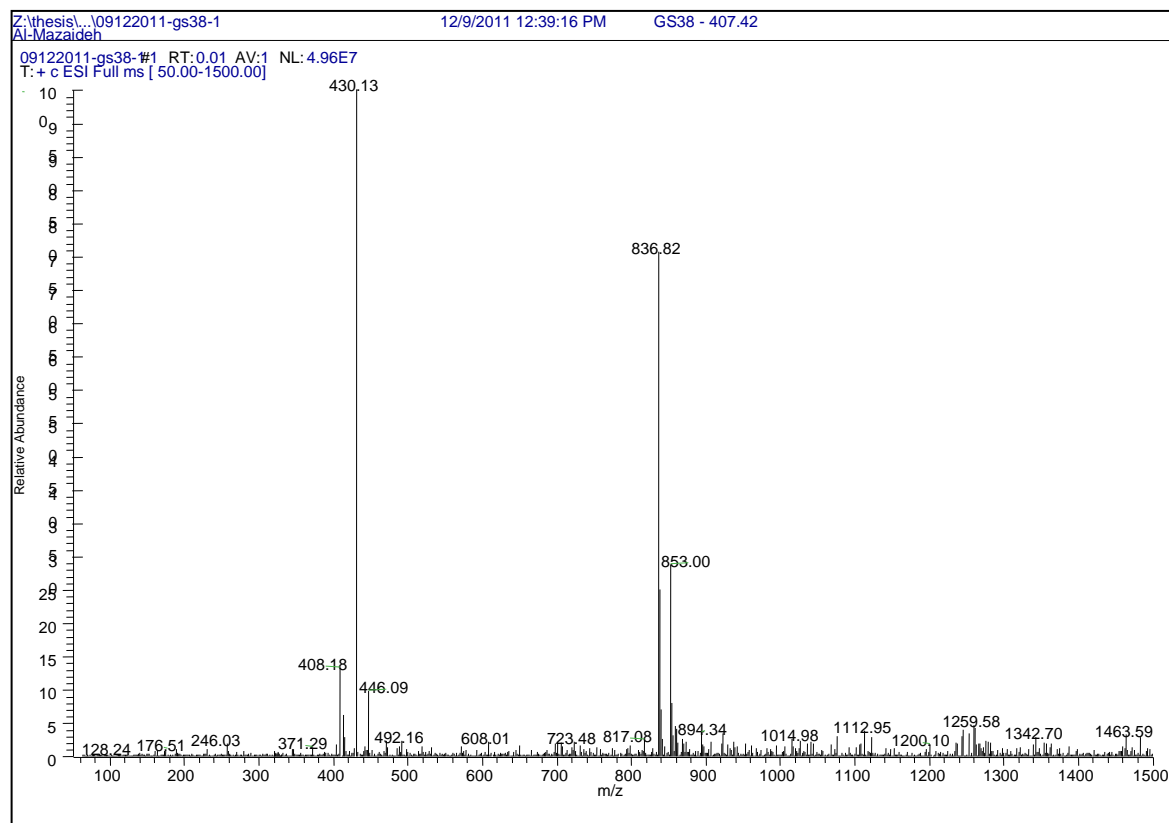
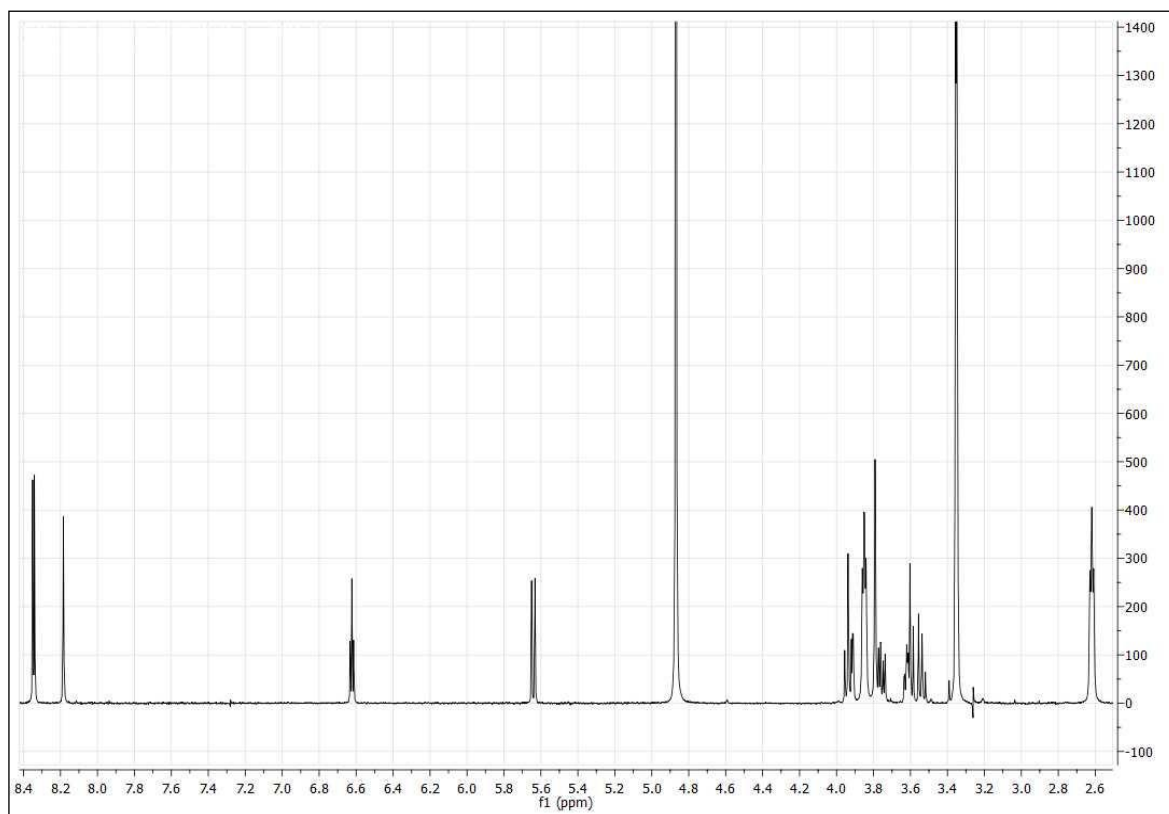
1-(2-Pyrimidinyl)-4-[(1-methyl-6-deoxy- α -D-glucopyranosid-6-yl)-(1H-1,2,3-triazol-4-yl)methyl]piperazine (GS35)

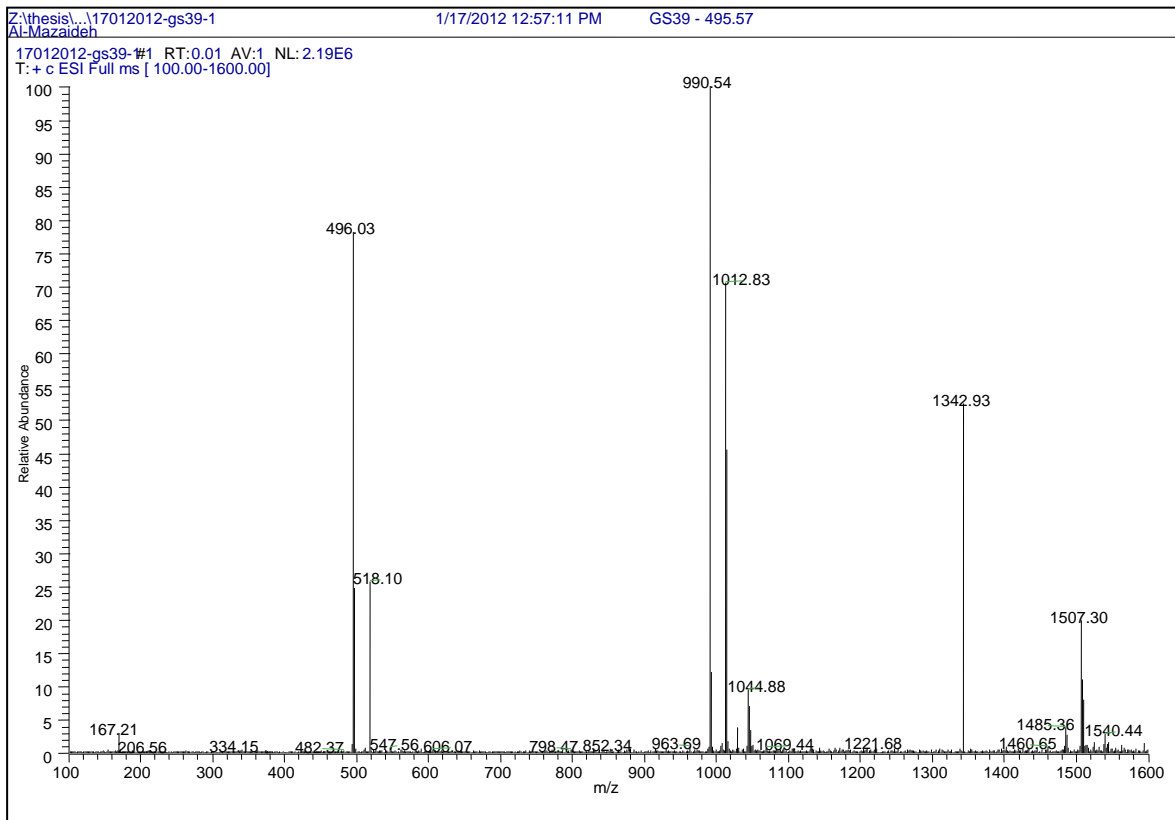
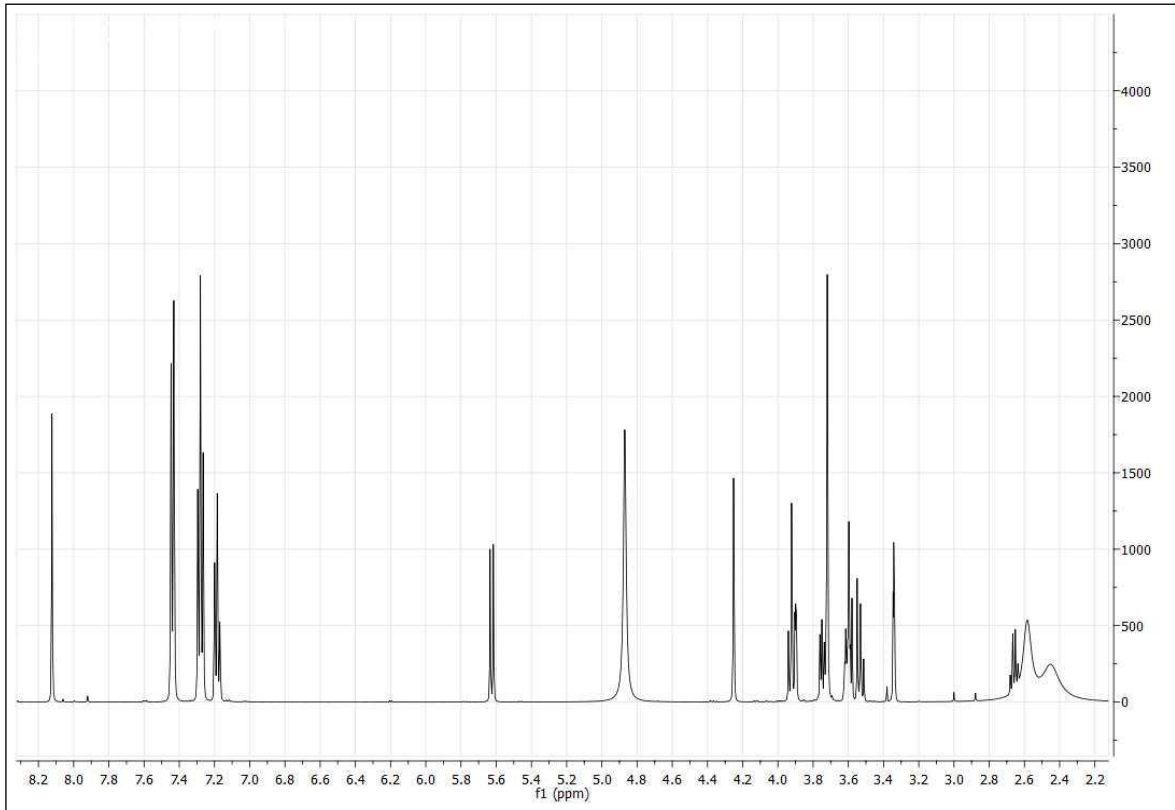
1-Benzhydryl-4-[(1-methyl-6-deoxy- α -D-glucopyranosid-6-yl)-(1H-1,2,3-triazol-4-yl)methyl]piperazine (GS36)



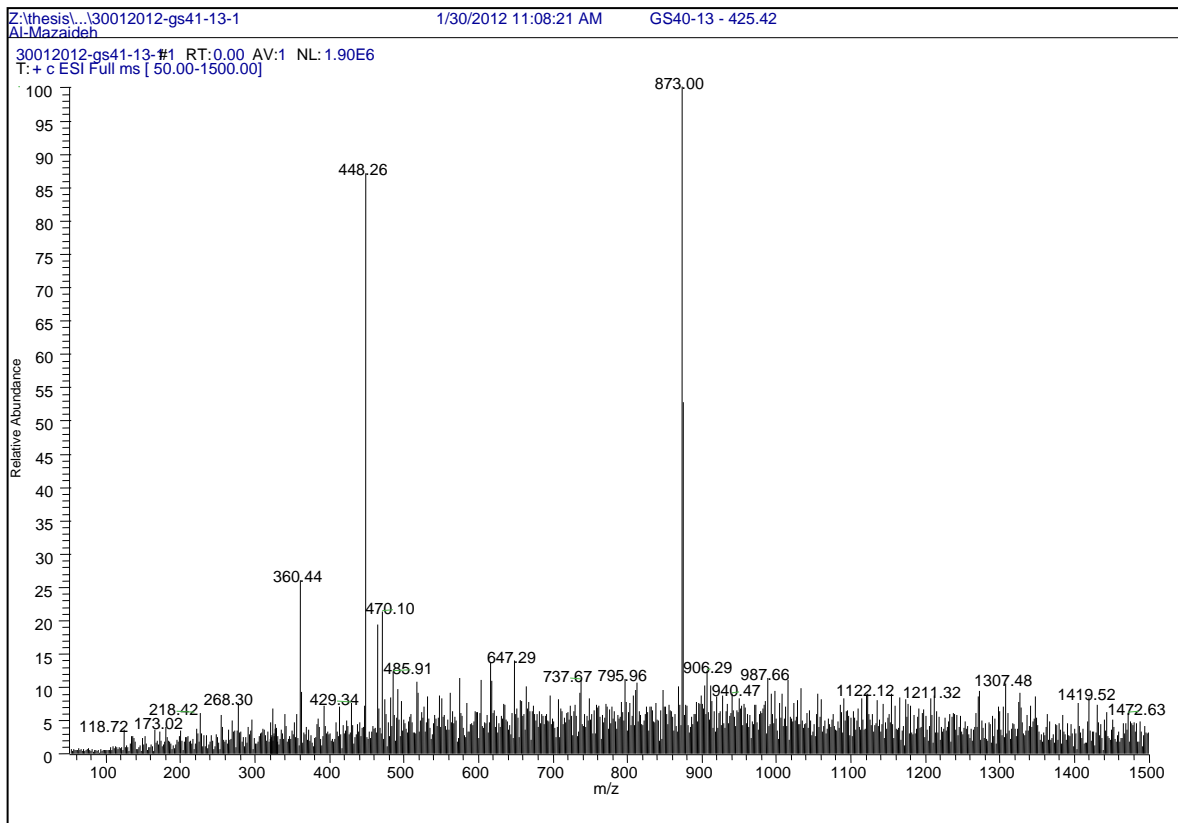
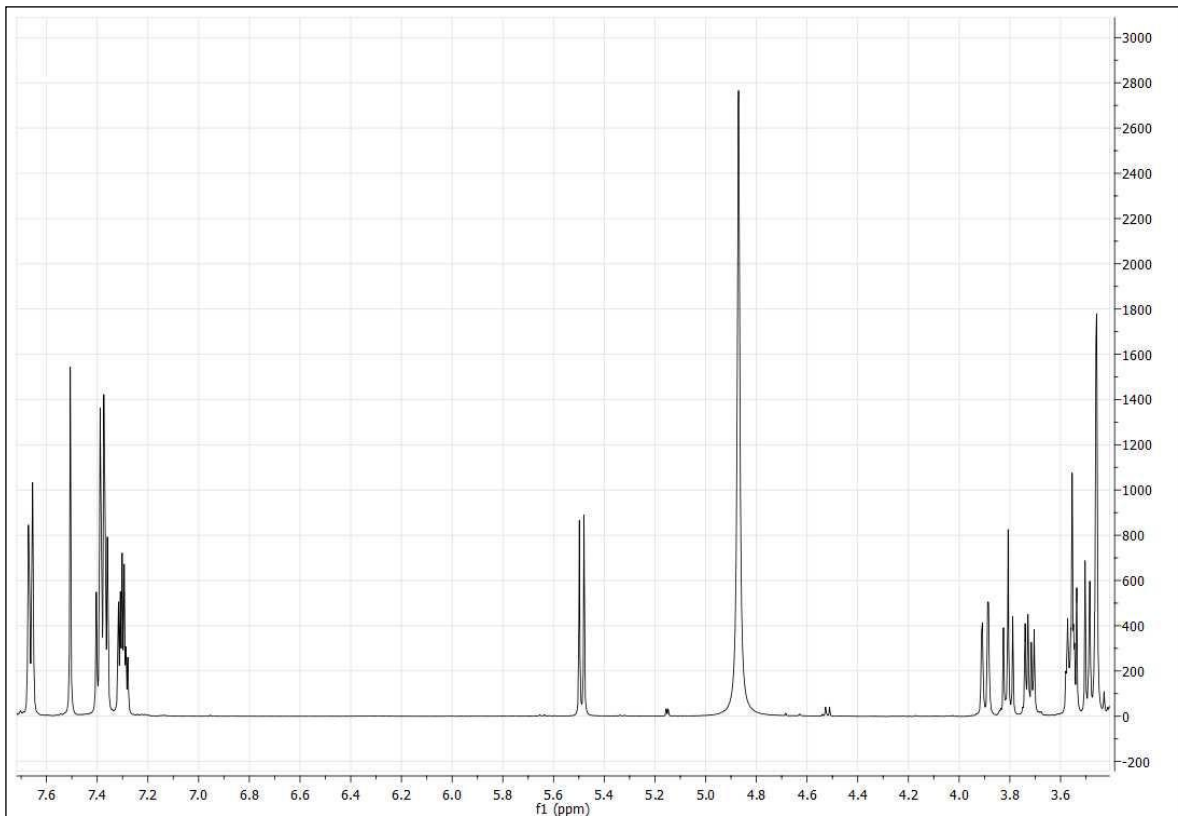
4-[(1-Methyl-6-deoxy- α -D-glucopyranosid-6-yl)-(1H-1,2,3-triazol-4-yl)methyl]-5,5-diphenyl-imidazolidine-2,4-dione (GS37)



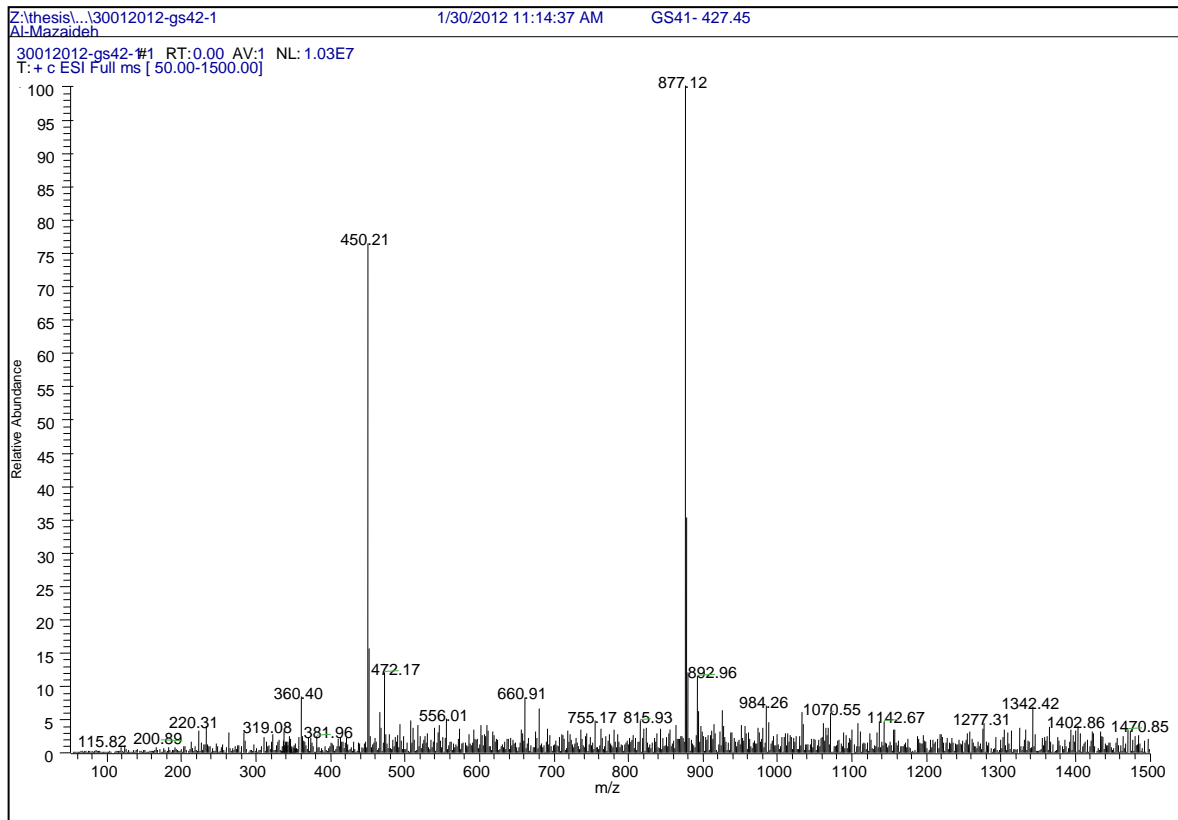
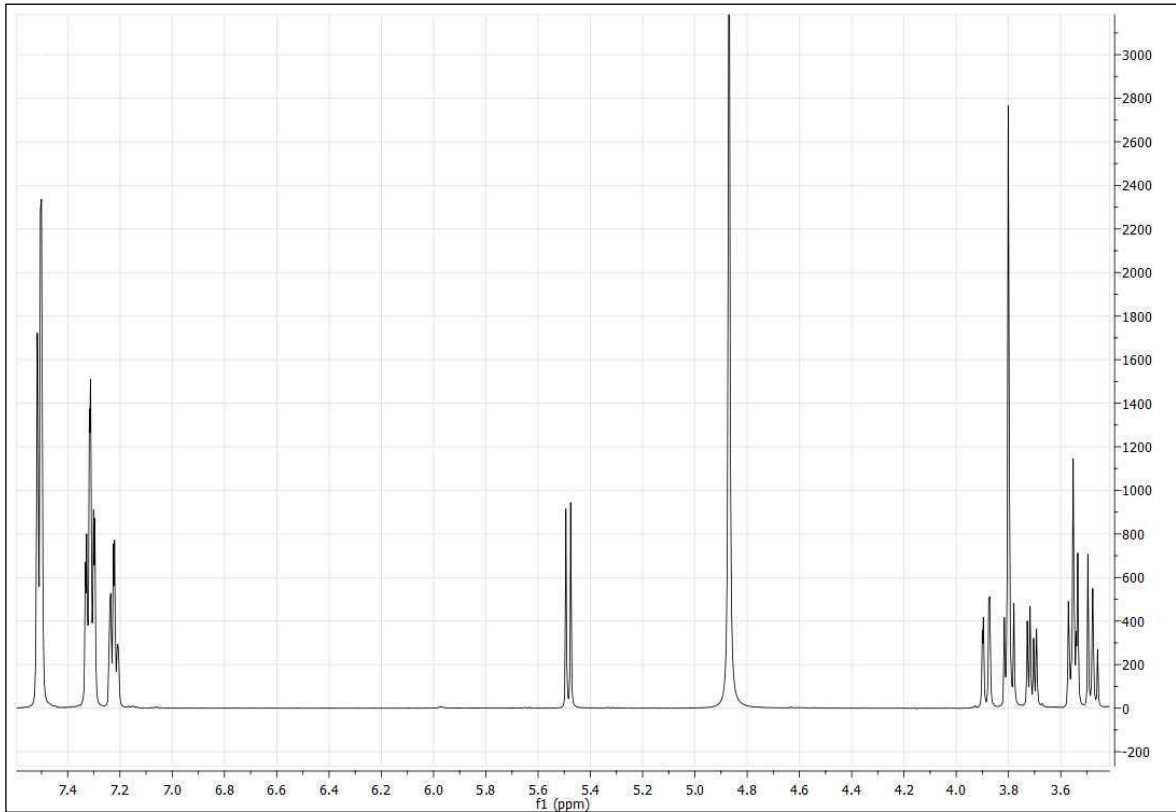
1-(2-Pyrimidinyl)-4-[1-(β -D-glucopyranosid-1-yl)-(1H-1,2,3-triazol-4-yl)methyl] piperazine (GS38)

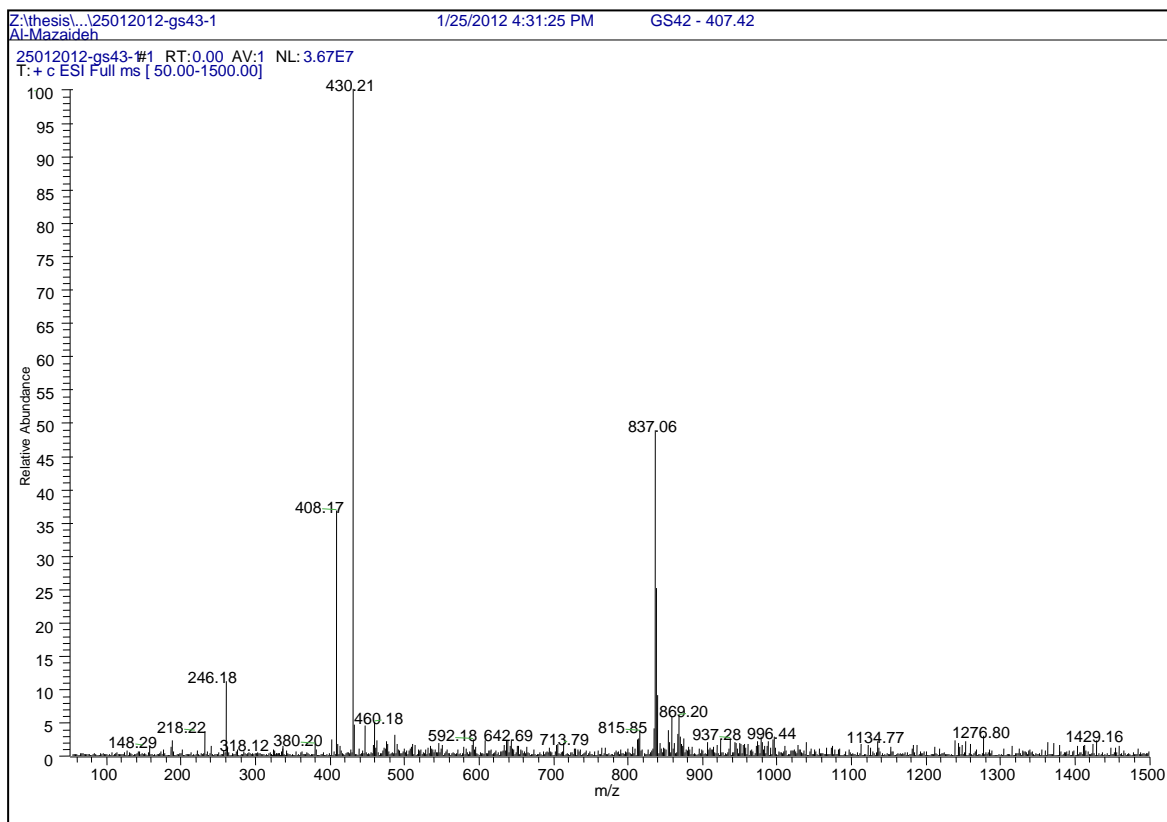
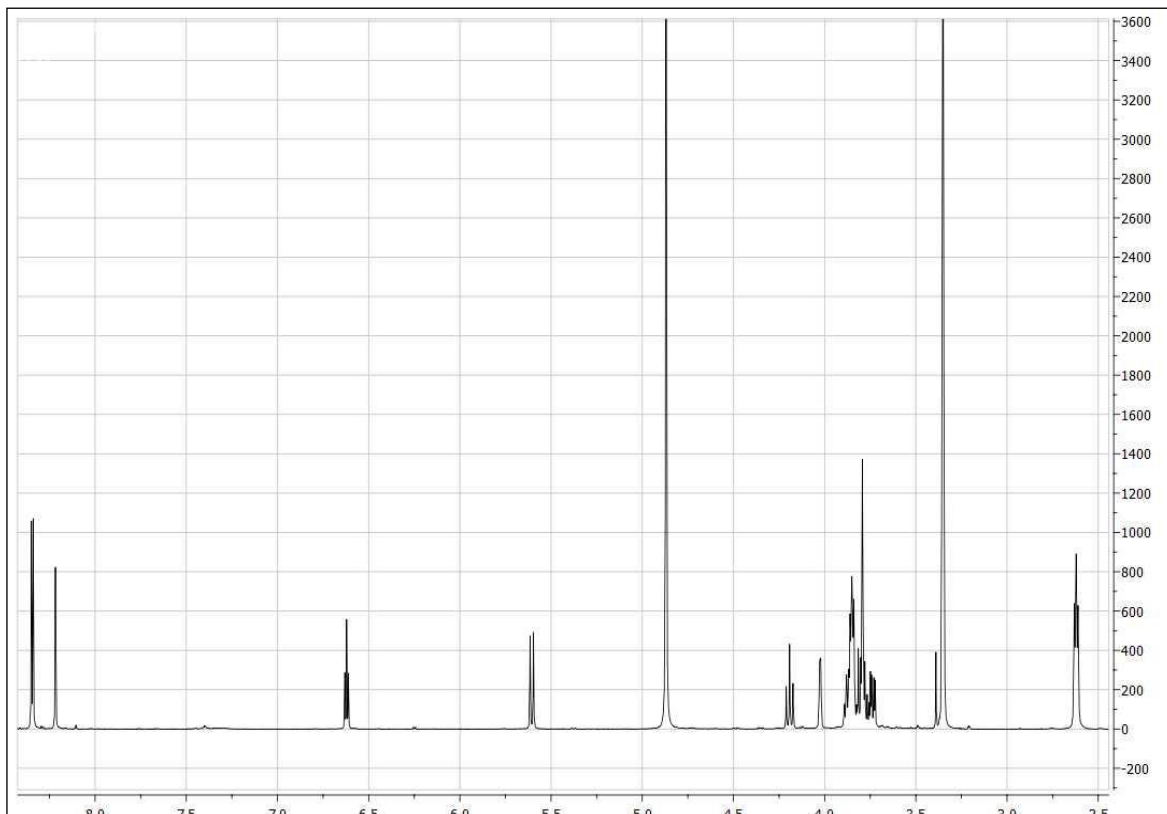
1-(Diphenylmethyl)-4-[1-(β -D-glucopyranosid-1-yl)-(1*H*-1,2,3-triazol-4-yl)methyl] piperazine (GS39)

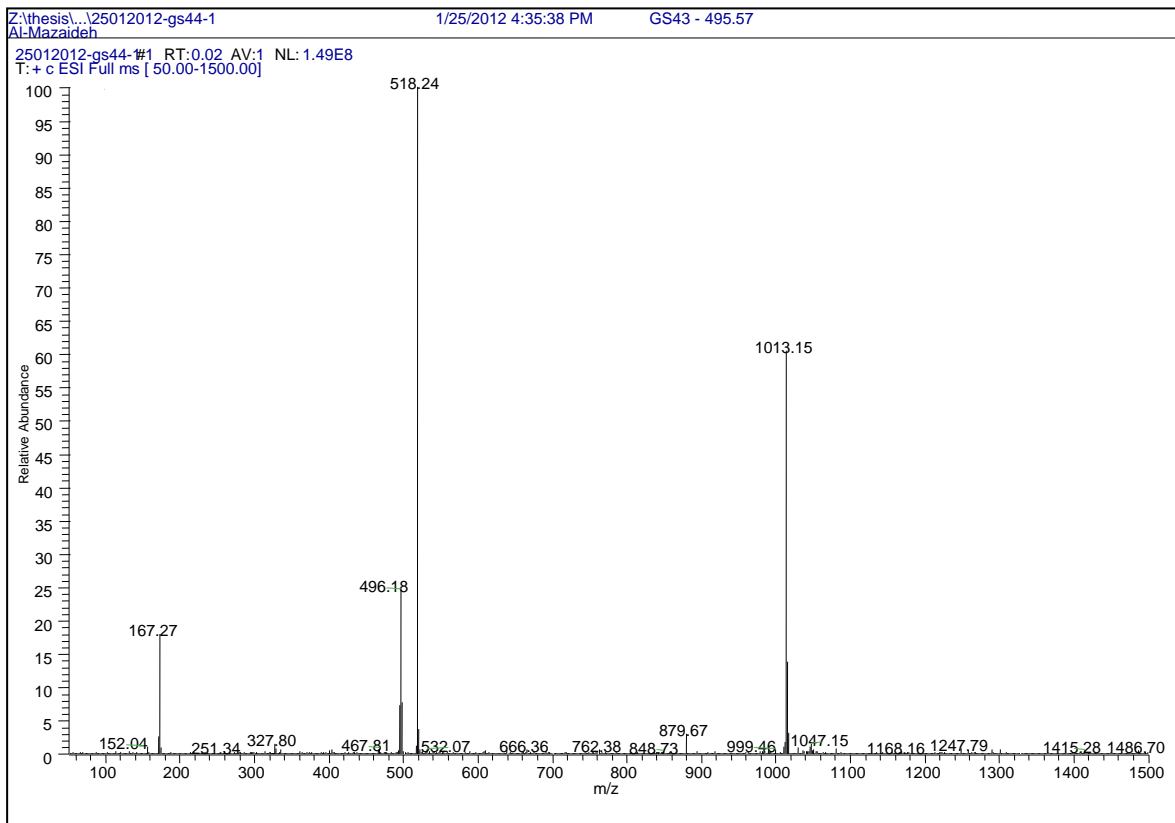
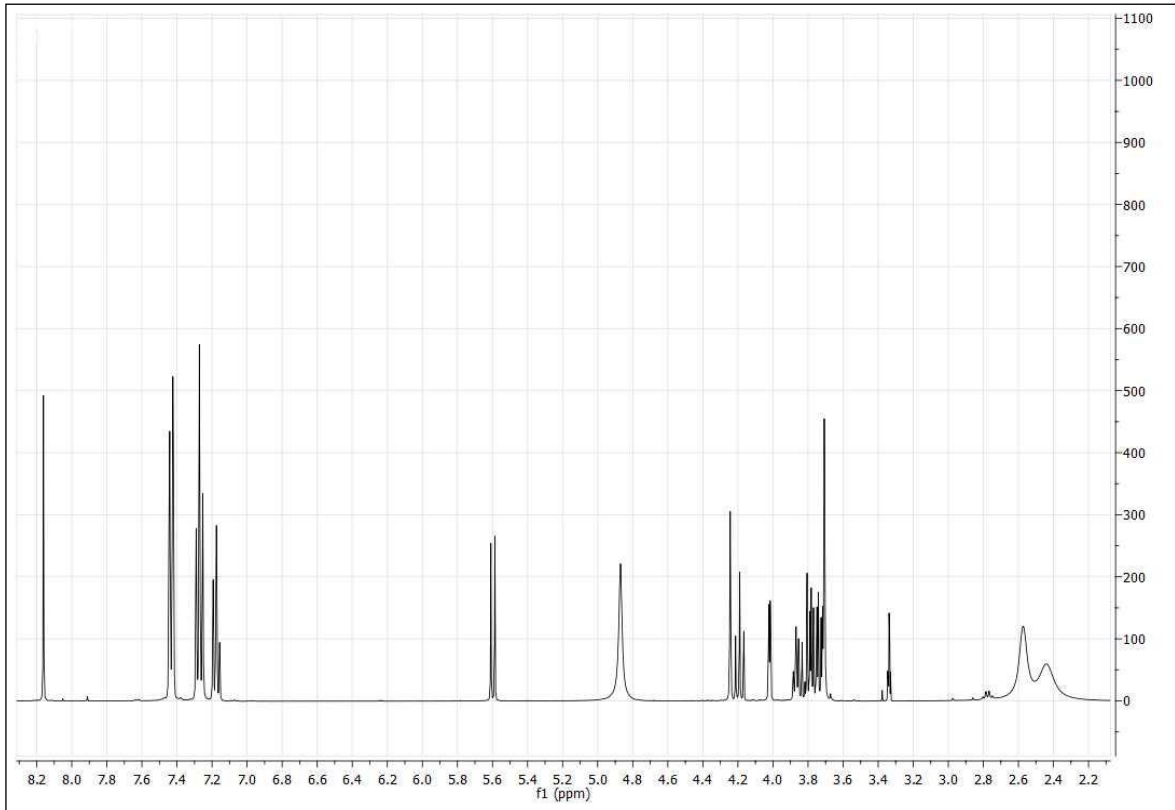
9-[1-(β-D-Glucopyranosid-1-yl)-(1H-1,2,3-triazol-4-yl)methyl]-9H-fluoren-9-ol (GS40)

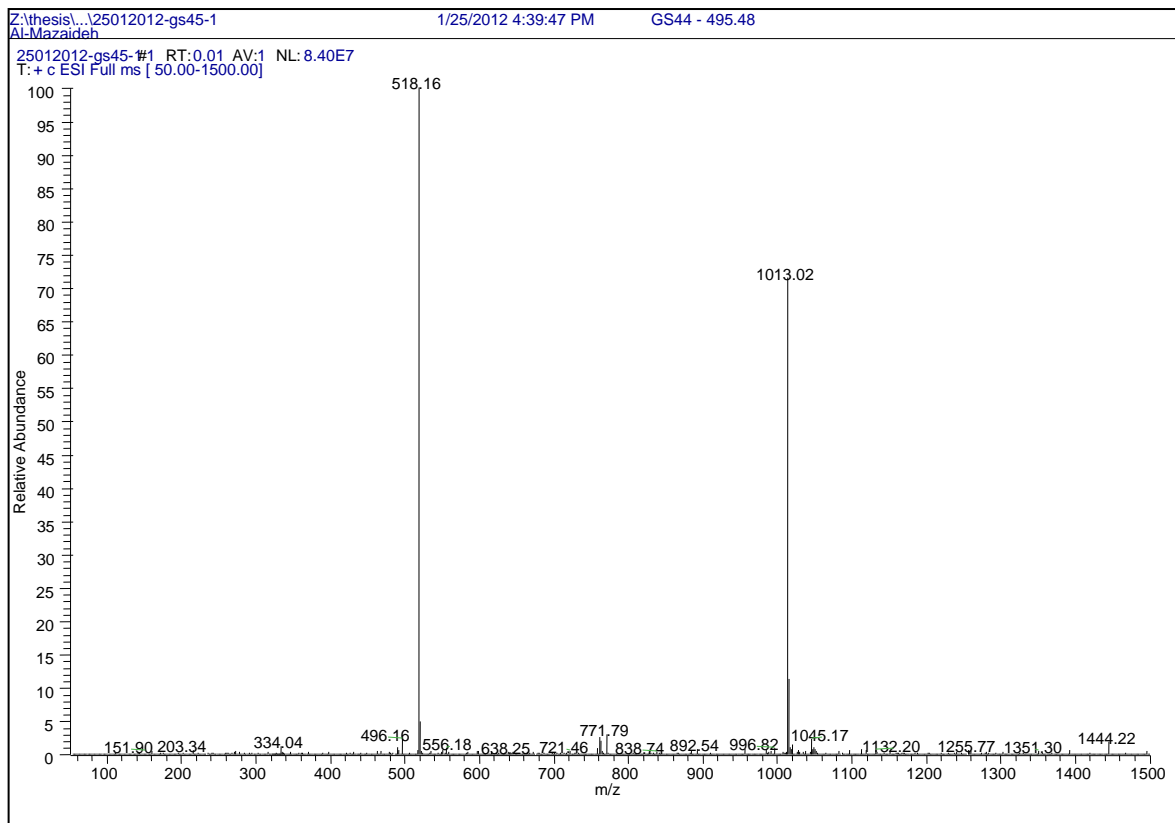
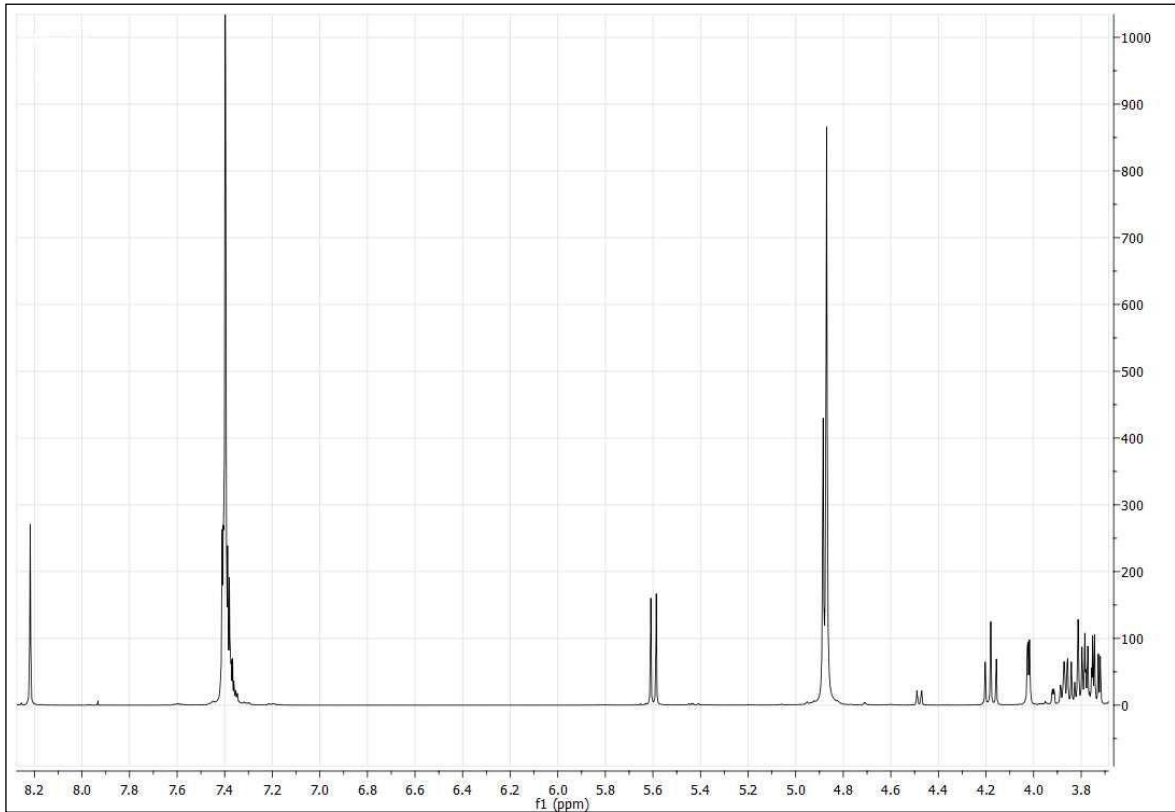


2-[1-(β -D-Glucopyranosid-1-yl)-(1*H*-1,2,3-triazol-4-yl)methyl]-1,1-diphenylethanol (GS41)

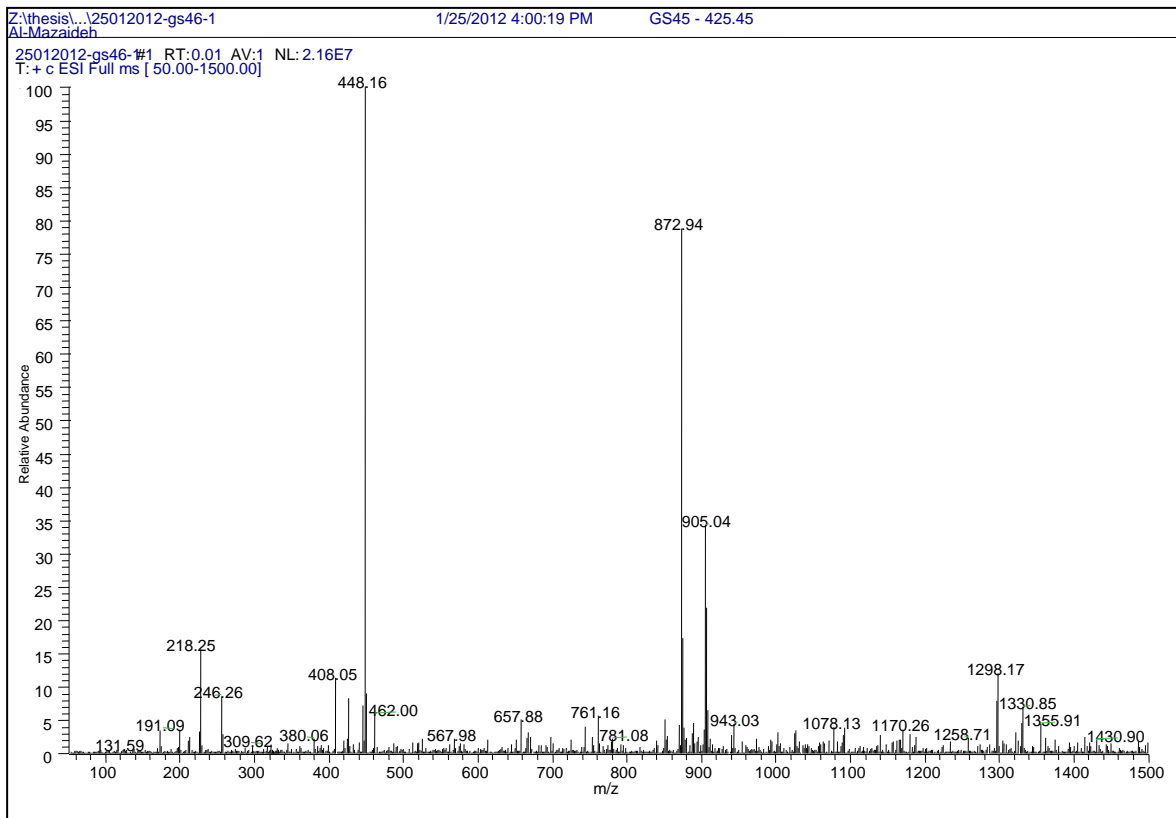
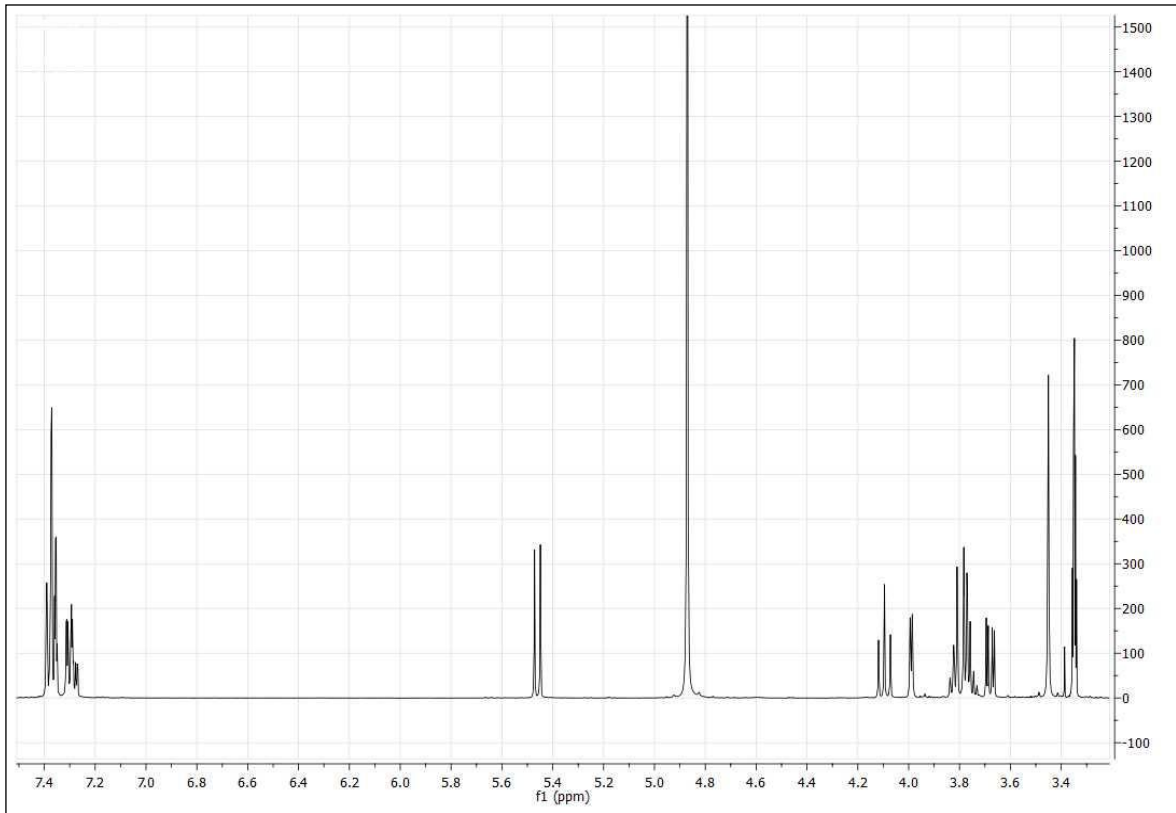


1-(2-Pyrimidinyl)-4-[1-(β -D-galactopyranosid-1-yl)-(1*H*-1,2,3-triazol-4-yl)methyl] piperazine (GS42)

1-(Diphenylmethyl)-4-[1-(β -D-galactopyranosid-1-yl)-(1*H*-1,2,3-triazol-4-yl)methyl]piperazine (GS43)

[1-(β -D-Galactopyranosid-1-yl)-(1H-1,2,3-triazol-4-yl)methyl]-5,5-diphenyl-imidazolidine-2,4-dione (GS44)

**9-[1-(β-D-Galactopyranosid-1-yl)-(1H-1,2,3-triazol-4-yl)methyl]-9H-fluoren-9-ol
(GS45)**



9 Acknowledgments

First and foremost, I would like to express my deep thanks and gratitude to my supervisor Prof. Dr. Wolfgang Sippl, who allowed me to perform this research in his group, as well as the hiring of the interesting topic and the scope for creativity. A special thanks to Dr. Matthias Schmidt for his considerable assistance, friendly service, practical advice, and guidance during this work.

Furthermore, I thank Prof. Dr. Bodo Dobner and his staff for their expertise and helpfulness. I also thank Mrs. Woigk for the production of ESI-MS spectra, and Dr. Ströhl the Department of Chemistry and his staff for carrying out the $^1\text{H-NMR}$ spectra.

I would also like to thank Mr. Alexander Rohe for his suggestions and contributions to the success of this work, especially in biochemical background. Thanks are extended to my colleagues, and whole staff in the department of medicinal chemistry, with whom I spent a so much precious time.

My thanks also go to German Erlenkamp, who performed the computer-based examinations and his suggestions brought me closer to the theoretical backgrounds.

Great thanks are owed to my wonderful family, my wife Haya and my daughter Rafef. The most special thanks belong to Haya, for her understanding about my leaving during all these years, selfless love, sustainable support, encouragement and great patience at all times, as well as standing beside me throughout my writing of this thesis and in my life. Haya has been my inspiration and motivation for continuing to improve my knowledge and move my career forward.

The present work was carried out at the Department of Medicinal Chemistry, Institute of Pharmacy, Martin-Luther-University Halle-Wittenberg, Halle (Saale), Germany, in the period 2009-2012. Finally, I want to express my thanks to Tafila Technical University TTU for financial support.

10 Curriculum Vitae

Ghassab Mohammad Ali Al-Mazaideh

Date of Birth: 25-08-1979

Place of Birth: Al Tafila, Jordan

Marital status: Married

Child: one daughter Rafef

Nationality: Jordanian

Email: ghassab.al-mazaideh@pharmazie.uni-halle.de

g_mazideh@yahoo.com

Education

1996-1997	Basira high secondary school, Al Tafila, Jordan.
1997-2001	Mu'tah university. Karak, Jordan. B.Sc in Chemistry.
2002-2005	Mu'tah uuniversity. Karak, Jordan. Master of Science (Physical chemistry). Title: Methylenecyclopentane and 1-Methylcyclopentene Tautomerism.
2009-present	Ph.D. student, Institute of Pharmacy, Department of Medicinal Chemistry, Martin-Luther-University Halle-Wittenberg. Supervisor: Prof. Dr. Wolfgang Sippl.

Work Experience and Training

2001-2005	Lecturer, Grandal Secondary School, Tafila, Jordan.
2006-2008	Teacher and Research Assistant, Department of Chemistry, Tafila Technical University TTU, Jordan.
10/2008-2/2009	Teacher Assistant, Faculty of Science, TU Chemnitz, Physical Chemistry/Electrochemistry.

Publications:

- Al-Rawajfeh, E., Al-Garalleh, M., Al-Mazaideh, G., AL-Rawashdeh, A., Khalil, S., *Understanding CaCO₃-Mg(OH)₂ scale formation: a semi-empirical MINDO-forces study of CO₂-H₂O system*, Chem. Eng. Comm. 2008, 195, p. 1026.
- Rohe, A., Göllner, C., Wichapong, K., Erdmann, F., Al-Mazaideh, G., Sippl, W., Schmidt, M., *Evaluation of potential Myt1 kinase inhibitors by TR-FRET based binding assay*, 2012. (Submitted).
- Further manuscripts are in preparation.

Posters:

- Al-Mazaideh, G., Sippl, W., Schmidt, M., *Synthesis and development of new potential ATP-competitive Myt1 kinase inhibitors*. DPhG-Tagung-Jena, 2009.
- Claudia, A., Philipp, P. Balgarov, Gollner, C, Al-Mazaideh, G., Erdmann, F., Sippl, W., Ruttinger, H., Schmidt, M., *Development of a CE based assay for determination of human Myt1 kinase activity*, DPhG-Tagung–Braunschweig 2010.
- Rohe, A., Erdmann, F., Philipp, C., Al-Mazaideh, G., Gollner, C., Sippl, W., Schmidt, M., *The human PKMYT1 as a target in Assay Development*, DPhG-Tagung–Innsbruck 2011.

11 Declaration of Independence

Hiermit versichere ich, dass ich die vorliegende Arbeit selbstständig und ohne Benutzung anderer als der angegebenen Hilfsmittel angefertigt habe.

Alle Stellen, die wörtlich oder sinngemäß aus veröffentlichten und nicht veröffentlichten Schriften anderer entnommen sind, sind als solche kenntlich gemacht.

Die Arbeit hat in gleicher oder ähnlicher Form noch keiner anderen Prüfungsbehörde vorgelegen.

Halle, March 2012

Ghassab M.Al-Mazaideh